Performance and Cost Assessment of a Coal Gasification Power Plant Integrated with a Direct-Fired sCO_2 Brayton Cycle

Nathan Weiland, Walter Shelton, Travis Shultz, Charles White, David Gray

September 18, 2017

NETL-PUB-21435

NATIONAL ENERGY TECHNOLOGY LABORATORY

Solutions for Today | Options for Tomorrow

About the National Energy Technology Laboratory

The National Energy Technology Laboratory (NETL), part of the United States (U.S.) Department of Energy (DOE) national laboratory system, is owned and operated by DOE. NETL supports DOE's mission to advance the energy security of the United States.

Disclaimer

Printed in the United States of America

Available to DOE and DOE contractors from the Office of Scientific and Technical Information (OSTI):

U.S. Department of Energy
Office of Scientific and Technical Information
P.O. Box 62
Oak Ridge, TN 37831-0062
www.osti.gov
Phone: (865) 576-8401
Fax: (865) 576-5728
Email: reports@osti.gov

Available to the public from the National Technical Information Service (NTIS):

U.S. Department of Commerce
National Technical Information Service
5301 Shawnee Road
Alexandria, VA 22312
www.ntis.gov
Phone: (800) 553-NTIS (6847) or (703) 605-6000
Fax: (703) 605-6900
Email: orders@ntis.gov

Author List:

National Energy Technology Laboratory (NETL)

Nathan Weiland
General Engineer

Walter Shelton
General Engineer

Travis Shultz
Supervisor, Energy Process Analysis Team

Mission Execution and Strategic Analysis (MESA)

Charles White
KeyLogic Systems, Inc.

David Gray
Formerly Noblis

This report was prepared by MESA for the U.S. DOE NETL. This work was completed under DOE NETL Contract Number DE-FE0025912. This work was performed under MESA Task 201.005.003.

All images in this report were created by NETL, unless otherwise noted.

The authors wish to acknowledge the excellent guidance, contributions, and cooperation of the NETL staff, particularly:

Nathan Weiland, NETL Technical Monitor

Richard Dennis, NETL Technology Manager Advanced Turbines

DOE Contract Number DE-FE0025912

This page intentionally left blank.

TABLE OF CONTENTS

LIST OF EXHIBITS

ACRONYMS AND ABBREVIATIONS

A-USC	Advanced Ultrasupercritical
AACE	Association for the Advancement of Cost Engineering
AGR	Acid gas removal
AHT	Advanced Hydrogen Turbine
Ar	Argon
Aspen	Aspen Plus®
ASU	Air separation unit
BEC	Bare erected cost
BFD	Block flow diagram
BFW	Boiler feedwater
BOP	Balance of plant
Btu	British thermal unit
Btu/lb	British thermal units per pound
CB&I	Chicago Bridge & Iron Company
CCCMP	Clean Coal and Carbon Management Program
CCF	Capital charge factor
CCS	Carbon capture and storage
CEPCI	Chemical Engineering Plant Cost Index
CF	Capacity factor
CH_4	Methane
CO	Carbon monoxide
CO_2	Carbon dioxide
COE	Cost of electricity
COS	Carbonyl sulfide
CPU	CO_2 purification unit
DCF	Discounted cash flow
DOE	Department of Energy
EOS	Equation of state
EPC	Engineer/procure/construct
EPCM	Engineering/procurement/ construction management
EPRI	Electric Power Research Institute
FG	Flue gas
FO	Fuel oil
ft	Foot, Feet
ft^3	Cubic foot
gal	Gallon
GE	General Electric
gpm	Gallons per minute
GT	Gas turbine
h, hr	Hour
H.O.	Home office
H_2	Hydrogen
H_2O	Water
H_2S	Hydrogen sulfide
HCl	Hydrochloric acid
Hg	Mercury
HHV	Higher heating value
hp	Horsepower
HP	High pressure
HRSG	Heat recovery steam generator
HTR	High-temperature recuperator
I&C	Instrumentation and control
IEAGHG	International Energy Agency Greenhouse Gas R&D Programme
IGCC	Integrated gasification combined cycle
IOU	Investor-owned utility
IP	Intermediate pressure
IRROE	Internal rate of return on equity
kg/hr	Kilogram per hour
kJ/kg	Kilojoule per kilogram
kPa	Kilopascal
kW, kWe	Kilowatt electric
kWh	Kilowatt-hour
kW_t	Kilowatt thermal
lb	Pound
LHV	Lower heating value
LMTD	Log mean temperature difference
LP	Low pressure
LRT	Lowest temperature for heat recovery
LT	Low temperature
LTR	Low-temperature recuperator
m	Meter
m^3/min	Cubic meters per minute
MAT	Minimum approach temperature
MC	Main compressor

MESA	Mission Execution and Strategic Analysis
MMBtu	Million British thermal units
MMBtu/hr	Million British thermal units per hour
mol%	Mole percent (percent by mole)
MPa	Megapascal
MW, MWe	Megawatt electric
MWh	Megawatt-hour
MWt	Megawatt thermal
N/A	Not applicable
N_2	Nitrogen
N_2O	Nitrous oxide
NETL	National Energy Technology Laboratory
NGCC	Natural gas combined cycle
NH_3	Ammonia
NIST	National Institute of Standards and Technology
NOx	Oxides of nitrogen
O&M	Operation and maintenance
O_2	Oxygen
O-H	Overhead
P	Pumping
PC	Pre-compression
PHX	Primary heat exchanger
POTW	Publicly-owned treatment works
ppmd	Parts per million dry
PR	Pressure ratio
PRB	Powder River Basin
psi	Pounds per square inch
psia	Pound per square inch absolute
psig	Pound per square inch gage
PSFM	Power Systems Financial Model
QGESS	Quality Guidelines for Energy System Studies
R&D	Research and development
RC	Recycle compressor
RGC	Radiant gas cooler
S_8	Octasulfur
sCO_2	Supercritical carbon dioxide
SCOT	Shell Claus Off-gas Treatment
SCR	Selective catalytic reduction
SGC	Syngas cooler
SO_2	Sulfur dioxide
SOx	Oxides of sulfur
SWS	Sour water stripper
T	Turbine
T&S	Transport and storage
TASC	Total as-spent cost
TG	Tail gas
TGTU	Tail gas treatment unit
THT	Transformational Hydrogen Turbine
TIT	Turbine inlet temperature
TOC	Total overnight cost
tonne	Metric ton (1,000 kg)
TPC	Total plant cost
U.S.	United States
V-L	Vapor liquid portion of stream (excluding solids)
vol%	Volume percent
W/K	Watt per Kelvin
WGCU	Warm gas clean-up unit
Wh/kg	Watt-hour per kilogram
WHB	Waste heat boiler
wt%	Weight percent
yr	Year
$/MMBtu	Dollars per million British thermal units
MM$	Millions of dollars
°C	Degrees Celsius
°F	Degrees Fahrenheit

This page intentionally left blank.

EXECUTIVE SUMMARY

The objective of the present study is to develop a cost and performance baseline for a coal syngas-fueled, direct-fired supercritical carbon dioxide (sCO_2) power plant using coal gasification, and to analyze the sensitivity of its net thermal efficiency and cost indicators to variations in select operating parameter and cost assumptions. The study results yield a net sCO_2 baseline plant efficiency of 37.7 percent on a HHV basis, which includes 97.6 percent carbon capture at a purity of 99.8 percent. This is significantly higher than the reference integrated gasification combined cycle (IGCC) plant using the same Shell gasifier, which has an efficiency of 31.2 percent with 90 percent carbon capture. Although it includes a high degree of uncertainty due to the low Technology Readiness Level of direct sCO_2 power cycles, the economic analysis estimates a cost of electricity (COE) of $137/MWh for the mature, commercial-scale sCO_2 plant (without CO_2 transport and storage (T&S) costs), yielding a 10 percent reduction in COE from the reference IGCC case. These results demonstrate the significant potential of direct sCO_2 power cycles for achieving the Department of Energy's (DOE) transformational power generation goals for coal-fueled power plants with carbon capture and storage (CCS). These results will be utilized in future studies that will focus on plant optimization to further minimize COE, based on potential sCO_2 plant improvements identified in sensitivity analyses and comparisons to other sCO_2 and IGCC studies.

The conceptual design for the baseline coal-fueled direct-fired sCO_2 power plant was developed by first analyzing the gasifier technology that would pair well with the direct-fired sCO_2 Brayton cycle, leading to the choice of a Shell gasifier based on its commercial availability, high cold gas efficiency, and syngas heat recovery capability. Based on a review of the literature on coal-fueled direct-fired sCO_2 power plants and a detailed analysis of the degrees of freedom in the sCO_2 cycle, performed previously at National Energy Technology Laboratory (NETL), a preliminary cycle configuration and state point was selected.

A detailed assessment of equations of state (EOS) best suited to analysis of sCO_2 working fluid mixtures present in direct sCO_2 cycles resulted in a switch to the Lee-Kessler-Plöcker EOS in the system model, improving the accuracy of the Aspen Plus® (Aspen) modeling results. Further, at the turbine inlet temperature (TIT) proposed for the preliminary baseline cycle, it was deemed necessary to incorporate blade cooling in the sCO_2 turbine. An empirical sCO_2 turbine blade cooling model was developed based on correlations to data in the direct sCO_2 literature. [1] While this decreased cycle efficiency, the resulting system model better-represents the actual processes present in a direct sCO_2 power cycle, and improves cycle model predictions going forward.

Several sensitivity analyses were performed to guide potential improvements in the plant configuration and operating conditions. It was determined that significant improvement to process efficiency can be realized by lowering the CO_2 cooler temperature, and by incorporating intercoolers in the sCO_2 pre-compressor. It was also determined that significant improvement to process efficiency can be realized by increasing the CO_2 TIT, at least up to 1204 °C (2200 °F). A change in the oxidant insertion point was examined as a way to extract additional high-quality heat from the syngas coolers. While it was found to slightly increase

process efficiency, there were many secondary impacts that indicate that such a change is not advisable.

Based on the results from the sensitivity analyses, a final cycle and baseline sCO_2 plant configuration was developed and the performance of the plant was estimated from an Aspen model and compared to the reference Shell gasifier IGCC case with CCS. The results are summarized in Exhibit ES-1, and show a baseline sCO_2 plant thermal efficiency of 37.7 percent on a higher heating value (HHV) basis, which is 6.5 percentage points higher than the reference IGCC case. Water consumption is also reduced by about 20 percent relative to the reference IGCC case.

Exhibit ES-1 Baseline direct sCO_2 plant and reference IGCC plant results comparison

Item	sCO_2 Baseline	IGCC Reference Case B1B [2]
Performance Results		
Gross Power (kWe)	777,080	673,400
Net Auxiliary Load (kWe)	-214,659	-176,660
Net Plant Power (kWe)	562,421	496,740
Net Plant Efficiency (HHV, %)	37.7	31.2
Cooling/Condenser Duty (kW_t)	-546,000	-371,000
Coal Feed Flowrate (kg/hr)	198,060	211,040
Thermal Input (kW_t)	1,492,815	1,590,722
Oxygen Flowrate (kg/hr)	391,242	160,514
Carbon Captured (%)	98.1	90.0
Captured CO_2 Purity (%)	99.8	99.4
Water Withdrawal ([m^3/min]/MWnet)	0.036	0.043
Economic Results (2011$)		
Total Plant Cost ($1,000)	2,060,211	1,977,603
Total Plant Cost ($/kW)	3,663	3,981
COE without T&S ($/MWh)	137.3	152.6
COE with T&S ($/MWh)	146.1	162.4

An economic analysis of the baseline sCO_2 plant design was performed and compared to the reference IGCC plant, also shown in Exhibit ES-1. Although the sCO_2 total plant cost (TPC) of $2.06 billion (2011 dollar-year basis) is 4 percent higher than the reference IGCC plant ($1.98 billion), the TPC on a $/kW basis is 8 percent lower than the IGCC case. The COE for the baseline sCO_2 plant is $137.3/MWh, without CO_2 T&S, 10 percent lower than for the reference IGCC plant ($152.6/MWh). Both the decrease in TPC on a $/kW basis and the decrease in COE are primarily due to the higher efficiency of the sCO_2 plant.

Given that many of the components of the sCO_2 cycle have never been built at commercial scale, there is considerable uncertainty in the capital cost estimates for these components. A rough sensitivity analysis shows that the TPC for the baseline sCO_2 plant would need to increase by 296 MM$ (14.4 percent) for the COE without T&S to rise to the same value as for the reference IGCC plant. Given that the TPC for the sCO_2 cycle components totals 262 MM$, there is a considerable buffer in the sCO_2 cycle component cost estimates for the baseline sCO_2 plant to show economic benefits relative to the reference IGCC plant. Examination of the sCO_2 baseline plant cost table shows that the cost of the gasifier account (gasifier, syngas coolers, air separation unit (ASU), and accessories) amounts to 49 percent of the plant's TPC, as shown in Exhibit ES-2. The most significant opportunities for reducing the capital costs of the baseline sCO_2 plant therefore lie in selecting a more cost-effective gasifier or in reducing syngas cooler or ASU costs, rather than in reducing costs of the sCO_2 cycle components.

Exhibit ES-2 Relative account costs for the baseline direct-fired sCO_2 plant TPC

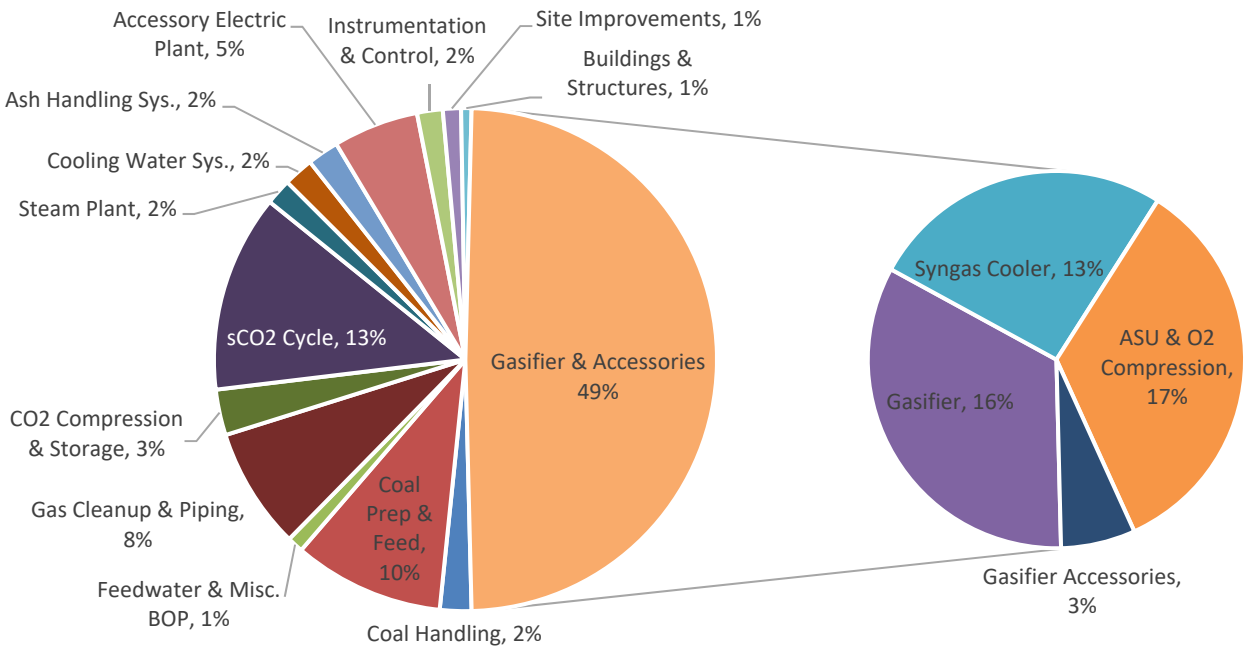

To that end, the techno-economic impact of eliminating the high-temperature syngas coolers was also examined. An initial screening level assessment indicated that this would result in a reduction in process efficiency of approximately 2 percentage points, but would also significantly reduce the cost of the syngas coolers, such that a lower overall COE is achievable with this change. This can be accomplished with an improved thermal integration scheme between the direct sCO_2 cycle and the gasification train, which will be examined in future studies of this plant design.

Finally, the results of this study are compared against other gasification-based sCO_2 [3] [4] and IGCC [2] [5] plant design studies. These comparisons suggest that investigation of quench-style gasifiers or General Electric (GE) gasifiers may also improve the cost and/or efficiency of the baseline sCO_2 plant design, and may also be pursued in follow-on studies.

1 INTRODUCTION

The Department of Energy's (DOE) Clean Coal and Carbon Management Program (CCCMP) provides a worldwide leadership role in the development of advanced coal-based electric power generation technologies with carbon capture and storage (CCS). The National Energy Technology Laboratory (NETL), as part of DOE's Office of Fossil Energy, implements research, development, and demonstration programs that address the challenges of reducing greenhouse gas emissions. This includes the techno-economic evaluation of advanced power cycles that will maximize system efficiency and performance, while minimizing CO_2 emissions and the costs of CCS.

Supercritical carbon dioxide (sCO_2) power cycles are a type of advanced power cycle under investigation at NETL and elsewhere, due to their potential for improved efficiency and cost relative to more conventional technologies. These cycles utilize high-pressure CO_2 as the primary working fluid, typically near or above the critical point of CO_2 (31 °C, 7.37 MPa, [88 °F, 1070 psi]), which both reduces the required compression power due to high sCO_2 density near the critical point, and reduces the inefficiency associated with phase change heat transfer at the cycle cooler. As a working fluid, CO_2 is abundant, inexpensive, non-toxic, and less corrosive than steam. Finally, due to the high cycle pressures, turbomachinery sizes are smaller and potentially less expensive than their air- or steam-based counterparts.

1.1 sCO_2 POWER CYCLES FOR FOSSIL FUELS

Supercritical CO_2 power cycles under investigation for use in fossil, concentrated solar, and nuclear power generation are typically based on a closed (indirect) recompression cycle design, as shown in Exhibit 1-1. Heat is transferred from the main thermal energy source (e.g., combustion, solar heating, etc.) to high-pressure sCO_2 working fluid through a primary heat exchanger (PHX), which is then expanded through a turbine (T) for power production. Thermal energy in the turbine exhaust is recovered through a high-temperature recuperator (HTR) and a low-temperature recuperator (LTR), to preheat the sCO_2 flow to the PHX. Most of the low-pressure flow exiting the LTR passes through a cooler and the main compressor (MC), while a portion bypasses the cooler and LTR through a recycle compressor (RC). This is done to better balance the recuperation heat duty, as the heat capacity of the low-pressure CO_2 near the critical point is much higher than that on the high-pressure side of the LTR.

Exhibit 1-1 Recompression sCO_2 power cycle

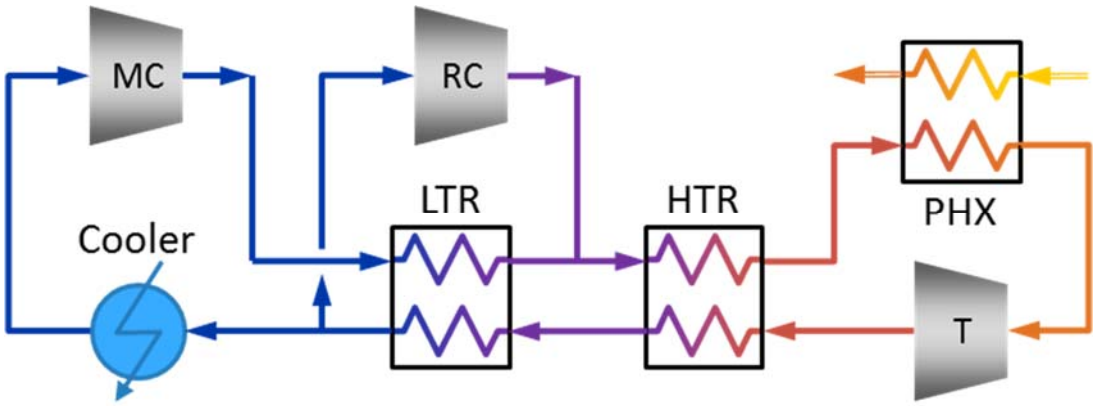

The recompression cycle has been shown to be one of the most efficient sCO_2 power cycles for concentrated solar and nuclear applications, since the high degree of recuperation dovetails nicely with these relatively constant-temperature heat sources. Additional consideration is required for efficient coupling of these indirectly-heated sCO_2 cycles to fossil-fueled heat sources, and is the subject of ongoing study. [6]

An alternative to these indirect sCO_2 cycles for fossil-fueled power are so-called direct-fired sCO_2 cycles, as shown in Exhibit 1-2. These cycles are attractive due to their high efficiency and inherent ability to capture CO_2 at storage-ready pressures. In these cycles, gaseous fuel is burned with oxygen in a highly-dilute sCO_2 environment, with the combustion products driving a turbine (T) to generate power. As with the indirect sCO_2 cycles, the thermal energy in the turbine exhaust is recuperated in a compact heat exchanger (Recup) to heat the CO_2 diluent flow to the combustor. After recuperation, water is condensed out of the product stream, followed by pre-compression (PC) to a pressure near the CO_2 critical pressure, additional cooling, and pumping (P) to the maximum cycle pressure. A portion of this stream is sent to a purification unit for CO_2 storage, while the bulk of the fluid is preheated in the recuperator and returned to the combustor.

Exhibit 1-2 Direct sCO_2 power cycle

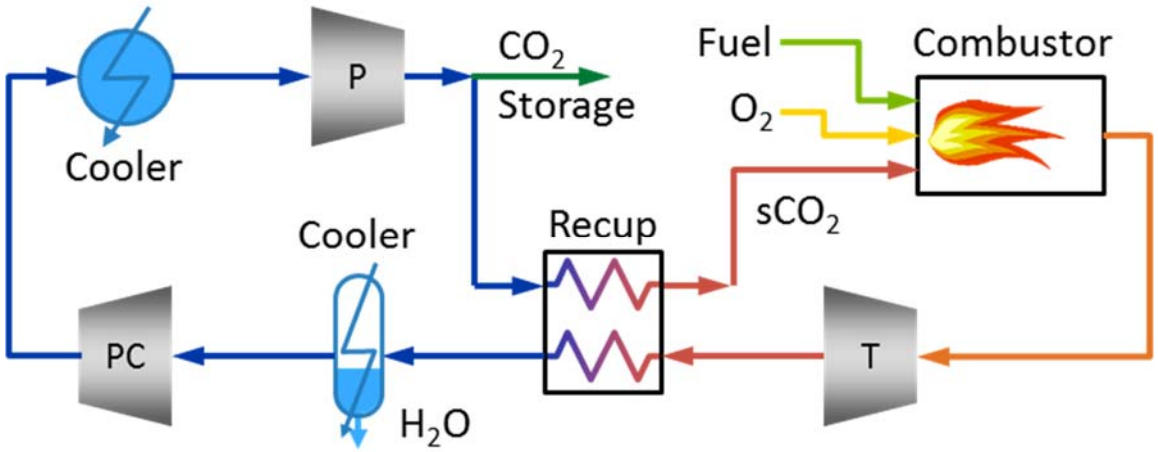

While direct and indirect sCO_2 cycles may share some common components (compressors, recuperators), they are very different cycles in many regards. The direct sCO_2 cycle is an open cycle with internal combustion, thus the working fluid contains impurities that enter the cycle through the oxygen stream (Ar, N_2), fuel stream (N_2), and through the combustion process (H_2O, CO, etc.). Recirculation rates in direct sCO_2 cycles are typically 90–95 percent, so the impurities constitute <10 percent of the cycle flow; however, their presence can have a significant adverse impact on the cycle compression power load, thereby reducing cycle efficiency. [1] [3]

Also, due to their high pressures and closed cycle nature, indirect sCO_2 cycle turbine inlet temperatures (TIT) are limited by the material constraints of the primary heat exchanger. This is directly analogous to steam Rankine cycles, where recent advances in nickel-alloy materials under the Advanced Ultrasupercritical (A-USC) research program have increased TITs to about 700–760 °C. [7] Since the direct sCO_2 cycle utilizes internal combustion without the need for transferring heat across a pressure difference, TITs can be much higher, resulting in higher cycle efficiencies than in indirect sCO_2 cycles. In this case, combustor liners and turbine blades must be cooled, similar to gas turbines. The recuperator, which exchanges heat at high pressure with recycled sCO_2, cannot be cooled, and represents the temperature/pressure design constraint of the system. If nickel alloys are used, this component can operate at inlet temperatures of 700–760 °C, though the high cost of these alloys also present challenges to the economic design of a direct sCO_2 plant. Turbine pressure ratios (PR) are typically about 8-12 for these cycles, and are limited by the need to maintain a high turbine exit pressure to enable a cost-effective, compact recuperator design.

At these PRs, the turbine exhaust/recuperator inlet constraint yields a TIT requirement of 1100–1200 °C (2012–2192 °F) at reasonable turbine efficiency. This presents unique challenges to the design of the oxy-combustor, which must operate at very high cycle pressures (20–30 MPa, [2900–4350 psi]) in a dilute sCO_2 combustion environment. High combustor pressures also preclude the use of solid fuels such as coal in this cycle due to difficulties with high-pressure coal feeding. Further, small flow passages in the recuperators and in the turbine seals would require extensive particulate ash cleaning at the high temperatures and pressures at the combustor exhaust, a technology that has not yet been developed. As a result, the use of coal as a fuel source in direct sCO_2 cycles necessitates the addition of a gasification process to convert the coal energy to syngas usable by the direct sCO_2 cycle.

The elevated pressures in a direct sCO_2 cycle leads to a high-power density cycle with a reduced turbomachinery footprint relative to conventional power generation technologies. Resulting reduced capital costs are somewhat offset by the need to contain the high pressures, but combined with the high efficiencies, mature direct-fired sCO_2 power plants have the potential to be competitive with conventional combined cycle plants with CCS, on a cost of electricity (COE) basis. [1] [8]

1.2 Direct sCO_2 Cycle Literature Review

Allam and colleagues have extensively studied the direct sCO_2 cycle. [8] [9] [10] Commercialization of this technology is being aggressively pursued by NET Power, 8 Rivers

Capital, and their collaborators, who are building a 25 MWe demonstration plant in Laporte, Texas. In their natural gas-fired version of this cycle, their literature suggests that net plant thermal efficiencies of 53 percent (higher heating value [HHV]) are achievable [9] with near 100 percent carbon capture. [10] Under slightly different assumptions, Foster Wheeler's modeling of this system yields a plant thermal efficiency of 50 percent (HHV), with 90 percent carbon capture. [1] Southwest Research Institute has evaluated alternative natural gas-fired direct sCO_2 cycles with reported plant thermal efficiencies of 48 percent. [11]

For comparison, NETL analyses of baseline natural gas combined cycle (NGCC) plants with 90 percent carbon capture yield a plant efficiency of 45.7 percent on an HHV basis. [2] The referenced plant included a state-of-the-art 2013 F-Class gas turbine with a sub-critical steam cycle. CO_2 capture was effected by the Cansolv process. [12] The efficiency penalty to add CO_2 capture in the NGCC case is 5.8 absolute percent. This efficiency reduction is caused primarily by the auxiliary loads of the capture system and CO_2 compression, as well as the significantly increased cooling water requirement that increases the auxiliary load of the cooling water pumps and the cooling tower fan. CO_2 capture results in a 31 MW increase in auxiliary load compared to the non-capture case.

A coal-fired version of NET Power's direct sCO_2 cycle has also been developed, in which coal is first gasified and partially-cleaned before syngas is burned in the sCO_2 cycle combustor. [9] In their baseline system, an entrained flow, dry-fed, slagging gasifier with water quench is used, which produces a modeled net plant thermal efficiency of 47.8 percent (HHV) on bituminous coal. [13] Variations in gasifier type, coal type, and heat recovery processes yield a range of HHV efficiencies from 43.3 percent to 49.7 percent. [13] [4]

The Electric Power Research Institute (EPRI) has also studied a syngas-fired direct sCO_2 power plant utilizing coal gasification in a slagging, entrained flow gasifier. [3] The study includes Shell's dry-fed gasifier design, and a steam bottoming cycle powered by the syngas cooler's thermal input. Their study of the effects of oxygen purity and coal carrier gas on the purity of the CO_2 in the power cycle's turbomachinery concludes that high oxygen purity (99.5 percent) and CO_2 carrier gas are required to produce a storage-ready stream of at least 95 percent CO_2 purity for permanent sequestration. The highest plant thermal efficiency attained was 39.6 percent (HHV), with 99.2 percent CO_2 capture rate, compared to 31.1 percent plant efficiency with 87 percent CO_2 capture in their integrated gasification combined cycle (IGCC) reference plant. The COE with this plant was also estimated at 133 $/MWh, compared to 138 $/MWh for the IGCC plant with carbon capture, though significant uncertainty in the sCO_2 capital cost was noted. [3]

1.3 Report Structure

The objective of the present study is to develop a cost and performance baseline for a coal syngas-fueled, direct-fired sCO_2 power plant using coal gasification, and to analyze the sensitivity of its net thermal efficiency and cost indicators to variations in select operating parameter and cost assumptions. The report first discusses the design basis for the plant, followed by a discussion of the design choices made in the assembly of the preliminary plant design. Section 4 describes the system model development and evolution. This includes a

summary of the performance of this preliminary plant design, as well as several sensitivity analyses that were reported on at the 5th Supercritical CO_2 Power Cycles Symposium in March 2016. [14] The conference paper detailing these results is available in Appendix A, and is used as a starting point for the remaining analyses presented in this report.

This preliminary plant configuration was used to assess different physical property methods for use in modeling syngas-fired sCO_2 cycles, as summarized in Section 4.2, resulting in a change in property methods. Details of the physical property analysis are described in a 2017 Turbo Expo paper, [15] which is included in this report as Appendix B. Under the new physical property method, a turbine cooling model was developed, as discussed in Section 4.3, leading to new plant performance and sensitivity analyses as reported in Section 4.4.

A final plant configuration and its performance is presented in Section 5. This was used to develop a preliminary capital cost estimate for the plant, which is presented in Section 6. Combined, these results will be utilized in future studies to optimize the plant to achieve the minimum COE.

2 DESIGN BASIS

The design bases from NETL's Bituminous Baseline Study [16] and Quality Guidelines for Energy System Studies (QGESS) series [17] [18] [19] [20] [21] [22] [23] [24] were adopted so that the results from this study would be consistent with established results and comparable to existing studies carried out by NETL.

The following sections describe environmental operating conditions, coal feedstock properties, water use, method of economic evaluation, and descriptions of advanced technologies within DOE's research and development (R&D) portfolio.

2.1 SITE CHARACTERISTICS

All plants in this study are assumed to be located at a generic plant site in the midwestern United States, with ambient conditions and site characteristics as presented in Exhibit 2-1 and Exhibit 2-2. [21]

Exhibit 2-1 Site ambient conditions

Parameter	Value
Elevation, (ft)	0
Barometric Pressure, MPa (psia)	0.10 (14.696)
Design Ambient Temperature, Dry Bulb, °C (°F)	15 (59)
Design Ambient Temperature, Wet Bulb, °C (°F)	11 (51.5)
Design Ambient Relative Humidity, %	60
Cooling Water Temperature (from cooling tower), °C (°F)	15.6 (60)

Exhibit 2-2 Site characteristics

Parameter	Value
Location	Greenfield, Midwestern U.S.
Topography	Level
Size, acres	300
Transportation	Rail
Ash/Slag Disposal	Off Site
Water	Municipal (50%)/Groundwater (50%)
Access	Land locked, having access by rail and highway
CO_2 Transport and Storage	Compressed to 15.3 MPa (2,215 psia), transported 100 kilometers (62 miles) and stored in a representative saline formation in the Illinois Basin

The land area for all cases assumes that 300 acres are required for the plant proper; the balance provides a buffer of approximately 0.25 miles to the fence line. In all cases, the power island

turbo-machinery is assumed to be enclosed in a turbine building. Other site-specific design parameters are not quantified for this study. Allowances for normal site access conditions and construction are included in the cost estimates.

2.2 Coal Characteristics

Coal properties from NETL's QGESS are shown in Exhibit 2-3 for the bituminous coal used in this study. [22]

Exhibit 2-3 Bituminous design coal analysis

Rank	Bituminous		
Seam	Illinois No. 6 (Herrin)		
Sample location	Franklin Co., Illinois		
Proximate analysis	**Dry basis, wt%**	**As fed, wt%**	**As received, wt%**
Moisture	0.0	5.00	11.12
Ash	10.91	10.36	9.70
Volatile matter	39.37	37.41	34.99
Fixed carbon	49.72	47.23	44.19
Ultimate analysis	**Dry basis, wt%**	**As fed, wt%**	**As received, wt%**
Carbon	71.72	68.14	63.75
Hydrogen	5.06	4.81	4.50
Nitrogen	1.41	1.34	1.25
Sulfur	2.82	2.68	2.51
Chlorine	0.33	0.31	0.29
Ash	10.91	10.36	9.70
Moisture	0.00	5.00	11.12
Oxygen[1]	7.75	7.36	6.88
Heating value	**Dry basis**	**As fed**	**As received**
HHV, kJ/kg	30,506	28,981	27,113
HHV, Btu/lb	13,126	12,470	11,666
LHV, kJ/kg	29,544	28,019	26,151
LHV, Btu/lb	12,712	12,056	11,252

[1] By difference;

2.3 Raw Water Withdrawal and Consumption

A water balance was performed for each case based on the major water consumers in the process. The total water demand for each subsystem was determined, and internal recycle

water available from various sources, such as condensate from syngas, was applied to offset the water demand. The difference between demand and recycle is defined as raw water withdrawal. Raw water withdrawal (or raw water makeup) represents the water removed from the ground or diverted from a surface water source for use in the plant. Raw water consumption is defined as the portion of raw water withdrawn that is evaporated, transpired, incorporated into products, or otherwise not returned to the water source from which it was withdrawn.

Raw water makeup is assumed to be provided 50 percent by a publicly-owned treatment works (POTW) and 50 percent from groundwater.

2.4 CARBON DIOXIDE CAPTURE

The direct sCO_2 plant produces a high-pressure exhaust stream that is typically greater than 98 mol% CO_2. In most direct sCO_2 systems studies, this stream is "capture-ready" and sent to carbon storage as-is. [3] [4] [9] In the present study, this stream is first sent through a carbon purification unit (CPU) to eliminate impurities and produce CO_2 at pipeline purity specifications as set forth in the NETL QGESS. [23] This increases the plant cost and reduces efficiency somewhat, but maintains consistency with other NETL studies, which meet this CO_2 purity specification.

2.5 CAPACITY FACTOR

This study assumes that each new plant would be dispatched any time it is available and capable of generating maximum capacity when online. Therefore, capacity factor and availability are equal. The capacity factor for all cases in this study was 80 percent.

The addition of CO_2 capture and other advanced technology to each case is assumed to have no impact on the capacity factor. This assumption was made to enable a comparison based on the impact of capital and variable operating costs only. Otherwise, any differences in anticipated availability between the conventional and advanced technology cases would impact the COE for the advanced technology cases and obfuscate the contribution due to performance and economics of the advanced technology under investigation.

2.6 COST ESTIMATING METHODOLOGY

The estimating methodology for capital costs, operation and maintenance (O&M) costs, and CO_2 transport and storage (T&S) costs is described in the following sections. The finance structure, basis for the discounted cash flow analysis, and COE calculations are also summarized. Additional details are available in NETL's QGESS series. [17] [18] [24]

2.6.1 Capital Costs

As illustrated in Exhibit 2-4, this study reports capital cost at four levels: bare erected cost (BEC), total plant cost (TPC), total overnight cost (TOC), and total as-spent cost (TASC). BEC, TPC, and TOC are overnight costs and are expressed in base-year dollars. The base year is the

first year of capital expenditure, which for this study is assumed to be 2011. TASC is expressed in mixed-year, current-year dollars over the entire five-year capital expenditure period.

Exhibit 2-4 Capital cost levels and their elements

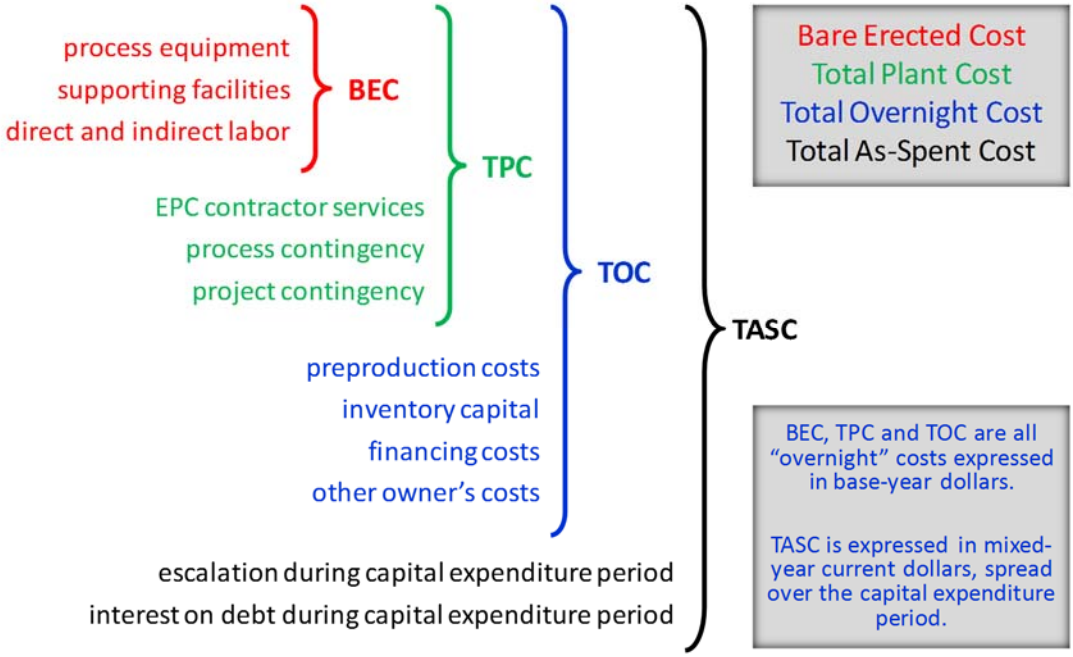

2.6.1.1 Cost Estimate Classification

As described in NETL's Bituminous Baseline Study, cost estimates for conventional configurations have an expected accuracy range of -15/+30 percent. [16] This accuracy range is consistent with the low side of a "Feasibility Study" (association for the Advancement of Cost Engineering International [AACE] Class 4). [25] NETL's pathway studies and other advanced technology assessments typically would be classified at the high (or more variable) end of the accuracy range for a Feasibility Study (-15/+50 percent) or low end of the accuracy range for a "Concept Screening" (Class 5, -20/+100 percent). The accuracy range depends on several factors given that the advanced technology cost and performance are based on a variety of sources (projections from pilot scale or preliminary lab data or from R&D goals or targets with minimal project definition). Given the present state of development for sCO_2 power cycles, and direct-fired sCO_2 cycles in particular, the cost estimate developed in this study is best described as a Class 4 Feasibility Study, with an estimated accuracy range of -15/+50 percent.

2.6.1.2 Technology Maturity

The cases examined in this study include technologies at different commercial maturity levels. To eliminate bias caused by the development status, the direct-fired sCO_2 plant is assumed to be "next-of-a-kind," just as the IGCC reference plant is categorized. As such, for common cost categories process and project contingencies were applied consistently, and process contingencies were estimated for non-commercial sCO_2 equipment items at similar magnitude as non-commercial IGCC equipment.

2.6.1.3 Contracting Strategy

Cost estimates are based on an engineering/procurement/construction management (EPCM) approach utilizing multiple subcontracts. This approach provides the Owner with greater control of the project while minimizing, if not eliminating, most of the risk premiums typically included in an engineer/procure/construct (EPC) contract price.

In a traditional lump sum EPC contract, the EPC contractor assumes all risk for performance, schedule, and cost. However, as a result of current market conditions, EPC contractors appear reluctant to assume that overall level of risk. Rather, the current trend appears to be a modified EPC approach where much of the risk remains with the Owner. Where contractors are willing to accept the risk in EPC type lump-sum arrangements, it is reflected in the project cost. In today's market, Contractor premiums for accepting these risks, particularly performance risk, can be substantial and increase the overall project costs dramatically.

The EPCM approach that is used as the basis for cost estimates in this study is anticipated to be the most cost effective approach for the Owner. While the Owner retains the cost and technology risks, those risks reduce with time as scope is better defined at the time of contract award(s). For this study, EPC fees are assumed to be 10 percent of the BEC, and include all home office engineering and procurement services, as well as field construction management costs.

2.6.1.4 Estimate Scope

Cost estimates in this study represent a complete power plant facility located on a generic site. The plant boundary limit is defined as the total plant facility within the "fence line," including coal receiving and water supply system, and terminating at the high voltage side of the main power transformers. CO_2 T&S cost is not included in the reported capital cost or O&M costs, but is calculated separately and added to the COE (see Section 2.6.3).

2.6.1.5 Capital Cost Assumptions

Capital and O&M costs are estimated using cost algorithms consistent with a conceptual level scope definition, which incorporates the following: 1) NETL Bituminous Baseline Study costs (estimated by WorleyParsons), 2) literature and/or vendor supplied costs, and 3) R&D target costs for advanced technologies. Plant size, number of process trains, sparing philosophy, and as much equipment-specific design as possible are incorporated into the cost algorithms.

For NETL's Bituminous Baseline Study, WorleyParsons developed capital cost estimates for each plant using the company's in-house database and conceptual estimating models for each of the specific technologies. This database and the respective models are maintained by WorleyParsons as part of a commercial power plant design base of experience for similar equipment in the company's range of power and process projects. A reference bottom-up estimate for each major component provides the basis for the estimating models.

2.6.1.6 Contingency

Process and project contingencies are included in cost estimates to account for unknown costs that are omitted or unforeseen due to a lack of complete project definition and engineering. Contingencies are added, because experience has shown that such costs are likely and

expected to be incurred even though they cannot be explicitly determined at the time the estimate is prepared.

Process contingency is intended to compensate for uncertainty in cost estimates caused by performance uncertainties associated with the development status of a technology. Process contingencies are applied to each equipment item or plant section based on its current technology development status.

AACE 16R-90 states that project contingency for a budget-type estimate (AACE Class 4 or 5) should be 15–30 percent of the sum of BEC, EPC fees, and process contingency. [25] This rule is used as a general guideline; however, some project contingency values occur below this range for very common, conventional technologies.

For consistency, process and project contingencies used in NETL's Bituminous Baseline Study form the basis for all major equipment in each plant section. As such, advanced technologies are assumed to embed expected costs in the BEC, when the advanced technology costs are based on R&D goals or targets. Any bottom-up cost estimates associated with advanced technologies include the appropriate level of contingency based on the completeness of the project definition and engineering before comparison is made to the R&D goals or targets used in this study for that advanced technology.

2.6.1.7 Owner's Costs

Exhibit 2-5 displays the method used to estimate Owner's costs. Interest and escalation during construction are not included as Owner's costs but are factored into the COE via the capital charge factor and are included in the TASC. Interest and escalation costs vary based on the capital expenditure period and the financing scenario (see Section 2.6.4.2).

Exhibit 2-5 Owner's costs included in TOC

Owner's Cost	Estimate Basis
Preproduction (Start-Up) Costs	• 6 months operating labor • 1-month maintenance materials at full capacity • 1-month non-fuel consumables at full capacity • 1-month waste disposal • 25% of one month's fuel cost at full capacity • 2% of TPC
Inventory Capital	• 0.5% of TPC for spare parts • 60-day supply (at full capacity) of fuel. Not applicable for natural gas • 60-day supply (at full capacity) of non-fuel consumables (e.g., chemicals and catalysts) that are stored on site. Does not include catalysts and adsorbents that are batch replacements, such as 1) water gas shift, carbonyl sulfide (COS), and selective catalytic reduction (SCR) catalysts, and 2) activated carbon
Land	• $3,000/acre (300 acres for all cases)
Financing Cost	• 2.7% of TPC

Owner's Cost	Estimate Basis
Other Owner's Costs	• 15% of TPC Significant deviation from this value is possible, because it is very site and owner specific. The lumped cost includes: - Preliminary feasibility studies, including a front-end engineering design study - Economic development (costs for incentivizing local collaboration and support) - Construction and/or improvement of roads and/or railroad spurs outside of site boundary - Legal fees - Permitting costs - Owner's engineering - Owner's contingency

2.6.2 O&M Costs

The operating costs and related maintenance expenses pertain to those charges associated with operating and maintaining a power plant over its expected life. There are two components to O&M costs: fixed O&M, which is independent of operating hours of power generation, and variable O&M, which is proportional to power generation.

2.6.2.1 Fixed O&M Costs

Fixed O&M costs are constant and are incurred whether or not the power plant is operating at any point in time. Fixed O&M costs are essentially a function of TPC.

- Operating Labor – The average base labor rate used to calculate annual labor cost is $39.70/hour. The associated labor burden is estimated at 30 percent of the base labor rate.
- Maintenance Labor – Maintenance labor cost is calculated from a correlation of maintenance labor cost (adjusted to 2011 dollars) as a function of TPC derived from prior NETL studies.
- Labor administration and Overhead Charges – These are assessed at a rate of 25 percent of the burdened O&M labor.
- Property Taxes and Insurance – Property taxes and insurance are assumed at 2 percent of the TPC.

2.6.2.2 Variable O&M Costs

Variable O&M costs used in this study are summarized in Exhibit 2-6 below.

Exhibit 2-6 Variable O&M parameters

Item	June 2011 Cost Basis
Bituminous Coal, $/MMBtu	2.9376
Bituminous Coal, $/ton	68.54
Water from POTW, $/1000 gal	1.67
Water Treatment Chemicals, $/lb	0.27
Activated Carbon, $/lb	1.63
COS Catalyst, $/$m^3$	3,751.70
Sulfinol Solvent, $/gal	10.05
Claus Catalyst, $/$ft^3$	203.15
Spent Mercury Catalyst Disposal, $/lb	0.65
Slag Disposal, $/ton	25.11
Sulfur Sales, $/ton	0

Consumables and Waste Disposal. The cost of consumables (including fuel) and waste disposal is determined based on individual rates of consumption/production, the unit cost of each specific commodity, and the plant annual operating hours.

Co-products and By-products. By-product quantities are determined in a manner similar to the consumables. However, due to the variable marketability of these by-products, no credit is taken for their potential salable value.

Maintenance Materials. Maintenance material cost is evaluated as a function of initial capital cost using an algorithm consistent with prior NETL studies. Maintenance materials consist primarily of the parts, supplies, and tools needed to perform scheduled major maintenance and overhauls on the major unit operations in the plant, particularly the prime movers. It also covers spare parts and supplies for unscheduled maintenance.

2.6.3 CO_2 Transport and Storage Costs

The cost of CO_2 T&S in a deep well saline formation is estimated using NETL's CO_2 Saline Storage Cost Model. Additional detail on development of these costs is available in the QGESS on Carbon Dioxide Transport and Storage Costs. [19]

CO_2 T&S costs are reported as first-year costs in $/tonne of CO_2, increasing at a nominal rate of 3 percent per year, consistent with the assumed general inflation rate. From the perspective of the CO_2 source (e.g., a power plant or other energy conversion facility), these costs are treated as a disposal cost for each tonne of CO_2 captured during the assumed 30-year operational period. From the pipeline and storage site's perspective, this cost represents the required revenue stream across the 30-year operational period to cover all costs and provide the required internal rate of return on equity (IRROE). All costs are reported in 2011 dollars.

CO_2 transport costs are based on a maximum daily flowrate of 11,000 tonnes/day through a generic 100 km (62 mile) dedicated pipeline. High-pressure (2,200 psig) CO_2 is provided at the plant gate of the energy conversion facility, and CO_2 exits the pipeline terminus at a pressure of 1,200 psig, remaining in a supercritical phase. The 12-inch pipe diameter is sized for transport using one boost recompression stage along the pipeline length. Transport costs are estimated to be $2.24/tonne CO_2.

Storage costs are based on NETL's CO_2 Saline Storage Cost Model. [26] This model provides detailed cost estimates for the injection and monitoring of CO_2 under United States (U.S.) Environmental Protection Agency regulations for Class VI injection wells, as well as monitoring and reporting requirements under Subpart RR of the Greenhouse Gas Reporting Rule.

The CO_2 Saline Storage Cost Model is used to determine storage costs in the Illinois Basin for a Midwestern plant location. Combined with CO_2 transport costs outlined above, the T&S costs are estimated at $11/tonne CO_2 for this study.

2.6.4 Finance Structure, Discounted Cash Flow Analysis, and COE

Global economic assumptions are listed in Exhibit 2-7. Finance structures (Exhibit 2-8) were chosen based on the assumed type of developer/owner (investor-owned utility [IOU] or independent power producer) and the assumed risk profile of the plant being assessed (low-risk or high-risk). For this study, the owner/developer is assumed to be an IOU. All sCO2 cases are considered to be high risk.

Exhibit 2-7 Global economic assumptions

Parameter	Value
Taxes	
Income Tax Rate	38% (Effective 34% Federal, 6% State)
Capital Depreciation	20 years, 150% declining balance
Investment Tax Credit	0%
Tax Holiday	0 years
Contracting and Financing Terms	
Contracting Strategy	EPCM (owner assumes project risks for performance, schedule, and cost)
Type of Debt Financing	Non-recourse (collateral that secures debt is limited to the real assets of the project)
Repayment Term of Debt	15 years
Grace Period on Debt Repayment	0 years
Debt Reserve Fund	None

Parameter	Value
Analysis Time Periods	
Capital Expenditure Period	5 years
Operational Period	30 years
Economic Analysis Period (used for IRROE)	35 years (capital expenditure period plus operational period)
Treatment of Capital Costs	
Capital Cost Escalation During Capital Expenditure Period (nominal annual rate)	3.6%
Distribution of Total Overnight Capital over the Capital Expenditure Period (before escalation)	10%, 30%, 25%, 20%, 15%
Working Capital	Zero for all parameters
% of Total Overnight Capital that is Depreciated	100%
Escalation of Operating Revenues and Costs	
Escalation of COE (revenue), O&M Costs, and Fuel Costs (nominal annual rate)	3.0%

Exhibit 2-8 Financial structure for IOU high risk and conventional projects

Type of Security	% of Total	Current (Nominal) Dollar Cost	Weighted Current (Nominal) Cost	After Tax Weighted Cost of Capital
Conventional				
Debt	50	4.5%	2.25%	-
Equity	50	12%	6%	-
Total	-	-	8.25%	7.39%
High Risk				
Debt	45	5.5%	2.475%	-
Equity	55	12%	6.6%	-
Total	-	-	9.075%	8.13%

2.6.4.1 Discounted Cash Flow Analysis and Cost of Electricity

NETL's Power Systems Financial Model (PSFM) is a nominal-dollar (current dollar) discounted cash flow (DCF) analysis tool. COE is the revenue received by the generator per net MWh during the power plant's first year of operation, *assuming that the COE escalates thereafter at a nominal annual rate equal to the general inflation rate, i.e., that it remains constant in real terms over the operational period of the power plant*. To calculate COE, the PSFM can be used to determine a base-year (2011) COE that, when escalated at an assumed nominal annual general

inflation rate of 3 percent, provides the stipulated IRROE over the entire economic analysis period (capital expenditure period plus 30 years of operation).

2.6.4.2 Estimating COE with Capital Charge Factors

For scenarios that adhere to the global economic assumptions listed in Exhibit 2-7 and utilize one of the finance structures listed in Exhibit 2-8, the following simplified equation can be used to estimate COE as a function of TOC, fixed O&M, variable O&M (including fuel), capacity factor, and net power output.

$$COE = \frac{\begin{matrix}first\ year \\ capital\ charge\end{matrix} + \begin{matrix}first\ year\ fixed \\ operating\ costs\end{matrix} + \begin{matrix}first\ year\ variable \\ operating\ costs\end{matrix}}{annual\ net\ megawatt\ hours\ generated}$$

$$COE = \frac{\{CCF\}\{TOC\} + OC_{FIX} + \{CF\}\{OC_{VAR}\}}{\{CF\}\{MWH\}}$$

where:

COE = revenue received by the generator ($/MWh, equivalent to mills/kWh) during the power plant's first year of operation (*but expressed in base-year dollars*), assuming that the COE escalates thereafter at a nominal annual rate equal to the general inflation rate, i.e., that it remains constant in real terms over the operational period of the power plant

CCF = capital charge factor taken from Exhibit 2-9 that matches the applicable finance structure and capital expenditure period

TOC = total overnight cost, *expressed in base-year dollars*

OC_{FIX} = the sum of all fixed annual operating costs, *expressed in base-year dollars*

OC_{VAR} = the sum of all variable annual operating costs, including fuel at 100 percent capacity factor, *expressed in base-year dollars*

CF = plant capacity factor, assumed to be constant over the operational period

MWH = annual net megawatt-hours of power generated at 100 percent capacity factor

The equation requires the application of one of the capital charge factors (CCF) listed in Exhibit 2-9. These CCFs are valid only for the global economic assumptions listed in Exhibit 2-7, the stated finance structure, and the stated capital expenditure period.

Exhibit 2-9 Capital charge factors for COE equation

Finance Structure	High Risk IOU	Conventional IOU
Capital Charge Factor (CCF)	0.124	0.116
5-Year TASC Multiplier	1.140	1.134

All factors in the COE equation are expressed in base-year dollars. The base year is the first year of capital expenditure, which for this study is assumed to be 2011. As shown in Exhibit 2-7, all factors (COE, O&M, and fuel) are assumed to escalate at a nominal annual general inflation rate of 3.0 percent. Accordingly, all first-year costs (COE and O&M) are equivalent to base-year costs when expressed in base-year (2011) dollars.

2.7 REFERENCE IGCC PLANT

A simplified block flow diagram (BFD) for an IGCC process based on the Shell gasifier with carbon capture is shown in Exhibit 2-10. This is used as a reference case for the current study, and is described in the Bituminous Baseline Study Rev 2b as Case B1B. [2]

Exhibit 2-10 IGCC reference plant block flow diagram

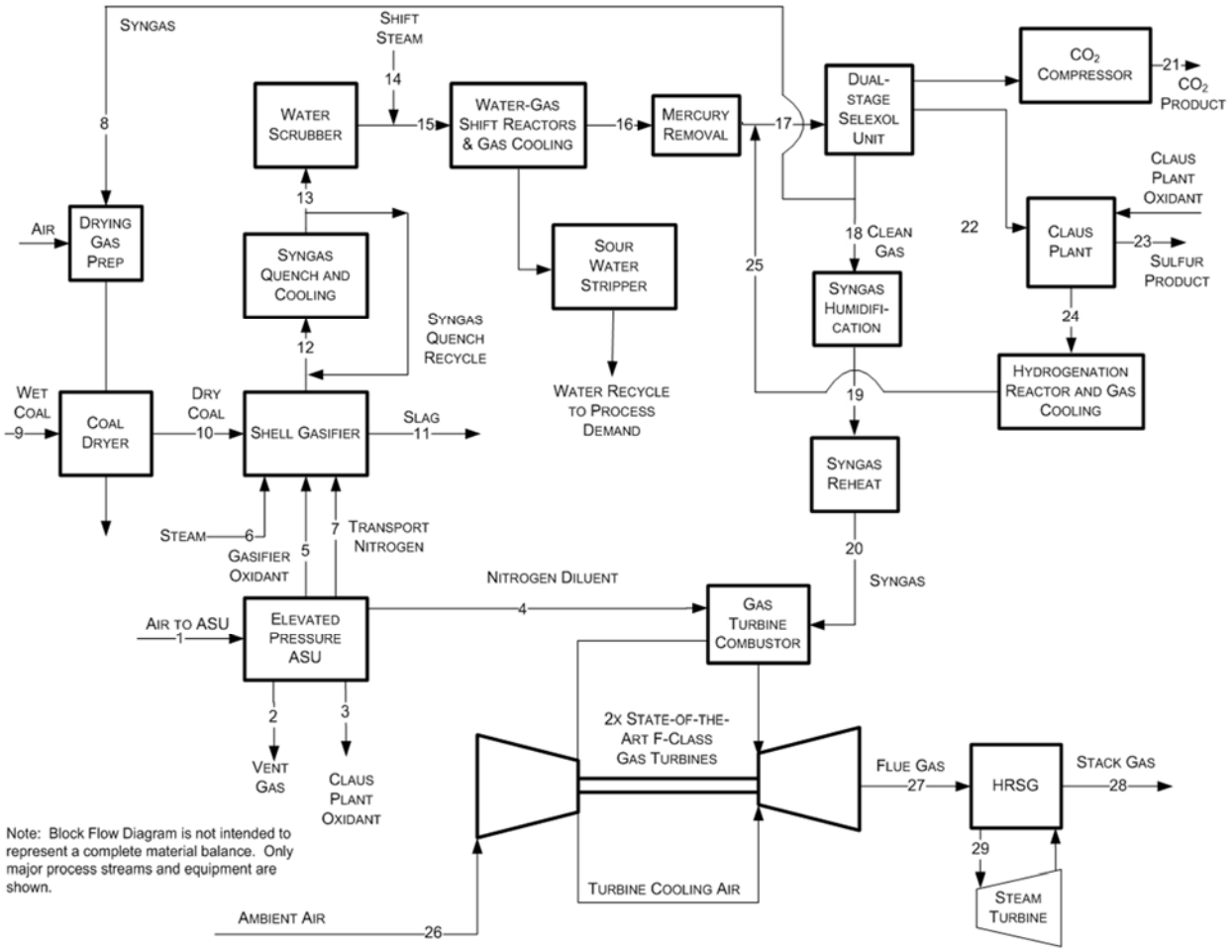

The gasifier island and gas cleanup sections in the IGCC are very similar to the corresponding sections in the coal-fired direct-fired sCO_2 power plant with a few notable differences. The IGCC plant utilizes an elevated pressure cryogenic air separation unit (ASU) designed to produce 95 percent purity oxygen and high-pressure nitrogen for use as a fuel diluent in the turbine. In the sCO_2 plant, the ASU is low pressure and is designed to produce 99.5 percent

purity oxygen to minimize argon and nitrogen contaminants in the sCO_2 cycle. Other systems studies have shown that the resulting reduction in CO_2 compression power due to higher sCO_2 purity more than offsets the increase in ASU power required to deliver higher purity oxygen to the cycle. [1] [3]

In the IGCC plant, decarbonization requires water gas shift reactors, which are located downstream of the syngas scrubber. The acid gas removal is a two-stage Selexol process that removes both H_2S and CO_2 as separate product streams. Finally, the IGCC plant uses nitrogen as the transport gas for the dry feed lock hopper system, whereas the sCO_2 plant uses CO_2 to improve sCO_2 purity and, hence, cycle performance. [3]

The IGCC plant's power island uses a combined cycle with two F-frame gas turbines operated on hydrogen-rich syngas and a single sub-critical Rankine bottoming cycle. The conventional hydrogen turbine has a firing temperature of 1137 °C, and a pressure ratio of 17.6. In the IGCC plant, there is further process integration with the use of byproduct nitrogen from the ASU as fuel gas diluent for power augmentation and NOx control in the gas turbine. [2]

While separate from the Reference case, the developed sCO_2 cycle will also be compared to cases from the Transformational Turbines Supplement to NETL's IGCC Pathway Study. [5] [27] This study considered the effects of hydrogen turbines and other advances on the performance and cost of an IGCC plant based on a General Electric (GE) gasifier with a radiant syngas cooler. This gasifier differs from the IGCC reference plant using the Shell gasifier in that the GE gasifier is slurry-fed while the Shell gasifier is dry-fed. In the Bituminous Baseline Study, this difference is shown to lead to different syngas compositions, which leads to changes in syngas cleanup requirements for the carbon capture cases, resulting in performance differences that must be accounted for in comparison to the sCO_2 plant. In the Transformational Turbines study, two hydrogen turbines were considered as replacements for the conventional hydrogen turbine: an Advanced Hydrogen Turbine (AHT) with a firing temperature of 1449 °C (2640 °F) and a pressure ratio of 23.8; and a Transformational Hydrogen Turbine (THT), with a firing temperature of 1704 °C (3100 °F) and a pressure ratio of 30.4. These cases are compared to the sCO_2 baseline plant in Section 7.

3 COAL-FIRED PLANT CONFIGURATION DEVELOPMENT

Exhibit 3-1 shows a table of potential gasification options to generate the syngas that will be used to fuel the direct-fired sCO_2 cycle. Although it is difficult to predict a priori which gasification technology is an optimal pairing with the direct sCO_2 cycle, the properties, requirements, and configurations for the gasification technologies can make them more or less advantageous in this service.

Exhibit 3-1 Gasification technology, coal rank, and gas cleaning options

Gasifier	Coal Type	Feed System	Coal Drying	Waste Heat Recovery	Comments
GE RGC	bituminous	water slurry	no	yes	WGCU, steam cycle or recuperation opportunities
GE QUENCH	bituminous	water slurry	no	no	conventional syngas cleaning
SHELL	bituminous subbituminous	lock hopper	yes	yes	WGCU, steam cycle or recuperation opportunities
SIEMENS	bituminous subbituminous	lock hopper	yes	no	conventional syngas cleaning
E-GAS (CB&I)	bituminous subbituminous	water slurry	no	yes	WGCU, steam cycle or recuperation opportunities
TRIG	subbituminous	lock hopper	yes	yes	WGCU, steam cycle or recuperation opportunities

3.1 CHOICE OF COAL

The direct sCO_2 cycle does not require a certain type of coal or coal properties and the choice of gasification technology strongly impacts the preference for coal type. The coal attributes that most strongly influence the efficiency of a direct sCO_2 power plant are heating value and moisture content. Thus, if all other factors are equal, bituminous coal is preferred. The choice of Illinois No. 6 bituminous coal allows for more direct comparisons of the proposed system to prior NETL systems analyses utilizing this as a reference fuel.

3.2 CHOICE OF GASIFIER

The gasifier list in Exhibit 3-1 is by no means comprehensive, but it does cover the range of gasifier types that have been the most commercially developed in the United States and for which good performance data are available. [2] [28] Factors that make the gasification technology preferable in this application are low auxiliary power and heat requirements (e.g., coal preparation and grinding or coal drying), high cold gas efficiency, and a configuration option for heat recovery from either raw or minimally quenched syngas. Another factor is whether the technology is amenable to utilizing advanced options for syngas cleaning that are currently being pursued in the DOE R&D portfolio. Overall, the Shell gasifier with syngas

coolers (SGCs) has most of the desired characteristics for pairing with a coal-fired direct-fired sCO_2 power plant, and is chosen for its high cold gas efficiency, low water usage, and low syngas hydrogen content.

3.3 Coal Dryer

The Shell gasifier employs a dry feed system utilizing lock hoppers to introduce coal across the pressure boundary into the gasifier. The coal is dried to 5 percent moisture to ensure uninterrupted flow through the lock hoppers. A slip stream of clean syngas is taken from downstream of the Sulfinol plant and combusted in air to provide the heat for drying. The combusted syngas, with an oxygen content of 6 vol%, is used to dry the coal in the coal mill.

3.4 Choice of Gas Clean-up

Multiple options are available for cleaning the syngas prior to combustion. Although advanced technology options for warm gas cleanup may offer a benefit to efficiency in this application, it was decided to use a commercially-available conventional technology. The efficiency benefits of warm-gas clean-up are offset by the need to compress the syngas to the high oxy-combustor pressure, which requires less auxiliary power for cold syngas resulting from conventional technologies. The chosen gas cleaning technology is Sulfinol, which is well-known and commercially-available.

An alternative to traditional syngas clean-up is promoted by NET Power for coal-fired direct sCO_2 plants, in which nitrogen- and sulfur-based syngas pollutants are removed with the water in the sCO_2 cycle. [9] [4] This eliminates the capital cost and efficiency losses associated with syngas cleaning, improving plant thermal efficiency by a reported 3 percentage points, [4] but requires special consideration of acid gas corrosion in the sCO_2 cycle. As this syngas cleanup technique requires additional development and validation, and increases the corrosion risk in the sCO_2 cycle, this approach is not considered in the present study.

3.5 Options for Thermal Integration

The choice of gasifier technology, gas cleanup technology, and other balance of plant (BOP) processes will impact the amount and quality of heat that can be effectively utilized in the sCO_2 cycle. The largest source of high-quality thermal energy available for heat integration is the high-temperature syngas cooler. In an IGCC plant, this is used to raise steam to generate power in a steam turbine bottoming cycle. A similar strategy is pursued in the direct sCO_2 EPRI study by Hume, [3] though the results show that only 5–7 percent of the gross plant power output is generated by the steam bottoming cycle.

In this study, a bottoming steam cycle was not considered to help reduce capital costs, though process steam is still raised in the syngas cooler, gasifier water wall, quench scrubber, and Claus unit. This steam is used as a process feed to the gasifier, and also supplies the process steam used in the ASU, Sulfinol reboiler, and sour water stripper reboiler.

Rather than raising steam with the additional heat available in the syngas cooler, other options for adding this heat to the direct sCO_2 cycle have been explored below, including preheating of

the syngas fuel streams and additional preheating of recycle sCO_2 to the oxy-combustor. Oxidant preheating was deemed to present a safety hazard in the syngas cooler, and was not considered. Other sources of waste heat that are utilized for various heating duties in the plant include the low-temperature syngas coolers, sour water stripper bottoms coolers, and the intercoolers for the syngas and gasifier oxygen compressors.

3.6 FINAL GASIFIER CONFIGURATION

The final gasifier technology option selected for this baseline case is a Shell gasifier with partial syngas quench using recycle syngas. The recycle syngas consists of approximately 32 percent of the syngas passing through the syngas coolers where it is cooled to approximately 241 °C (465 °F). The recycle syngas mixes with the raw syngas cooling it to 1093 °C (2000 °F). The partially quenched syngas transfers heat to cold sinks in the sCO_2 power cycle followed by additional syngas cooling to generate process steam. Additional details on the Shell gasifier modeling approach can be found in the NETL Bituminous Baseline Study. [2]

Oxygen for the gasifier, sCO_2 oxy-combustor, and Claus plant comes from a low-pressure cryogenic ASU. An oxygen purity of 99.5 percent is chosen to minimize nitrogen and argon impurities, which increase the required compression power in the sCO_2 cycle, thereby reducing cycle efficiency. [3] This is partially offset by the increase in ASU power requirement needed to produce high-purity oxygen and also increases the cost of the ASU. Modeling details for the ASU can be found in the NETL Bituminous Baseline Study. [2] Oxygen for the sCO_2 oxy-combustor is compressed in a four-stage compressor with three inter-coolers at an assumed isentropic efficiency of 85 percent. Intercooler stages assume an exit temperature 35 °C (95 °F) with water knock-out, and 69 kPa (10 psi) pressure drop per stage.

Desulfurization is done using a combination of Sulfinol and a Claus/Shell Claus Off-gas Treating (SCOT) unit. [2] Exhibit 3-2 shows a simplified BFD for the whole plant. Advanced heat integration options are not depicted.

The cleaned syngas leaving the Sulfinol unit is compressed to the combustor pressure in a two-stage compressor with a single inter-cooler and an assumed isentropic efficiency of 85 percent. The intercooler exit temperature is 35 °C (95 °F) with water knock-out, and assumes a 69 kPa (10 psi) pressure drop. Compressed syngas is preheated to 732 °C (1350 °F) in the syngas cooler, and enters the combustor along with oxygen and recycled working fluid.

The effluent from the combustor enters the CO_2 turbine and is expanded to a pressure that cools the working fluid sufficiently to enter the recuperator. An upper limit of 760 °C (1400 °F) was chosen for this location based on the high temperature and pressure limits of nickel-based alloys, which represent a major constraint on the system design. [10] The working fluid is cooled in the recuperator by heating the recycled CO_2. The cooled working fluid exiting the cold end of the recuperator undergoes further cooling to condense out water and undergo recompression. Most of this recompressed stream is recycled to the recuperator and then to the oxy-combustor. Most of the purged portion of the recompressed working fluid enters a CO_2 purification unit and that product stream is sent for sequestration. A portion of the purge stream is recycled to the gasifier lock hoppers as a transport gas, which is required to maintain sCO_2 purity and low compression power requirements. [3]

Exhibit 3-2 Simplified syngas-fueled sCO_2 cycle configuration

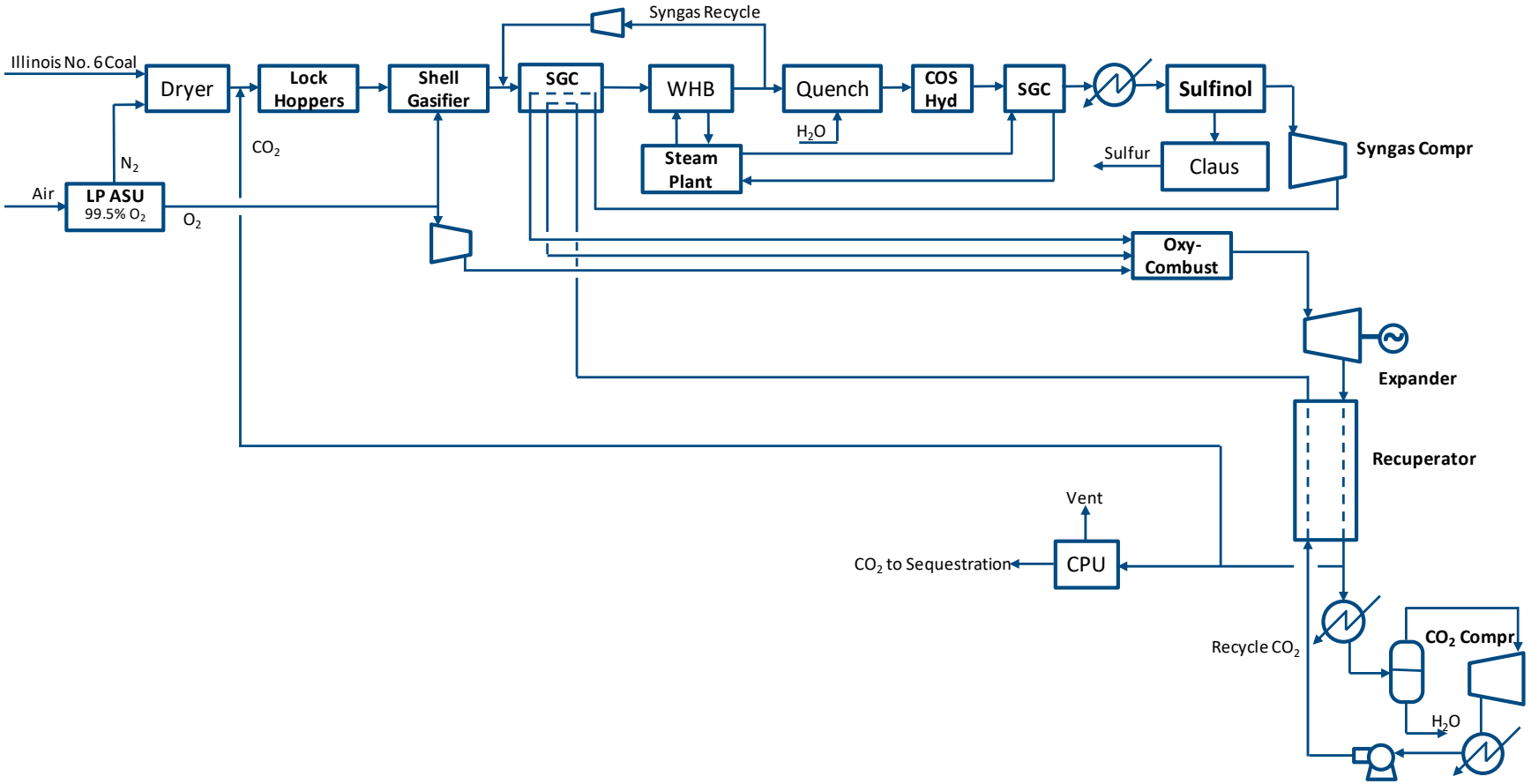

3.7 sCO_2 Brayton Cycle Options

Numerous configuration and state point options exist within the direct-fired sCO_2 power cycle. The following sections provide a brief discussion of the options and ramifications for their selection. Finally, a recommendation is made for an initial baseline plant.

3.7.1 Combustor

The primary design decisions for the combustor are exit temperature, amount of excess oxygen, whether to do staged combustion, and whether to preheat the feed streams. The combustor exit temperature has been set initially to 1149 °C (2100 °F) based on a review of similar studies in the literature. [1] [3] [9]

As the amount of excess oxygen in the combustor increases, the oxygen levels in the working fluid increase, which, in turn, increases the power requirement for recompression and negatively impacts process efficiency. However, if the excess oxygen is too low, incomplete combustion occurs, which also leads to the buildup of impurities (primarily CO) in the working fluid and a lower process efficiency. It was decided to use an excess oxygen of 1 percent relative to the amount required for complete combustion, and assume that the combustor could be designed to attain essentially complete conversion of the fuel. This assumption may be removed in future studies to assess the impact of incomplete combustion on cycle performance.

While a multi-stage combustor design has some advantages (comparable to reheating in a steam cycle), it was not considered in this Baseline study, because the added complexity to the model would not lead to a higher fidelity or more accurate result.

Generally preheating the feed streams to the combustor increases efficiency by reducing the amount of fuel required to attain a desired TIT. Consideration of preheating options was guided by the pinch analysis to determine whether the use of preheating is worthwhile.

3.7.2 sCO_2 Turbine

The primary design decisions for the sCO_2 turbine are TIT, pressure ratio, exit pressure, and whether to use reheat.

While cycle efficiency increases monotonically with TIT, real turbines require cooling to keep the blades at or below the maximum temperature for that material. The cooling requirement increases as the TIT increases and at some point, the cycle efficiency drops with an increase in TIT. It was decided to use 1149 °C (2100 °F) as the TIT in the initial study and perform a sensitivity analysis over the range 1149–1204 °C (2100–2200 °F), as discussed in Section 4.4.5.

Most prior analyses used a turbine PR in the range of 8–10 with exit pressure (P_{exit}) below the critical pressure, P_c. The PR must be sufficient to cool the turbine exhaust to a temperature that can be used in the recuperator. It was decided to initially use a PR of 10 and perform a sensitivity analysis on PR and P_{exit} to determine optimum values, as discussed in Section 4.4.6.

While reheating has been employed to improve efficiency in other power cycles, it is not thermodynamically beneficial to pursue reheating with the present cycle configuration, and thus was not employed in this study. Reheating in this context would involve partial expansion to an intermediate pressure in the turbine, followed by a second combustor and expansion in a lower pressure turbine. For a constant overall pressure ratio and a limitation on the turbine exhaust temperature entering the recuperator, the use of multistage combustion requires a lower exhaust temperature at the outlet of each combustor stage relative to a single stage combustor. This serves to lower the average temperature of heat addition relative to the non-reheated case, which thermodynamically results in a less efficient cycle. Further, the addition of a reheat stage would partially negate an advantage of the CO_2 turbine by having relatively small size.

3.7.3 Recuperator

The primary design decisions for the recuperator are the target effectiveness, maximum temperature, and whether to integrate other process heating/cooling with the recuperator.

In general, increasing the recuperator effectiveness increases the sCO_2 Brayton cycle efficiency by increasing the amount of thermal recuperation of the turbine's exhaust. Generally, the limiting factor is the cold end minimum temperature approach, although in some configurations, the pinch point occurs in the recuperator interior. For the initial configuration described in Appendix A, a minimum temperature approach of 10 °C (18 °F) was selected. This arbitrary value was based on prior NETL sensitivity studies that did not include quantitative cost estimation. A more definitive economic optimization to determine the minimum approach temperature is planned for future work.

As the maximum allowable recuperator temperature increases, the cycle efficiency increases, but the materials needed for high-temperature service at elevated pressures are very expensive. It was decided to limit the maximum recuperator temperature to 760 °C (1400 °F) for the initial Baseline configuration.

In some applications, it is possible to increase the recuperator effectiveness and the cycle efficiency by transferring process heat into the cold end of the recuperator. [9] [10] This is the region where the cold side thermal capacitance typically exceeds the hot side thermal capacitance due to the increase in heat capacity of CO_2 near its critical point. Supplemental heating applied in this region would increase the recuperator effectiveness and increase the amount of heat that can be utilized in the cycle. Although supplemental recuperator heating was not used in this study, future work will evaluate whether it is advantageous in this application.

3.7.4 CO_2 Cooler/Condenser

Condensing the working fluid at the main cooler has the advantage of reducing the power requirement to recompress the working fluid. However, this may require impractically low cooler temperatures, even when very high-purity oxygen with little excess is used.

The attainable cold sCO_2 temperature used in this study is determined as follows. For the design basis Midwest location (Exhibit 2-1), the cooling water temperature at the exit of the cooling tower is 15.6 °C (60 °F), and the allowable temperature rise is 11 °C (20 °F). [21] In a counterflow water/sCO_2 condenser arrangement, the pinch point at the CO_2 saturated vapor conditions is about midway through the heat exchanger, since some cooling of the sCO_2 entering the hot side of the condenser is required to attain a saturated vapor state. Assuming then that half of the allowable cooling water temperature rise is associated with condensation of the CO_2, the cooling water temperature at the pinch point is 21.1 °C (70 °F). For liquid-liquid heat exchange in a shell and tube heat exchanger, a 5.5 °C (10 °F) approach temperature can be assumed. [21] Assuming that a cooler can be designed to this approach temperature for water/sCO_2, similar to 10 °C or less approach temperatures in sCO_2/sCO_2 recuperators, this results in a cold CO_2 temperature of 26.7 °C (80 °F), which is used throughout the study. Cold CO_2 temperatures assumed in other studies include 29.4 °C (85 °F) [3] and 20 °C (68 °F). [10] Given the range of possible cold sCO_2 temperatures, a sensitivity analysis was performed to determine if further cooling of the CO_2 is advantageous, as discussed in Section 4.4.3.

4 MODEL DEVELOPMENT AND EVOLUTION

4.1 INITIAL BASELINE PERFORMANCE RESULTS AND SENSITIVITY ANALYSES

Appendix A presents the performance results for the initial baseline case. The net plant efficiency of this initial baseline was high, especially when compared to the reference IGCC plant. However, the design variables for the sCO_2 cycle configuration were not optimized and a series of sensitivity analyses were performed to determine if further improvements could be achieved. The results of these sensitivity analyses are also shown in Appendix A. The sensitivity analysis to turbine exit pressure showed that the efficiency could be increased by lowering the turbine exit pressure from the initial setting. The sensitivity analyses to compressor pressure and turbine inlet pressure showed that the efficiency increases monotonically with both design variables. The sensitivity analysis to cooler pressure showed that the initial design point cooler pressure yielded the maximum efficiency and nearly the maximum specific power. The sensitivity analysis to cooler temperature showed that the efficiency varies inversely with cooler temperature with a sharp increase in efficiency occurring at a cooler temperature below 30 °C (86 °F). As would be expected, efficiency decreases with increasing cycle pressure drop and minimum approach temperature and the sensitivity analyses shown in Appendix A quantify this impact for the initial cycle design. The sensitivity analysis on the percentage of excess oxygen fed to the combustor showed that both process efficiency and specific power drop approximately 0.01 percentage point for every 1 percentage point increase in the excess oxygen, up to 5 percent.

4.2 PHYSICAL PROPERTY METHOD ASSESSMENT

Accurate modeling of sCO_2 power cycles requires high accuracy in determining the physical properties of CO_2, particularly near its critical point of 31 °C (88 °F) and 7.37 MPa (1069 psi). The Span-Wagner equation of state (EOS) is the most accurate property method available for processes consisting of pure CO_2. [29] The Span-Wagner EOS is incorporated into the REFPROP physical property method developed by the National Institute of Standards and Technology (NIST), [30] and is used by most researchers in modeling indirect sCO_2 power cycles. For a direct-fired sCO_2 power cycle, however, the working fluid is not pure CO_2 and it changes composition at various points in the cycle. Unfortunately, there is a limited set of mixtures available for which REFPROP can be reliably used and there are several species present in a coal-fired direct-fired sCO_2 cycle that REFPROP cannot handle. Even with a relatively simplified system with the trace components eliminated, simulations made using REFPROP required excessive computation times and are infeasible. A series of comparative analyses were performed to identify the best physical property method in Aspen Plus® (Aspen) to use for direct-fired sCO_2 cycles, as described in Appendix B.

The results of that study indicated that the LK-PLOCK property method, based on the Lee-Kesler-Plöcker EOS, was the most accurate method to use for the coal-fueled direct-fired sCO_2 power plant analyses. This prompted a change from the PR-BM property method, used in the preliminary analysis of Appendix A, to the LK-PLOCK property method, used in the remainder

of this study. This result is consistent with the conclusion from the previous NETL study CO_2 Compressor Simulation User Manual [31] on CO_2 compression modeling.

4.3 CO_2 TURBINE MODEL WITH BLADE COOLING

The CO_2 turbine entrance temperature in the baseline case is 1149 °C (2100 °F). Conventional combustion turbines require blade cooling at temperatures this high; this is also expected to be the case with the direct-fired sCO_2 cycle. Several effects can be expected when blade cooling is introduced to the process model including 1) a significant drop in process efficiency for non-regenerative cooling, 2) a modest drop in process efficiency for regenerative cooling, 3) a shift in the optimum sCO_2 cycle state point, 4) a change in turbine exit temperature, and 5) a change in mass flow distribution through the turbine. In addition, it may be necessary to re-examine the process heat integration scheme. Finally, as TIT increases and additional cooling flow is required, a maximum in process efficiency is likely to occur.

The literature on direct-fired sCO_2 cycles was reviewed and two reports were identified where blade cooling was included and the approach discussed. In *Regen-SCOT: Rocket Engine-Derived High Efficiency Turbomachinery for Electric Power Generation*, [32] the system analyzed was a direct-fired natural gas oxy-fired sCO_2 Brayton cycle with a steam Rankine bottoming cycle. The turbine cooling systems considered included both regenerative (working fluid) and non-regenerative (steam) cooling; however, the sCO_2 TIT and exhaust temperature used were over 150 °C higher than those used in the present study. Although a turbine cooling data correlation could be derived, its predictive accuracy was deemed low due to the disparity in sCO_2 turbine conditions, thus this study was not used.

To develop a turbine cooling model, data was taken from chapter D.2 of the International Energy Agency Greenhouse Gas R&D Programme (IEAGHG) report, *Oxy-combustion Turbine Power Plants,* [1] a performance assessment of the NET Power cycle. The sCO_2 cycle conditions were a good match for the baseline case. Only non-regenerative (open loop) cooling was used. The process flow diagram and stream table were adequate to determine the blade cooling stream flows. Data were provided for three TITs of 1100 °C (2012 °F), 1150 °C (2102 °F), and 1200 °C (2192 °F). Although specifics of the model implementation and cooling flow distribution between stages were not described in the report, the results correlated well and a reasonable approach for determining the cooling flow distribution was developed as discussed below.

To accommodate turbine blade cooling, a number of revisions were made to the preliminary Aspen turbine model: 1) the CO_2 turbine model was revised to have seven stages, 2) the pressure ratio for each turbine stage was made approximately equal, 3) the recuperator was split into a LTR and a HTR with the LTR cold side exit temperature set to a cooling bleed temperature of 399 °C (750 °F) [1] [33] the LTR cold side exit stream was split into multiple cooling bleeds (one for each cooled turbine stage) with the remainder entering the HTR, and 5) the cooling bleed streams were mixed with the working fluid exiting each turbine stage.

A piecewise continuous spline correlation, based on the IEAGHG report data, was derived for the total cooling bleed flow required, as a fraction of turbine inlet flow, as shown in Exhibit 4-1. The cooling bleed flow to each stage was based on the temperature of the stream entering the

stage, T_n, where the ratio of cooling bleed at stage *n+1* to the cooling bleed at stage *n* was set equal to $(T_{n+1} - T_{max}) / (T_n - T_{max})$. Based on the correlation in Exhibit 4-1, T_{max} is 860 °C (1580 °F), and no cooling was used if the temperature of the stream entering a turbine stage was less than 860 °C (1580 °F). This is consistent with the IEAGHG report, in which a maximum metal temperature of 860 °C (1580 °F) was considered. [1] Based on this analysis, only the first five turbine stages are cooled in the Aspen model of the sCO_2 turbine. This is roughly consistent with the direct sCO_2 turbine developed by Toshiba, in which the first four stages of the seven-stage turbine are cooled. [34]

Exhibit 4-1 Cooling bleed as a function of turbine inlet temperature

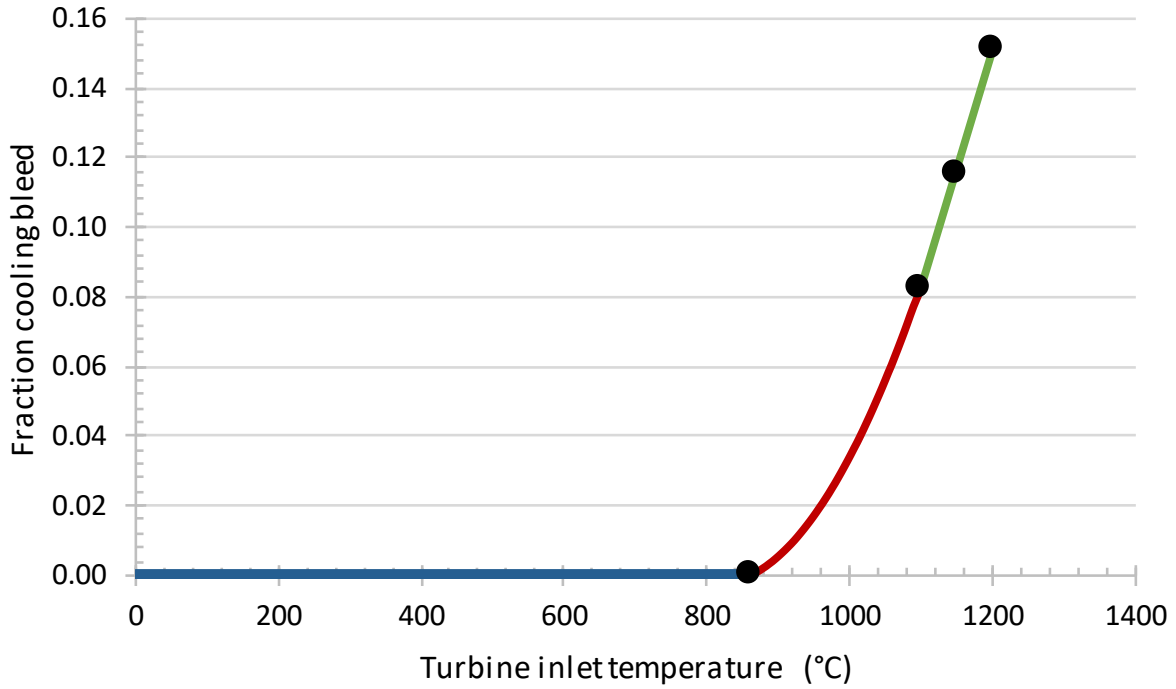

The approach employed here is largely empirical, based on the results from the IEAGHG model. A physical sCO_2 turbine blade cooling model is currently under development, and will be used in future analyses of direct sCO_2 systems to improve model accuracy.

4.4 Process Analysis and Sensitivity Analyses

Utilizing the preliminary plant design from *Performance baseline for direct-fired sCO_2 cycles* [14] (shown in Appendix A) with the LK-PLOCK property method and the turbine cooling model described in Section 4.3, a revised plant design was modeled in Aspen to better represent the actual conditions likely to be present in a syngas-fired direct sCO_2 cycle. Sensitivity analyses were performed on this revised model as discussed in the sub-sections below, to optimize the revised model for overall performance. Based on these results, a final plant design is presented in Section 5.

4.4.1 Sensitivity to Pre-compressor Intercooling

A sensitivity analysis was performed on the number of stages used for the pre-compressor under the assumption that intercoolers would cool the working fluid to the same temperature as the CO_2 cooler (26.7 °C) between each compressor stage. A 1.38 kPa (2 psia) pressure drop was assumed for each intercooler [35] and the pressure ratio was kept approximately equal for each compressor stage. No adjustment was made to the compressor isentropic efficiency. Exhibit 4-2 shows a plot of the pre-compressor power as a function of the number of compressor stages. As expected, the compressor power decreases as the number of stages increases and the compression comes closer to becoming isothermal. However, the rate of decrease in compressor power drops off rapidly after 3–4 stages.

Exhibit 4-3 shows a plot of overall process efficiency and specific power as a function of the number of pre-compressor stages. The qualitative behavior of the process efficiency and specific power is just opposite of that for the compressor power as both efficiency and specific power increase with the number of compressor stages but at an ever-diminishing rate.

Although the choice of the number of compressor stages is ultimately an economic optimization, an initial selection of four compressor stages was made based on performance results.

Exhibit 4-2 Pre-compressor power as a function of the number of compressor stages

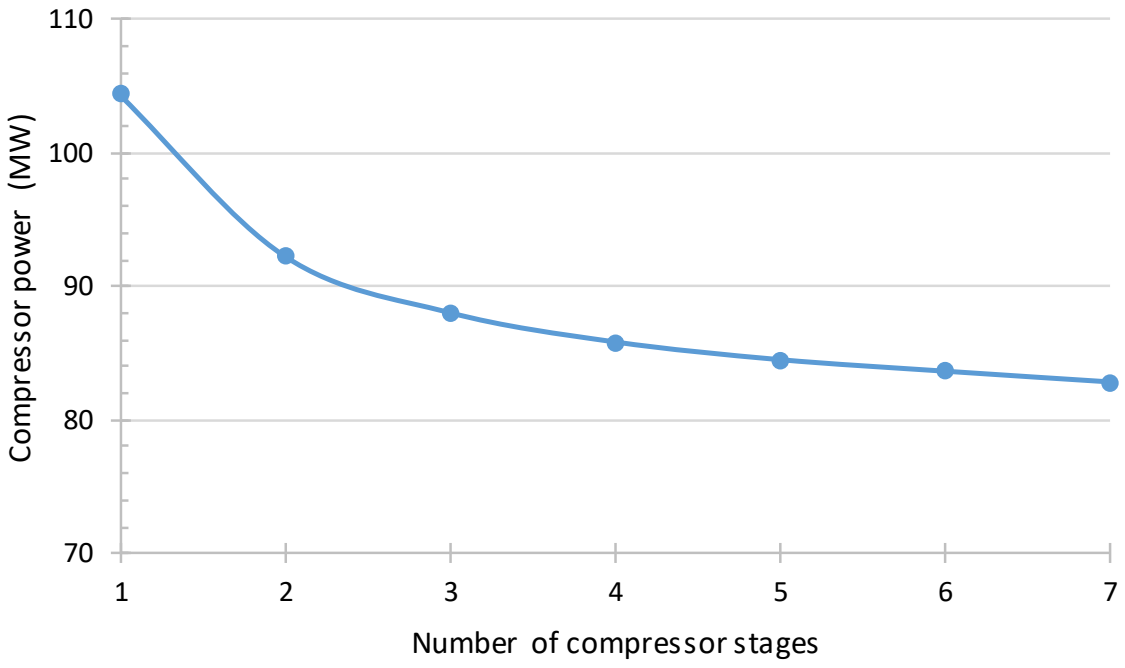

Exhibit 4-3 Process efficiency and specific power as a function of the number of compressor stages

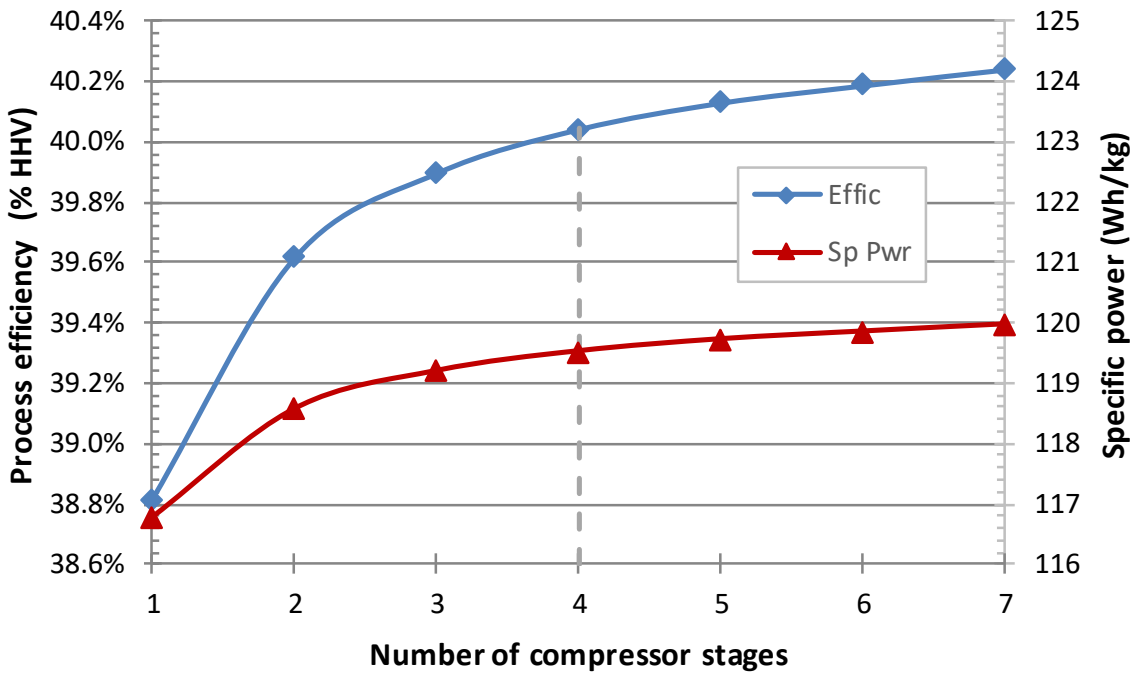

4.4.2 Sensitivity to Pump Intercooling

An analogous sensitivity analysis to the pre-compressor intercooling sensitivity analysis was performed on the pump. As with the pre-compressor, intercooling to the CO_2 cooler temperature was used with an assumed intercooler pressure drop of 1.38 kPa (2 psia) per intercooler. No adjustment was made to the pump efficiency. Exhibit 4-4 shows a plot of overall process efficiency and specific power as a function of the number of pump stages. The magnitude of the sensitivity of process efficiency and specific power to the number of stages is significantly less than was observed with the pre-compressor. Because of this low sensitivity and the fact that process efficiency is adversely impacted with more than two pump stages, the initial process configuration used contained a single pump stage with no cooling.

Exhibit 4-4 Process efficiency and specific power as a function of the number of pump stages

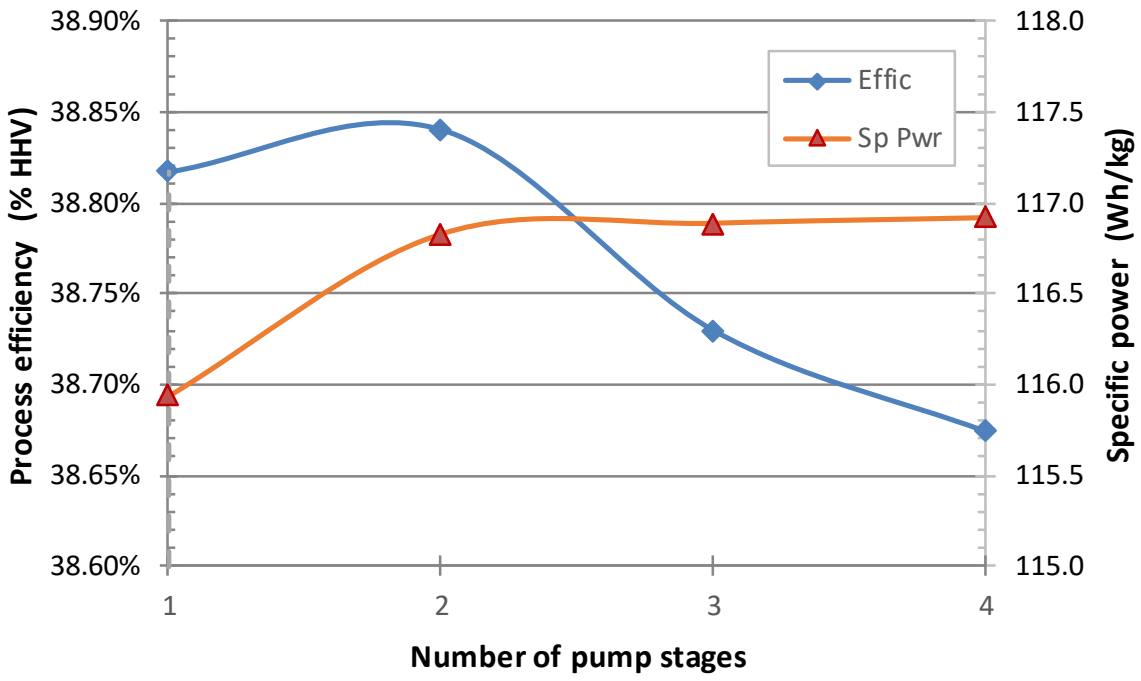

4.4.3 Sensitivity to Cooler Temperature and Pressure

In *Performance baseline for direct-fired sCO2 cycles* [14] (shown in Appendix A), sensitivity analyses were run on the cooler temperature and pressure separately. In this sensitivity analysis, the temperature and pressure were varied simultaneously. It is expected that there will be a relationship observed between pressure at maximum process efficiency and the saturation pressure at a given cooler temperature. The sensitivity analysis to pressure was run at six cooler temperatures: 21.1, 23.9, 25.6, 26.7, 27.8, 29.4 °C (70, 75, 78, 80, 82, and 85 °F) and the point of maximum efficiency identified. Exhibit 4-5 plots the maximum process efficiency versus the cooler temperature. Also shown is the calculated specific power, which is the net plant power output divided by the maximum sCO_2 cycle flowrate, i.e., the flowrate exiting the turbine. The results indicate that there is considerable benefit to be realized if the cooler temperature can be lowered. The achievable cold sCO_2 temperature is limited by the temperature of the coolant or ambient conditions at the cold sink, however, and is set to 26.7 °C in the current study per the discussion in Section 3.7.4. Optimal cooler pressures largely follow the CO_2 saturation pressure down to 25.6 °C (78 °F), and deviate to lower optimal pressures as cooling temperature further decreases, yielding only partial condensation of the CO_2 within the cooler.

Exhibit 4-5 Sensitivity of process efficiency to cooler temperature

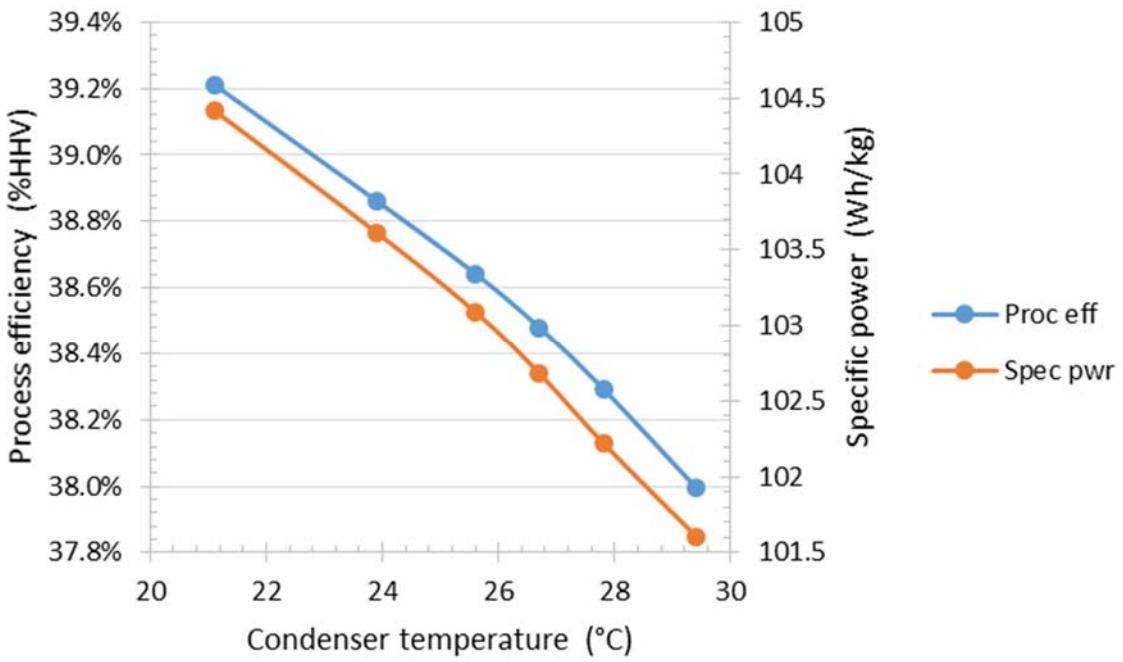

4.4.4 Assessment of Moving the Oxygen Injection Point to the sCO_2 Pump Outlet

In the preliminary studies, the oxygen feed from the ASU was fed directly to the sCO_2 combustor, though other studies have suggested that this stream can be premixed with recycle sCO_2 prior to entering the cold side of the recuperator to gain an efficiency advantage by preheating the oxygen. [1] [36] In the present system model, the expected impacts of inserting the oxygen just after the pump are 1) an increase in the thermal capacitance on the cold side of the recuperator due to increased mass flow, which leads to a decrease in recuperator effectiveness and an increased driving force in the recuperator; 2) an increase in the extent of oxygen preheating before the combustor, which leads to an increase in working fluid flow rate and cycle output and an increase in cycle efficiency; 3) creation of an oxygen bypass to the combustor via the turbine cooling flow, which leads to an increase in oxygen concentration in the working fluid and an increase in the oxygen make-up requirement; and 4) an increase in the concentration of N_2, O_2, and Ar in the working fluid, which leads to a lower cooler temperature to attain condensation and introduces the need for a O_2 compressor after cooler to preserve recuperator effectiveness. Exhibit 4-6 compares the summary performance results for the baseline case compared to a case with a modified oxygen insertion point.

Exhibit 4-6 Comparison of baseline and modified oxygen insertion point cases

sCO_2 Cycle Results	Original O_2 Insertion	Modified O_2 Insertion
Recuperator effectiveness	0.928	0.910
Recuperator LMTD °C (°F)	27.7 (49.9)	31.2 (56.2)
CO_2 flow rate to turbine (kg/hr)	6,712,223	6,770,282
Net cycle output (kWe)	775,627	778,657
O_2 mole fraction in purge	0.00049	0.0059
O_2 make-up flow rate (kg/hr)	241,052	243,099
Process efficiency (% HHV)	38.86	39.04

The CO_2 cooler temperature had to be lowered to 23.9 °C (75 °F) to attain complete condensation. The overall process efficiency increases 0.18 percentage points compared to the baseline case with the same cooler temperature; however, the oxygen bypass via the turbine cooling flow is likely to increase plant capital costs due to increased ASU capacity and oxygen scrubbing requirements in the CPU. As a result, movement of the oxygen injection point was not incorporated into the final plant configuration in this study, though given its potential benefits, future studies will consider alternative oxygen preheating schemes to optimize the plant's COE.

4.4.5 Sensitivity to Increased Turbine Inlet Temperature

The final baseline case configuration with blade cooling was run at a TIT of 1204 °C (2200 °F), as opposed to the initial TIT of 1149 °C (2100 °F). This is adjusted by reducing the recycle CO_2 flow to the combustor. The required cooling bleed increases from ~11.5 percent to ~15 percent, per the turbine blade cooling model discussed in Section 4.3. [1] There was no change in the number of turbine stages requiring cooling. The higher TIT resulted in a more even distribution of coolant amongst stages. The turbine exit temperature was estimated to be 761 °C (1402 °F) and the overall process efficiency was 38.89 percent (0.5 percentage point increase). Exhibit 4-7 compares the overall system performance at the two TITs.

Exhibit 4-7 System performance sensitivity to turbine inlet temperature

Item	Turbine Inlet Temperature	
	1149 °C	1204 °C
Gross Power (kWe)	769,240	776,003
Net Auxiliary Load (kWe)	-195,524	-195,978
Net Plant Power (kWe)	573,716	580,025
Net Plant Efficiency (HHV, %)	38.4	38.9
Cooling Duty (kW_t)	-554,000	-485,000
Coal Feed Flowrate (kg/hr)	198,060	198,060
Thermal Input (kW_t)	1,492,815	1,492,815
Oxygen Flowrate (kg/hr)	391,224	391,243

4.4.6 Sensitivity to Turbine Exit Pressure

Sensitivity of the cycle performance to turbine exit pressure was previously analyzed in the preliminary studies (see Appendix A) with a maximum temperature constraint of 1149 °C (2100 °F) applied at the turbine inlet. Given the improved system performance shown in Section 4.4.5 for a TIT of 1204 °C (2200 °F), as well as the capability to model the effects of turbine cooling flows absent in the preliminary studies, the sensitivity analysis on turbine exit pressure was repeated for the 1204 °C TIT case. The results are shown in Exhibit 4-8. The turbine exit pressure was varied from 3.0 MPa (435 psia) to 3.83 MPa (550 psia). As the turbine exit pressure increases, so does the turbine exit temperature. Over the range of turbine exit pressures examined, the turbine exit temperature ranged from 725 °C (1337 °F) to 760 °C (1400 °F). The maximum turbine exit temperature was limited to 760 °C so the maximum turbine exit pressure was limited to 3.83 MPa.

The specific power decreases significantly and monotonically as the turbine exit pressure increases, whereas the process efficiency passes through a maximum at a turbine exit pressure of 3.55 MPa (515 psia), and is minimally impacted by turbine exit pressure. It should be noted that in the region of turbine exit pressures between 3.45 and 3.83 MPa (500 and 555 psia), the process efficiency curve is quite flat and other factors, such as cost, may lead to the selection of an alternate state point for the cycle, though 3.55 MPa (515 psia, shown as a dashed line in Exhibit 4-8) is chosen for the final plant design.

Exhibit 4-8 Sensitivity of process efficiency to turbine exit pressure

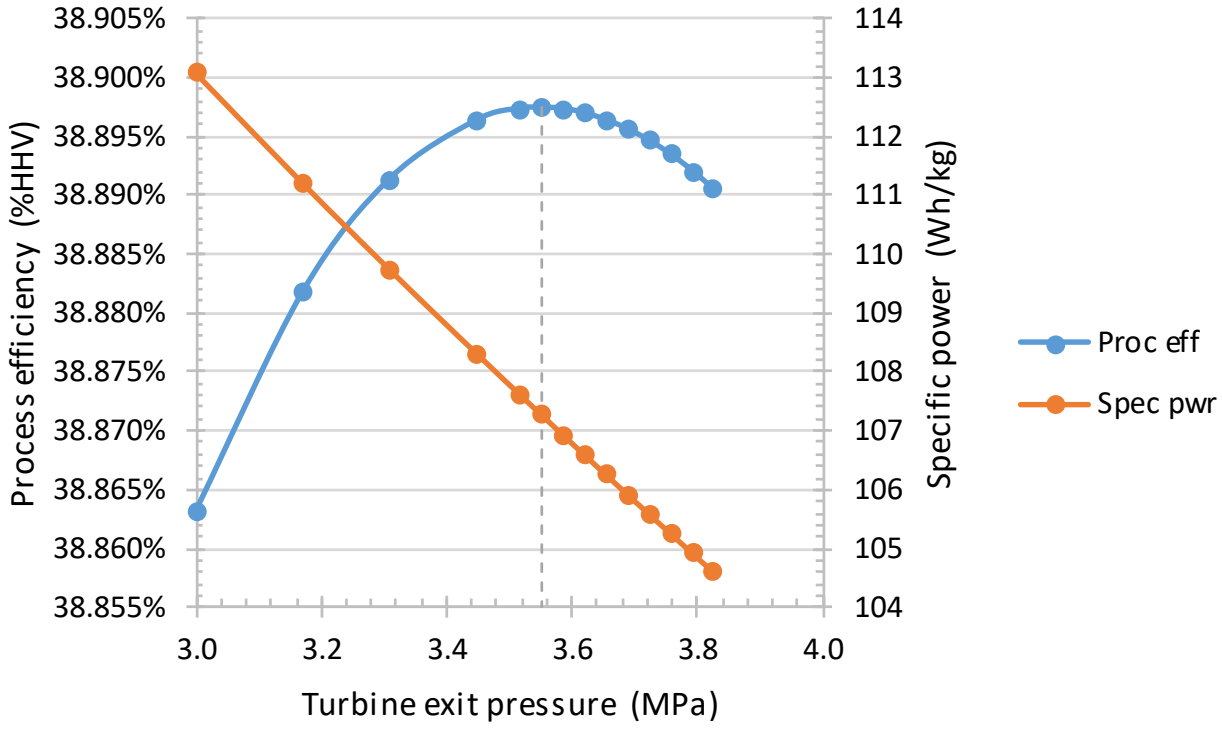

4.4.7 Effect of Eliminating High-Temperature sCO_2 Heating in the Syngas Cooler

In the baseline configuration, high-pressure recycle sCO_2 exiting the HTR is heated further in the syngas cooler prior to injection into the sCO_2 oxy-combustor. This helps recover more heat from the gasification process, but may be very expensive to implement due to the high cost of nickel alloy materials required for the piping runs and syngas heat exchanger. The total thermal input to the process is 1,493 MWt and for the baseline case, the high temperature syngas/sCO_2 heater duty is 49.8 MWt (3.3 percent). If this SGC duty is not recovered, the drop in plant thermal efficiency is approximately 1.8 percentage points. This is analogous (but different magnitude) to the 2.9 percentage point plant efficiency drop in the GE IGCC with quench compared to the GE IGCC with radiant cooler. [2] This heat exchanger has been retained in the final plant design so that its costs can be estimated, enabling a determination of its effect on COE as discussed in Section 6.3.2.

5 FINAL BASELINE COAL-FIRED DIRECT-FIRED sCO_2 POWER PLANT

5.1 FINAL PLANT CONFIGURATION

Based on the results of the model enhancements and sensitivity analyses discussed in the above sections, the preliminary cycle design (shown in Appendix A) [14] was revised to the final recommended plant configuration. To summarize, major changes from the preliminary cycle model, as well as their effects on its net thermal efficiency, include:

1. A change to the Lee-Kessler-Plöcker EOS (LKPLOCK property method) for evaluating the sCO_2 cycle (+0.45 percentage points thermal efficiency)
2. Addition of a turbine blade cooling model (-1.4 percentage points)
3. Addition of three stages of compressor intercooling (+1.2 percentage points)
4. Increasing the TIT from 1149 °C to 1204 °C (+0.5 percentage points)
5. Increasing the turbine exit pressure from 30 to 35.5 bars (+0.03 percentage points)

Final operating point variables are shown in Exhibit 5-1; Exhibit 5-2 shows a simplified process flow diagram for the final process; Exhibit 5-3 shows the detailed stream table for the streams identified in Exhibit 5-2. Note that there is closure in the material balances in Exhibit 5-2 and Exhibit 5-3, though energy balances cannot be calculated from this information, as steam heating and cooling processes are not included to improve clarity.

Exhibit 5-1 Final baseline sCO_2 power cycle configuration

Section	Parameter	Final Baseline
Combustor	O_2 purity	99.5%
	Excess O_2	1%
	Stages	1
	Pressure drop	689 kPa
	Preheating	None
Expander	Inlet temp	1204 °C (2200 °F)
	PR, P_{exit}	8.4, 3.55 MPa
	Blade Cooling	15.0%
Recuperator	Extent	Maximum
	Max temp	750 °C (1382 °F)
	Min T_{app}	10 °C (18 °F)
CO_2 cooler	Cooler/condenser	26.7 °C (80 °F)
	Cooling source	Cooling tower
Recompression	CO_2 bypass	None
CO_2 pressurization	Compr/pump	Compr (7.4 MPa)/pump (30.8 MPa)
CPU	Presence	H_2O condenser, deoxy
	Impurities	H_2O, O_2, Ar, N_2, HCl, SO_2
	Streams	Working fluid/Seq CO_2

Exhibit 5-2 Process flow diagram for coal-fired direct-fired sCO₂ power plant

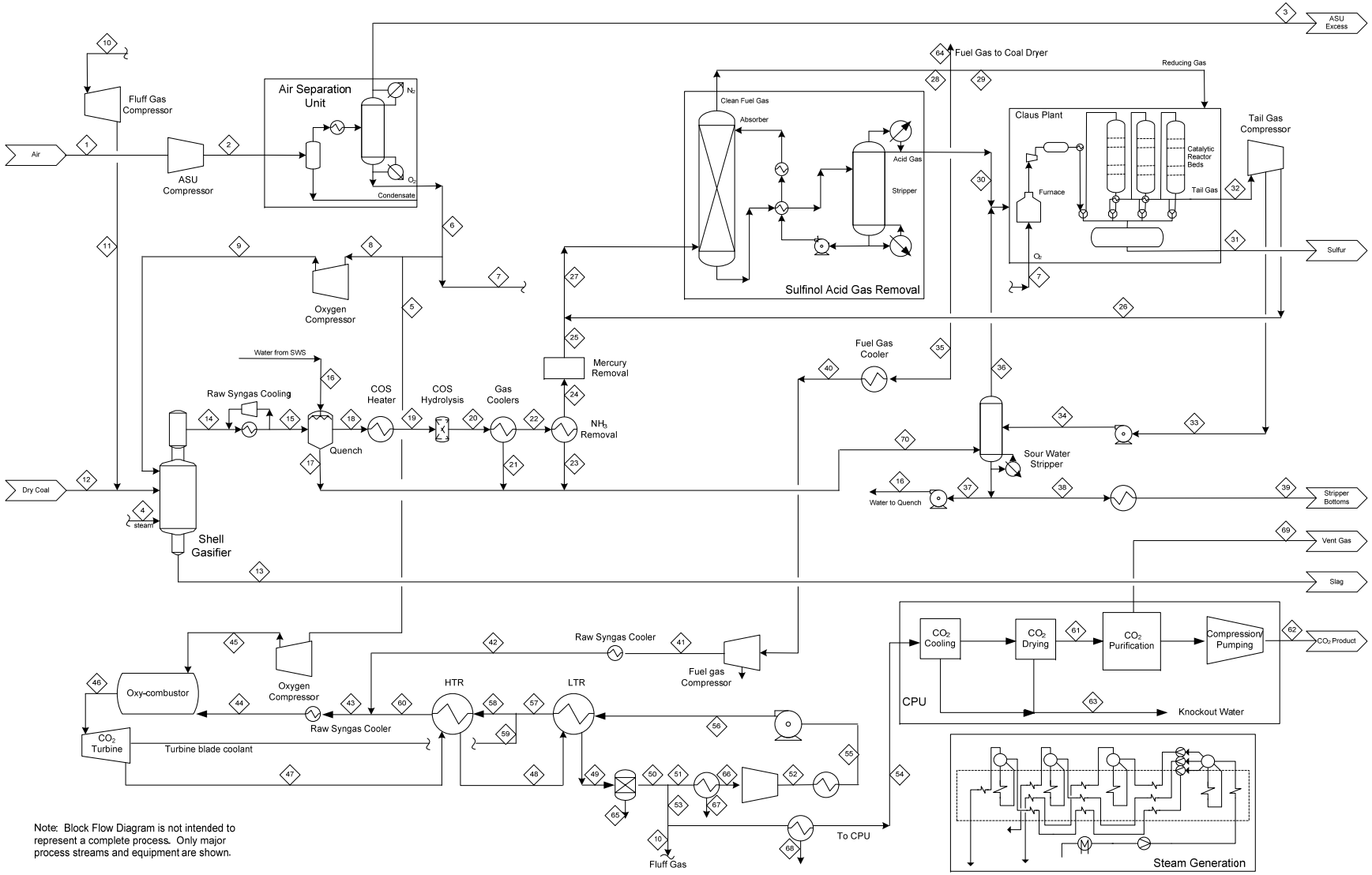

Exhibit 5-3 Stream table for coal-fired direct-fired sCO_2 power plant

Stream	1	2	3	4	5	6	7	8	9	10	11	12	13	14	15
V-L Mole Fraction															
CO_2	0.0003	0.0003	0.0004	0	0	0	0	0	0	0.9718	0.9718	0	0	0.0400	0.0400
H_2O	0.0099	0.0099	0.0125	1.0000	0	0	0	0	0	0.0136	0.0136	0	0	0.0590	0.0590
Ar	0.0092	0.0092	0.0105	0	0.0044	0.0044	0.0044	0.0044	0.0044	0.0050	0.0050	0	0	0.0015	0.0015
O_2	0.2074	0.2074	0.0015	0	0.9950	0.9950	0.9950	0.9950	0.9950	0.0005	0.0005	0	0	0	0
N_2	0.7732	0.7732	0.9751	0	0.0006	0.0006	0.0006	0.0006	0.0006	0.0090	0.0090	0	0	0.0055	0.0055
CO	0	0	0	0	0	0	0	0	0	0	0	0	0	0.6221	0.6221
CH_4	0	0	0	0	0	0	0	0	0	0	0	0	0	0.0001	0.0001
H_2	0	0	0	0	0	0	0	0	0	0	0	0	0	0.2612	0.2612
COS	0	0	0	0	0	0	0	0	0	0	0	0	0	0.0009	0.0009
H_2S	0	0	0	0	0	0	0	0	0	0	0	0	0	0.0082	0.0082
HCl	0	0	0	0	0	0	0	0	0	0	0	0	0	0.0010	0.0010
NH_3	0	0	0	0	0	0	0	0	0	0	0	0	0	0.0007	0.0007
SO_2	0	0	0	0	0	0	0	0	0	0	0	0	0	0	0
S_8	0	0	0	0	0	0	0	0	0	0	0	0	0	0	0
Total	1.0000	1.0000	1.0000	1.0000	1.0000	1.0000	1.0000	1.0000	1.0000	1.0000	1.0000	0	0	1.0000	1.0000
V-L Flow rate (kg_{mole}/hr)	58,945	58,945	46,731	720	7,527	12,214	98	4,590	4,590	948	948	0	0	17,162	17,162
V-L Flow rate (kg/hr)	1,700,975	1,700,975	1,309,733	12,972	241,106	391,242	3,124	147,013	147,013	41,213	41,213	0	0	366,665	366,664
Solids Flow rate (kg/hr)	0	0	0	0	0	0	0	0	0	0	0	185,303	19,837	0	0
Temperature (°C)	15	38	8	332	19	19	33	19	301	76	121	60	1455	1455	241
Pressure (MPa, abs)	0.10	0.46	0.10	5.79	0.11	0.11	0.86	0.11	5.10	3.45	5.62	0.10	4.24	4.24	3.96
Steam Table Enthalpy (kJ/kg)*	30.23	52.31	19.64	3,121.38	16.46	16.39	29.44	16.39	284.71	54.38	90.46	---	---	2,409.72	462.66
AspenPlus Enthalpy (kJ/kg)**	-97.57	-75.49	-139.51	-12,829.82	-6.37	-6.43	6.61	-6.43	261.89	-8,850.88	-8,814.79	-1,105.17	1,716.19	-2,390.51	-4,337.56
Density (kg/m^3)	1.2	5.1	1.2	20.7	1.4	1.4	10.9	1.4	34.2	57.8	83.3	---	---	6.3	19.8
V-L Molecular Weight	28.857	28.857	28.027	18.015	32.031	32.031	32.031	32.031	32.031	43.485	43.485	---	---	21.365	21.365
V-L Flow rate (lb_{mole}/hr)	129,949	129,949	103,022	1,587	16,594	26,928	215	10,118	10,118	2,089	2,089	0	0	37,836	37,836
V-L Flow rate (lb/hr)	3,749,945	3,749,945	2,887,417	28,599	531,538	862,527	6,886	324,103	324,103	90,858	90,858	0	0	808,344	808,341
Solids Flow rate (lb/hr)	0	0	0	0	0	0	0	0	0	0	0	408,517	43,732	0	0
Temperature (°F)	59	100	45	629	65	65	90	65	573	168	250	140	2650	2650	465
Pressure (psia)	14.7	66.7	14.7	840.0	15.9	15.9	125.0	15.9	740.0	500.0	814.7	14.7	614.7	614.7	574.7
Steam Table Enthalpy (Btu/lb)*	13.0	22.5	8.4	1,342.0	7.1	7.0	12.7	7.0	122.4	23.4	38.9	---	---	1,036.1	198.9
AspenPlus Enthalpy (Btu/lb)**	-42.0	-32.5	-60.0	-5,516.2	-2.7	-2.8	2.8	-2.8	112.6	-3,805.5	-3,789.9	-475.2	737.9	-1,027.8	-1,864.9
Density (lb/ft^3)	0.076	0.321	0.076	1.296	0.091	0.091	0.679	0.091	2.138	3.612	5.201	---	---	0.394	1.237

* - Steam Table Reference conditions are 32.02°F & 0.089 psia

** - Aspen Plus thermodynamic reference state is the component's constituent elements in an ideal gas state at 25°C and 1 atm

Exhibit 5-3 Stream table for coal-fired direct-fired sCO_2 power plant (continued)

Stream	16	17	18	19	20	21	22	23	24	25	26	27	28	29	30
V-L Mole Fraction															
CO_2	0	0.0002	0.0366	0.0366	0.0374	0.0004	0.0430	0.0006	0.0433	0.0433	0.7865	0.0507	0.0444	0.0444	0.3991
H_2O	0.9994	0.9976	0.1381	0.1381	0.1373	0.9958	0.0070	0.8726	0.0016	0.0016	0.0017	0.0016	0.0014	0.0014	0.0087
Ar	0	0	0.0013	0.0013	0.0013	0	0.0015	0	0.0015	0.0015	0.0030	0.0016	0.0016	0.0016	0.0001
O_2	0	0	0	0	0	0	0	0	0	0	0	0	0	0	0
N_2	0	0	0.0050	0.0050	0.0050	0	0.0058	0	0.0058	0.0058	0.0780	0.0065	0.0063	0.0063	0.0184
CO	0	0.0002	0.5702	0.5702	0.5702	0.0003	0.6567	0.0003	0.6608	0.6608	0.0920	0.6551	0.6665	0.6665	0.0243
CH_4	0	0	0.0001	0.0001	0.0001	0	0.0001	0	0.0001	0.0001	0	0.0001	0.0001	0.0001	0
H_2	0	0.0001	0.2394	0.2394	0.2394	0.0001	0.2757	0.0001	0.2774	0.2774	0.0193	0.2748	0.2796	0.2796	0.0111
COS	0	0	0.0008	0.0008	0	0	0	0	0	0	0	0	0	0	0
H_2S	0	0.0001	0.0074	0.0074	0.0082	0.0003	0.0094	0.0004	0.0095	0.0095	0.0191	0.0096	0	0	0.5382
HCl	0	0.0014	0.0003	0.0003	0.0003	0.0011	0.0001	0.0226	0	0	0.0003	0	0	0	0
NH_3	0.0006	0.0003	0.0008	0.0008	0.0008	0.0019	0.0006	0.1033	0	0	0	0	0	0	0
SO_2	0	0	0	0	0	0	0	0	0	0	0	0	0	0	0
S_8	0	0	0	0	0	0	0	0	0	0	0	0	0	0	0
Total	1.0000	1.0000	1.0000	1.0000	1.0000	1.0000	1.0000	1.0000	1.0000	1.0000	1.0000	1.0000	1.0000	1.0000	1.0000
V-L Flow rate (kg_{mole}/hr)	9,662	8,103	18,721	18,721	18,721	2,466	16,255	102	16,153	16,153	164	16,317	16,027	23	290
V-L Flow rate (kg/hr)	174,050	146,227	394,486	394,486	394,486	44,518	349,968	1,868	348,100	348,100	6,592	354,692	343,868	485	10,824
Solids Flow rate (kg/hr)	0	0	0	0	0	0	0	0	0	0	0	0	0	0	0
Temperature (°C)	171	155	155	233	233	70	66	23	35	35	38	35	43	43	40
Pressure (MPa, abs)	4.24	3.89	3.89	3.86	3.79	3.65	3.65	3.62	3.62	3.62	3.86	3.62	3.60	3.60	3.62
Steam Table Enthalpy (kJ/kg)*	752.03	665.35	515.20	628.63	628.09	269.11	104.34	5.14	50.95	50.95	35.02	50.53	60.75	60.75	40.05
AspenPlus Enthalpy (kJ/kg)**	-15,191.46	-15,233.21	-5,087.61	-4,974.18	-4,974.18	-15,606.67	-4,191.08	-14,049.34	-4,192.09	-4,192.09	-7,954.89	-4,262.14	-4,240.61	-4,240.61	-4,632.04
Density (kg/m^3)	838.2	856.6	23.1	19.4	19.0	948.3	27.9	954.3	30.4	30.4	60.0	30.7	29.4	29.4	52.2
V-L Molecular Weight	18.015	18.047	21.072	21.072	21.072	18.050	21.530	18.356	21.550	21.550	40.231	21.738	21.456	21.456	37.289
V-L Flow rate (lb_{mole}/hr)	21,300	17,863	41,272	41,272	41,272	5,437	35,835	224	35,611	35,611	361	35,972	35,332	50	640
V-L Flow rate (lb/hr)	383,708	322,370	869,679	869,679	869,679	98,144	771,535	4,119	767,416	767,416	14,533	781,949	758,087	1,070	23,862
Solids Flow rate (lb/hr)	0	0	0	0	0	0	0	0	0	0	0	0	0	0	0
Temperature (°F)	339	311	311	450	451	157	150	73	95	95	100	95	108	108	104
Pressure (psia)	615.0	564.7	564.7	559.7	549.7	529.7	529.7	524.7	524.7	524.7	559.5	524.7	521.7	521.7	524.7
Steam Table Enthalpy (Btu/lb)*	323.3	286.1	221.5	270.3	270.0	115.7	44.9	2.2	21.9	21.9	15.1	21.7	26.1	26.1	17.2
AspenPlus Enthalpy (Btu/lb)**	-6,531.6	-6,549.5	-2,187.4	-2,138.7	-2,138.7	-6,710.1	-1,802.0	-6,040.5	-1,802.4	-1,802.4	-3,420.2	-1,832.5	-1,823.3	-1,823.3	-1,991.6
Density (lb/ft^3)	52.327	53.480	1.440	1.208	1.185	59.205	1.743	59.578	1.900	1.900	3.748	1.917	1.837	1.837	3.257

* - Steam Table Reference conditions are 32.02°F & 0.089 psia

** - Aspen Plus thermodynamic reference state is the component's constituent elements in an ideal gas state at 25°C and 1 atm

Exhibit 5-3 Stream table for coal-fired direct-fired sCO_2 power plant (continued)

Stream	31	32	33	34	35	36	37	38	39	40	41	42	43	44	45
V-L Mole Fraction															
CO_2	0	0.3470	0.0013	0.0013	0.0444	0.0591	0	0	0	0.0444	0.0444	0.0444	0.8822	0.8822	0
H_2O	0	0.5595	0.9981	0.9981	0.0014	0.4839	0.9982	0.9982	0.9982	0.0014	0.0014	0.0014	0.0013	0.0013	0
Ar	0	0.0013	0	0	0.0016	0.0002	0	0	0	0.0016	0.0016	0.0016	0.0047	0.0047	0.0044
O_2	0	0	0	0	0	0	0	0	0	0	0	0	0.0005	0.0005	0.9950
N_2	0	0.0343	0	0	0.0063	0.0004	0	0	0	0.0063	0.0063	0.0063	0.0088	0.0088	0.0006
CO	0	0.0405	0	0	0.6665	0.0613	0	0	0	0.6665	0.6665	0.6665	0.0722	0.0722	0
CH_4	0	0	0	0	0.0001	0	0	0	0	0.0001	0.0001	0.0001	0	0	0
H_2	0	0.0085	0	0	0.2796	0.0333	0	0	0	0.2796	0.2796	0.2796	0.0303	0.0303	0
COS	0	0	0	0	0	0	0	0	0	0	0	0	0	0	0
H_2S	0	0.0085	0.0001	0.0001	0	0.0353	0	0	0	0	0	0	0	0	0
HCl	0	0.0004	0.0005	0.0005	0	0.0033	0.0015	0.0015	0.0015	0	0	0	0	0	0
NH_3	0	0	0	0	0	0.3231	0.0003	0.0003	0.0003	0	0	0	0	0	0
SO_2	0	0	0	0	0	0	0	0	0	0	0	0	0	0	0
S_8	1.0000	0	0	0	0	0	0	0	0	0	0	0	0	0	0
Total	1.0000	1.0000	1.0000	1.0000	1.0000	1.0000	1.0000	1.0000	1.0000	1.0000	1.0000	1.0000	1.0000	1.0000	1.0000
V-L Flow rate (kg_{mole}/hr)	19	373	209	209	15,809	45	9,673	1,161	1,161	15,809	15,809	15,809	145,920	145,920	7,527
V-L Flow rate (kg/hr)	4,959	10,367	3,768	3,768	339,210	894	174,535	20,952	20,952	339,210	339,210	339,210	6,038,535	6,038,535	241,106
Solids Flow rate (kg/hr)	0	0	0	0	0	0	0	0	0	0	0	0	0	0	0
Temperature (°C)	160	171	38	39	43	124	170	170	66	33	170	708	707	733	146
Pressure (MPa, abs)	0.43	0.32	0.32	1.03	3.60	0.45	0.79	0.79	0.79	3.56	30.82	30.70	30.70	30.68	30.89
Steam Table Enthalpy (kJ/kg)*	9,544.28	1,117.56	142.26	144.72	60.75	1,299.94	745.83	745.83	255.30	46.89	234.18	1,054.77	762.89	796.77	110.28
AspenPlus Enthalpy (kJ/kg)**	477.66	-9,751.94	-15,769.79	-15,767.34	-4,240.61	-7,993.40	-15,160.37	-15,160.37	-15,650.90	-4,254.47	-4,067.32	-3,246.73	-7,848.44	-7,814.56	87.46
Density (kg/m^3)	30.9	2.4	981.8	981.2	29.4	2.7	839.3	839.3	953.6	30.1	154.4	73.3	142.0	138.3	262.2
V-L Molecular Weight	256.528	27.821	18.060	18.060	21.456	19.953	18.043	18.043	18.043	21.456	21.456	21.456	41.382	41.382	32.031
V-L Flow rate (lb_{mole}/hr)	43	822	460	460	34,853	99	21,326	2,560	2,560	34,853	34,853	34,853	321,693	321,693	16,594
V-L Flow rate (lb/hr)	10,933	22,855	8,306	8,306	747,817	1,970	384,778	46,191	46,191	747,817	747,817	747,817	13,312,468	13,312,468	531,538
Solids Flow rate (lb/hr)	0	0	0	0	0	0	0	0	0	0	0	0	0	0	0
Temperature (°F)	320	339	100	101	108	255	338	338	150	90	337	1306	1303	1350	295
Pressure (psia)	63.0	46.5	46.5	150.0	521.7	65.0	115.0	115.0	115.0	516.7	4,470.0	4,452.0	4,452.0	4,450.0	4,480.0
Steam Table Enthalpy (Btu/lb)*	4,103.6	480.5	61.2	62.2	26.1	558.9	320.7	320.7	109.8	20.2	100.7	453.5	328.0	342.6	47.4
AspenPlus Enthalpy (Btu/lb)**	205.4	-4,192.9	-6,780.3	-6,779.2	-1,823.3	-3,436.8	-6,518.2	-6,518.2	-6,729.1	-1,829.2	-1,748.8	-1,395.9	-3,374.5	-3,359.9	37.6
Density (lb/ft^3)	1.932	0.151	61.294	61.256	1.837	0.169	52.396	52.396	59.534	1.880	9.640	4.578	8.866	8.631	16.371

* - Steam Table Reference conditions are 32.02°F & 0.089 psia

** - Aspen Plus thermodynamic reference state is the component's constituent elements in an ideal gas state at 25°C and 1 atm

Exhibit 5-3 Stream table for coal-fired direct-fired sCO_2 power plant (continued)

Stream	46	47	48	49	50	51	52	53	54	55	56	57	58	59	60
V-L Mole Fraction															
CO_2	0.9541	0.9580	0.9580	0.9580	0.9718	0.9718	0.9839	0.9718	0.9830	0.9839	0.9839	0.9839	0.9839	0.9839	0.9839
H_2O	0.0316	0.0276	0.0276	0.0276	0.0136	0.0136	0.0013	0.0136	0.0022	0.0013	0.0013	0.0013	0.0013	0.0013	0.0013
Ar	0.0049	0.0050	0.0050	0.0050	0.0050	0.0050	0.0051	0.0050	0.0051	0.0051	0.0051	0.0051	0.0051	0.0051	0.0051
O_2	0.0005	0.0005	0.0005	0.0005	0.0005	0.0005	0.0005	0.0005	0.0005	0.0005	0.0005	0.0005	0.0005	0.0005	0.0005
N_2	0.0089	0.0089	0.0089	0.0089	0.0090	0.0090	0.0091	0.0090	0.0091	0.0091	0.0091	0.0091	0.0091	0.0091	0.0091
CO	0	0	0	0	0	0	0	0	0	0	0	0	0	0	0
CH_4	0	0	0	0	0	0	0	0	0	0	0	0	0	0	0
H_2	0	0	0	0	0	0	0	0	0	0	0	0	0	0	0
COS	0	0	0	0	0	0	0	0	0	0	0	0	0	0	0
H_2S	0	0	0	0	0	0	0	0	0	0	0	0	0	0	0
HCl	0	0	0	0	0	0	0	0	0	0	0	0	0	0	0
NH_3	0	0	0	0	0	0	0	0	0	0	0	0	0	0	0
SO_2	0	0	0	0	0	0	0	0	0	0	0	0	0	0	0
S_8	0	0	0	0	0	0	0	0	0	0	0	0	0	0	0
Total	1.0000	1.0000	1.0000	1.0000	1.0000	1.0000	1.0000	1.0000	1.0000	1.0000	1.0000	1.0000	1.0000	1.0000	1.0000
V-L Flow rate (kg_{mole}/hr)	145,969	167,984	167,984	167,984	165,591	154,028	152,126	11,563	10,494	152,126	152,126	152,126	130,111	22,015	130,111
V-L Flow rate (kg/hr)	6,279,641	7,243,980	7,243,980	7,243,980	7,200,803	6,697,969	6,663,665	502,834	459,431	6,663,665	6,663,665	6,663,665	5,699,326	964,339	5,699,326
Solids Flow rate (kg/hr)	0	0	0	0	0	0	0	0	0	0	0	0	0	0	0
Temperature (°C)	1205	750	498	76	76	76	42	76	35	27	66	400	400	400	708
Pressure (MPa, abs)	29.99	3.55	3.52	3.48	3.45	3.45	7.40	3.45	2.93	7.29	30.82	30.75	30.75	30.75	30.70
Steam Table Enthalpy (kJ/kg)*	1,449.73	843.59	536.76	56.45	54.38	54.38	-56.25	54.38	2.21	-202.94	-166.61	355.53	355.53	355.53	745.52
AspenPlus Enthalpy (kJ/kg)**	-7,511.17	-8,104.92	-8,411.76	-8,892.06	-8,850.88	-8,850.88	-8,924.10	-8,850.88	-8,868.42	-9,070.78	-9,034.45	-8,512.31	-8,512.31	-8,512.31	-8,122.32
Density (kg/m^3)	96.7	17.8	23.5	58.8	57.8	57.8	210.2	57.8	58.4	643.0	804.1	228.6	228.6	228.6	150.6
V-L Molecular Weight	43.021	43.123	43.123	43.123	43.485	43.485	43.804	43.485	43.780	43.804	43.804	43.804	43.804	43.804	43.804
V-L Flow rate (lb_{mole}/hr)	321,800	370,334	370,334	370,334	365,060	339,568	335,374	25,492	23,135	335,374	335,374	335,374	286,840	48,534	286,840
V-L Flow rate (lb/hr)	13,844,006	15,969,974	15,969,974	15,969,974	15,874,785	14,766,246	14,690,619	1,108,540	1,012,855	14,690,619	14,690,619	14,690,619	12,564,651	2,125,968	12,564,651
Solids Flow rate (lb/hr)	0	0	0	0	0	0	0	0	0	0	0	0	0	0	0
Temperature (°F)	2200	1382	928	168	168	168	108	168	95	80	150	752	752	752	1306
Pressure (psia)	4,350.0	515.0	510.0	505.0	500.0	500.0	1,073.0	500.0	425.0	1,058.0	4,470.0	4,460.0	4,460.0	4,460.0	4,452.0
Steam Table Enthalpy (Btu/lb)*	623.3	362.7	230.8	24.3	23.4	23.4	-24.2	23.4	0.9	-87.3	-71.6	152.9	152.9	152.9	320.5
AspenPlus Enthalpy (Btu/lb)**	-3,229.4	-3,484.7	-3,616.6	-3,823.2	-3,805.5	-3,805.5	-3,836.9	-3,805.5	-3,813.0	-3,900.0	-3,884.4	-3,659.9	-3,659.9	-3,659.9	-3,492.2
Density (lb/ft^3)	6.038	1.113	1.470	3.669	3.612	3.612	13.120	3.612	3.646	40.143	50.198	14.273	14.273	14.273	9.401

* - Steam Table Reference conditions are 32.02°F & 0.089 psia

** - Aspen Plus thermodynamic reference state is the component's constituent elements in an ideal gas state at 25°C and 1 atm

Exhibit 5-3 Stream table for coal-fired direct-fired sCO_2 power plant (continued)

Stream	61	62	63	64	65	66	67	68	69	70
V-L Mole Fraction										
CO_2	0.9852	0.9980	0	0.0444	0.0013	0.9839	0.0007	0.0007	0.2820	0.0002
H_2O	0	0	1.0000	0.0014	0.9987	0.0013	0.9993	0.9993	0	0.9960
Ar	0.0051	0	0	0.0016	0	0.0051	0	0	0.2835	0
O_2	0.0005	0	0	0	0	0.0005	0	0	0.0291	0
N_2	0.0092	0.0020	0	0.0063	0	0.0091	0	0	0.4053	0
CO	0	0	0	0.6665	0	0	0	0	0	0.0003
CH_4	0	0	0	0.0001	0	0	0	0	0	0
H_2	0	0	0	0.2796	0	0	0	0	0	0.0001
COS	0	0	0	0	0	0	0	0	0	0
H_2S	0	0	0	0	0	0	0	0	0	0.0001
HCl	0	0	0	0	0	0	0	0	0	0.0015
NH_3	0	0	0	0	0	0	0	0	0	0.0017
SO_2	0	0	0	0	0	0	0	0	0	0
S_8	0	0	0	0	0	0	0	0	0	0
Total	1.0000	1.0000	1.0000	1.0000	1.0000	1.0000	1.0000	1.0000	1.0000	1.0000
V-L Flow rate (kg_{mole}/hr)	10,471	10,284	23	195	2,392	152,126	1,902	121	187	10,671
V-L Flow rate (kg/hr)	459,016	452,288	415	4,173	43,178	6,663,665	34,304	2,189	6,728	192,613
Solids Flow rate (kg/hr)	0	0	0	0	0	0	0	0	0	0
Temperature (°C)	38	38	38	43	76	27	27	35	33	136
Pressure (MPa, abs)	2.90	15.27	2.90	3.60	3.45	3.41	3.41	2.93	0.11	1.03
Steam Table Enthalpy (kJ/kg)*	3.35	-212.22	200.16	60.75	401.46	-14.55	141.79	185.51	25.47	567.37
AspenPlus Enthalpy (kJ/kg)**	-8,860.67	-9,161.97	-15,984.91	-4,240.61	-15,760.84	-8,882.40	-16,031.21	-15,987.61	-3,075.15	-15,308.04
Density (kg/m^3)	56.8	804.8	981.1	29.4	943.9	74.0	992.2	984.1	1.5	800.3
V-L Molecular Weight	43.836	43.978	18.015	21.456	18.049	43.804	18.033	18.033	36.025	18.050
V-L Flow rate (lb_{mole}/hr)	23,084	22,673	51	429	5,274	335,374	4,194	268	412	23,525
V-L Flow rate (lb/hr)	1,011,941	997,109	914	9,200	95,189	14,690,619	75,627	4,826	14,832	424,633
Solids Flow rate (lb/hr)	0	0	0	0	0	0	0	0	0	0
Temperature (°F)	100	100	100	108	168	80	80	95	90	276
Pressure (psia)	420.0	2,215.0	420.0	521.7	500.0	495.0	495.0	425.0	15.8	150.0
Steam Table Enthalpy (Btu/lb)*	1.4	-91.2	86.1	26.1	172.6	-6.3	61.0	79.8	11.0	243.9
AspenPlus Enthalpy (Btu/lb)**	-3,809.7	-3,939.2	-6,872.7	-1,823.3	-6,776.4	-3,819.0	-6,892.6	-6,873.9	-1,322.2	-6,581.7
Density (lb/ft^3)	3.545	50.245	61.249	1.837	58.929	4.622	61.944	61.438	0.097	49.960

* - Steam Table Reference conditions are 32.02°F & 0.089 psia

** - Aspen Plus thermodynamic reference state is the component's constituent elements in an ideal gas state at 25°C and 1 atm

5.2 Final Baseline Plant Performance

Exhibit 5-4 shows the overall performance summary for the final baseline case. The gross power for the sCO_2 cycle includes the auxiliary power requirement for the CO_2 pre-compressor (70,468 kWe) and the CO_2 pump (67,256 kWe). The estimated process efficiency of 37.7 percent (HHV basis) is the same as the preliminary baseline case (shown in Appendix A), [14] but also includes a realistic model for required turbine cooling flows absent in the preliminary studies, and corrects an oxygen compression power error in that study. This efficiency is still quite high for a coal-fired power plant with CCS, and 6.5 percentage points higher than the reference IGCC plant. [2] Additional performance comparisons are made to other sCO_2 and IGCC studies in Section 7.

Exhibit 5-4 Coal-fired direct sCO_2 final baseline case performance results

Item	sCO_2 Baseline	IGCC Reference Case B1B [2]
Gross Power (kWe)	777,080	673,400
Net Auxiliary Load (kWe)	-214,659	-176,660
Net Plant Power (kWe)	562,421	496,740
Net Plant Efficiency (HHV, %)	37.7	31.2
Cooling/Condenser Duty (kW_t)	-546,000	-371,000
Coal Feed Flowrate (kg/hr)	198,060	211,040
Thermal Input (kW_t)	1,492,815	1,590,722
Oxygen Flowrate (kg/hr)	391,242	160,514
Carbon Captured (%)	98.1	90.0
Captured CO_2 Purity (%)	99.8	99.4
Water Withdrawal ([m^3/min]/MWnet)	0.036	0.043

Exhibit 5-5 shows the breakdown of the auxiliary power requirements in the plant.

Exhibit 5-5 Coal-fired direct sCO_2 final baseline and IGCC reference plant auxiliary power requirements

Auxiliary Load Summary		
	sCO_2 Baseline	IGCC Reference Case B1B
Coal Handling, kWe	-447	-460
Coal Milling, kWe	-2,037	-2,170
Coal Dryer Air Blower, kWe	-140	N/A
Slag Handling, kWe	-492	-550
Air Separation Unit Auxiliaries, kWe	-1,000	-1,000
Air Separation Unit Main Air Compressor, kWe	-79,001	-59,740
Gasifier Oxygen Compressor, kWe	-20,057	-9,460
sCO_2 Oxygen Compressor, kWe	-44,120	N/A
Nitrogen Compressors, kWe	N/A	-32,910
Fuel Gas Compressor	-35,240	N/A
CO_2 Fluff Gas Compressor	-413	N/A
Feedwater Pumps, kWe	-92	-3,500
Syngas Recycle Compressor, kWe	-869	-790
CO_2 Compression, kWe	-15,934	-30,210
Acid Gas Removal, kWe	-457	-18,650
Combustion Turbine Auxiliaries, kWe	-1,000	-1,000
Steam Turbine Auxiliaries, kWe	N/A	-100
Circulating Water Pumps, kWe	-3,984	-4,380
Miscellaneous Water Pumps, kWe	-10	-1,760
Cooling Tower Fans, kWe	-2,579	-2,270
Claus Plant/TGTU Auxiliaries, kWe	-250	-250
Claus Plant TG Recycle Compressor, kWe	-595	-1,830
Miscellaneous Balance of Plant, kWe	-3,000	-3,000
Transformer Losses, kWe	-2,943	-2,630
Total Auxiliaries, kWe	**-214,659**	**-176,660**

5.3 Plant Material Balances

Exhibit 5-6, Exhibit 5-7, and Exhibit 5-8 show the overall carbon, sulfur, and water balances for the plant, respectively. The carbon balance shows that of the carbon in the coal feed, 97.6 percent is captured in the CO_2 product. The major sources of uncaptured carbon are the coal dryer and CPU vent gas. Approximately 0.08 percent of the coal sulfur is discharged in the product CO_2.

The water balance assumes that the blowdown streams from the cooling tower and boilers are discharged and that the condensate streams and excess water from the sour water stripper (SWS) bottoms can be recycled untreated to the cooling tower. The total water withdrawal is 20.42 m^3/min (5,396 gpm).

Exhibit 5-6 Carbon balance for coal-fired direct-fired sCO_2 final baseline

Carbon In		Carbon Out	
	kg/hr (lb/hr)		kg/hr (lb/hr)
Air to ASU	231 (510)	Purge CO_2 knock-out	1 (2)
Air to coal dryer	8 (17)	ASU vent stream	231 (510)
Coal feed	126,252 (278,339)	CO_2 pre-cooler knock-out	37 (81)
		CO_2 pre-cooler knock-out	15 (34)
		CO_2 product	123,271 (271,767)
		Coal dryer vent	1,669 (3,679)
		CPU vent	633 (1,395)
		Slag	631 (1,392)
		Claus tail gas vent	2 (4)
Total	**126,491 (278,866)**	**Total**	**126,491 (278,866)**

Exhibit 5-7 Sulfur balance for coal-fired direct-fired sCO_2 final baseline

Sulfur In		Sulfur Out	
	kg/hr (lb/hr)		kg/hr (lb/hr)
Coal feed	4,964 (10,944)	CO_2 pre-cooler knock-out	0 (1)
		CO_2 product	4 (9)
		Product sulfur	4,959 (10,933)
Total	**4,964 (10,944)**	**Total**	**4,964 (10,944)**

Exhibit 5-8 Water balance for coal-fired direct-fired sCO_2 final baseline

Water Use	Water Demand	Internal Recycle	Raw Water Withdrawal	Process Water Discharge	Raw Water Consumption
	m^3/min (gpm)	m^3/min (gpm)	m^3/min (gpm)	m^3/min (gpm)	m^3/min (gpm)
Cooling Tower	21.86 (5,774)	–	21.86 (5,774)	5.46 (1,443)	16.39 (4,330)
Quench water	2.90 (767)	2.90 (767)	–	–	–
BFW Makeup	0.25 (66)	–	0.25 (66)	–	0.25 (66)
CPU condensate 1	–	0.01 (2)	-0.01 (-2)	–	-0.01 (-2)
CPU condensate 2	–	0.04 (10)	-0.04 (-10)	–	-0.04 (-10)
sCO_2 condensate 1	–	0.72 (190)	-0.72 (-190)	–	-0.72 (-190)
sCO_2 condensate 2	–	0.57 (151)	-0.57 (-151)	–	-0.57 (-151)
SWS Bottoms excess	–	0.35 (92)	-0.35 (-92)	–	-0.35 (-92)
HP Blowdown	–	–	–	0.00 (1)	0.00 (-1)
IP Blowdown	–	–	–	0.02 (4)	-0.02 (-4)
LP Blowdown	–	–	–	0.02 (4)	-0.02 (-4)
Total	**25.01 (6,607)**	**4.59 (1,211)**	**20.42 (5,396)**	**5.46 (1,443)**	**14.96 (3,952)**

5.4 Air Emissions

The plant is expected to have low levels of air emissions of Hg, particulates, NOx, and SO_2. Although quantitative estimates for these emissions were not made, their amounts are expected to be as low as or lower than those for the reference IGCC plant. The emissions of Hg and particulates should be the same as the reference IGCC plant on a per kg of coal fed basis since the gasification, particulate removal, and Hg removal technologies are the same in both cases. The NOx emissions should be lower in the sCO_2 case because the combustor is oxy-fired and operates at a lower temperature than the air-fired combustor in the reference IGCC gas turbine. The SO_2 emissions should also be lower than the IGCC reference plant since both plants use comparable sulfur removal technologies and the sCO_2 plant includes a cooler stage with water knockout that should assist in removing SO_2 from the vent gas.

5.5 Plant Thermal Integration

Exhibit 5-9 is a T-Q diagram for the sCO_2 cycle recuperators. The plot shows both the hot side (red line) and cold side (blue line) of the recuperator. The dashed vertical line denotes the break point between the LTR and HTR. At this line, the cold side T-Q plot slopes up and approaches the hot side T-Q line. This is because at that point the cooling bleed is taken off so in the HTR the thermal capacitance of the cold side falls below the thermal capacitance of the hot side.

Exhibit 5-9 T-Q diagram for sCO_2 cycle recuperator

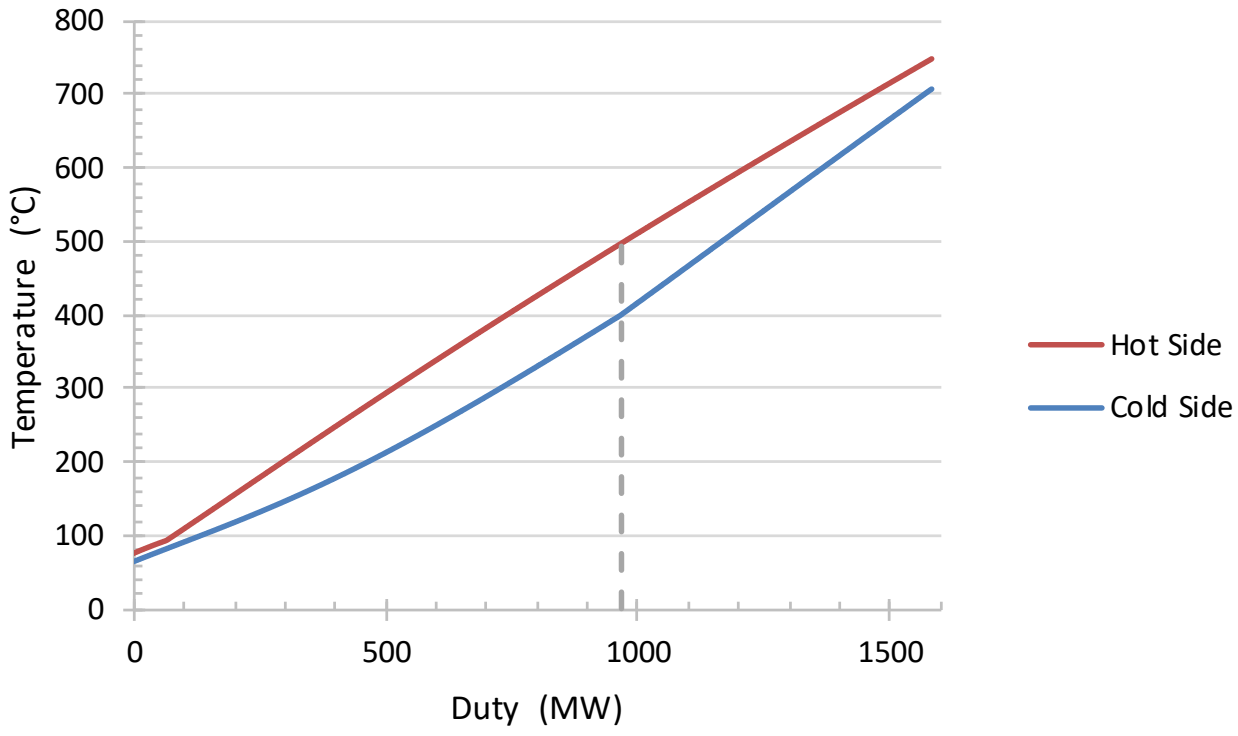

Starting at the cold end of the LTR, the temperature approach is 10.3 °C (18.6 °F), which is slightly higher than the minimum design specification of 10 °C in Exhibit 5-1. It remains almost constant, rising slightly through the first 7 percent by duty of the LTR and then begins to noticeably increase. The maximum temperature approach is at the hot end of the LTR and is 98 °C (176 °F). This is the same as the temperature approach at the cold end of the HTR, but as noted above, the temperature approach falls from the cold end to the hot end of the HTR. At the hot end of the HTR, the temperature approach is 43 °C (77 °F).

The LTR duty is 967 MW (3298 MMBtu/hr) and the HTR duty is 617 MW (2107 MMBtu/hr) giving a total recuperator duty of 1584 MW (5405 MMBtu/hr).

The heat integration scheme for the plant was derived based on a pinch analysis. The hot streams available in the process include the high and low-temperature syngas coolers, the gasifier, the Claus unit, the SWS bottoms cooler, the oxygen compressor intercooler, and the fuel gas intercooler. The primary cold sinks were the steam plant and the CO_2 and syngas feeds to the combustor. Exhibit 5-10 shows the hot and cold source streams used to perform the pinch analysis.

Exhibit 5-10 Hot and cold source streams for pinch analysis

Stream	Tin (°C)	Tout (°C)	Duty (MW)
Hot source			
High-temperature syngas cooler	1093	649	107.7
Intermediate temperature syngas cooler	649	241	91.5
Low-temperature syngas cooler	233	151	14.2
Claus boiler	1093	1093	7.1
Sulfur condenser	649	160	3.9
Gasifier	1316	1316	29.9
Sour water stripper bottoms cooler	170	151	0.6
Syngas compressor intercooler	158	151	0.9
Gasifier oxygen compressor intercooler	269	151	4.6
Cold source			
COS hydrolysis reactor preheater	221	232	12.4
HP evaporator	335	331	3.8
HP economizer	233	335	1.9
IP evaporator	225	225	49.8
IP economizer	148	229	1.3
LP evaporator	148	148	52.8
IP economizer	104	148	0.7
Deaerator	93	104	0.2
BFW economizer	15	93	1.3
CO_2 recycle preheater	706	732	57.4
Syngas preheater	169	707	77.2
Coal dryer air preheater	34	131	1.5

Exhibit 5-11 shows the T-Q diagram for the heat integration scheme. The total amount of heat recovered is 260 MW (888 MMBtu/hr), the minimum approach temperature (MAT) is 11.8 °C (21 °F), and the lowest temperature for heat recovery (LRT) from the hot side is 151 °C (304 °F). Based on the large temperature differences present in Exhibit 5-9 and Exhibit 5-11, there is significant potential for further heat integration between the gasifier, sCO_2 cycle, and auxiliary processes, to improve heat transfer effectiveness and overall plant efficiency. This will be pursued in NETL's ongoing studies of these cycles.

Exhibit 5-11 T-Q diagram for process heat integration

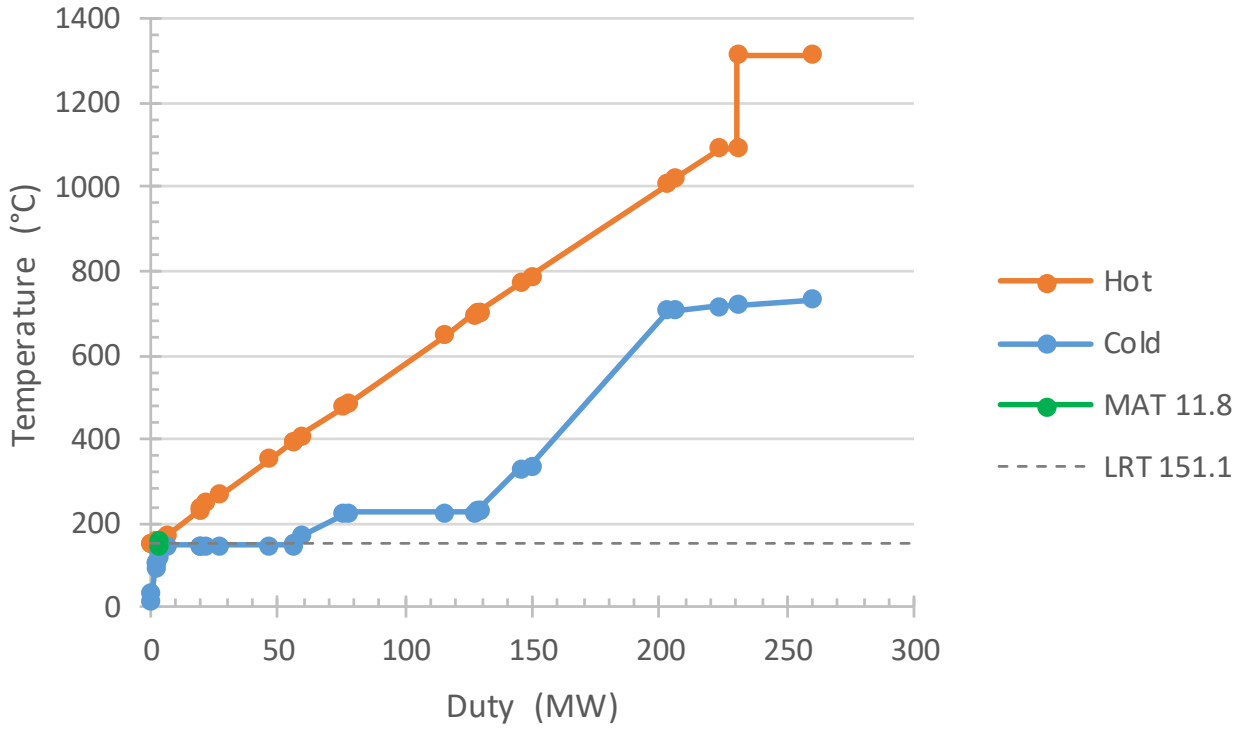

6 ECONOMIC ANALYSIS

6.1 CAPITAL COST ESTIMATE METHODOLOGY

Aside from the thermal power cycle and extra heat recovery units, the balance of plant unit operations and equipment items are analogous to those found in the reference IGCC plant, except that the steam plant only produces steam for process needs and the high temperature syngas coolers are used to heat CO_2, not just steam. The cost estimates for these items were based on a combination of vendor data, estimates from Worley-Parsons, power law scaling, and correlations that were fit to historical cost estimates published in previous NETL reports. [2] [16]

The components in the sCO_2 power cycle are not present in the reference plant and new cost algorithms had to be derived for these units. In addition, an adjustment was made to the syngas cooler cost algorithm to account for differences in the cold side fluid between steam and CO_2. The following sections describe the approaches used for each of these components.

6.1.1 CO_2 Oxy-Turbine

The approach taken to costing the sCO_2 turbine is based on Toshiba's turbine design, which employs inner and outer casings to contain the high system pressure, similar to the design of a high-pressure (HP) steam turbine. [37] In this approach, the outer casing can contain most of the pressure using conventional low-temperature materials, with the more expensive high temperature and pressure materials reserved for the inner casing, which is actively cooled. The cost of the outer casing is based on known costs for a similarly-sized HP steam turbine, and amounts to about $4M in 2011 dollars. [37]

For cost estimating purposes, the oxy-combustor, CO_2 expander, and inner casing, as well as all bearings, seals, and associated equipment, were treated as being analogous to a conventional gas turbine without the compressor. The sCO_2 unit was sized based on the volumetric throughput of the working fluid, and assumed to be configured as a split-flow turbine, similar to HP steam turbines, to reduce or eliminate the thrust bearing requirements. A review of gas turbine specifications at comparable firing temperatures showed that a Trent 60 gas turbine uses roughly half of the total volumetric throughput of the sCO_2 turbine, thus the cost of two Trent 60s, one for each flow path of the split-flow turbine, were used as the base capital cost for the mature sCO_2 turbine. The BEC for these gas turbines was obtained from the Gas Turbine World Handbook [38], and an 18 percent deduction was applied for the cost of the unneeded compressors, based on gas turbine manufacturer feedback. The cost of the outer casing was added to this number to arrive at the total BEC cost of the sCO_2 oxy-turbine. In addition, consistent with the syngas-fired turbine in the reference plant, a process contingency of 5 percent of the BEC is applied to this sub-account due to the unique operating conditions of the combustor and turbine.

This method of arriving at a cost for the sCO_2 turbine is crude, and carries with it a high degree of uncertainty, yet the final TPC cost of $51.5M was deemed to be reasonable for a mature sCO_2 oxy-turbine of this size and type. A more rigorous approach would involve a

determination of the turbine speed, preliminary sizing of the turbine rotor and blading, followed by blade stress analyses, etc., which was deemed to be outside the scope of this project. These costs can be updated at a later point should more cost information or analyses become available for this new type of turbine.

6.1.2 Low-Temperature CO_2 Recuperator

Equipment costs of the CO_2 recuperators are based on a report by Aerojet Rocketdyne. [39] In this report, low-temperature recuperator modules are sized for 3 MW each, with a BEC of $152,000 per module, including labor and module interconnection piping. The LTR for the baseline case has a heat duty of 967 MW (3298 MMBtu/hr). The recuperator cost algorithm adjusts the reported cost by the ratio of average log mean temperature difference between the reference recuperators in the Aerojet Rocketdyne report and the current recuperators. A material cost adjustment is added to the LTR algorithm to account for the higher operating pressure compared to the reference case, leading to a baseline LTR cost of $0.294/(W/K).

6.1.3 High-Temperature CO_2 Recuperator

In the reference source for the HTRs, [39] the modules are sized for 8 MW each, with a BEC of $97,625 per module. The HTR for the baseline case has a heat duty of 617 MW (2107 MMBtu/hr). As with the LTR cost scaling algorithm, the HTR cost is also scaled by the log mean temperature difference and adjusted for higher operating pressure relative to the Aerojet Rocketdyne study. An additional material cost adjustment is added to the HTR algorithm to account for higher operating temperature. When the hot side fluid is at or below 600 °C, the HTR cost is $0.253/(W/K) and for temperatures above 600 °C the HTR cost is $1.318/(W/K), with units assumed to be installed in series. The lower specific cost of the HTR modules, relative to the LTR modules, can be attributed to reduced distribution/interconnection piping requirements associated with the larger duty per module, as well as potential design differences required to meet the pressure drop specifications in the study.

6.1.4 CO_2 Pre-cooler and CO_2 Condenser

The cost estimates for the CO_2 pre-cooler and the CO_2 condenser were based on the same algorithm as the LTR, with a cost of $0.294/(W/K). The pre-cooler has a heat duty of 127 MW (433 MMBtu/hr) and the condenser has a heat duty of 272 MW (927 MMBtu/hr) in the baseline case.

6.1.5 CO_2 Compressor & Pump

The cost estimates for the CO_2 pre-compressor and the pump were scaled based on vendor data for the main and bypass compressors for a utility scale recompression Brayton sCO_2 cycle. The scaling algorithm used divided the equipment cost into three components with one component dependent on required power (60 percent), another component dependent on volumetric flow rate to the compressor (20 percent), and the final component dependent on the temperature of the stream entering the main compressor stage (20 percent).

6.1.6 O_2 and Syngas Compressors

The cost estimates for the O_2 and syngas compressors used in the sCO_2 cycle were based on a cost algorithm that scaled the cost based on the power requirement of the compressor. [40] The cost was adjusted to 2011 dollars using the Chemical Engineering Plant Cost Index (CEPCI). The cost algorithm estimated a total cost for installation materials and labor based on a Lang factor and this cost was arbitrarily split as 40 percent for materials and 60 percent for labor.

6.1.7 CO_2 System Piping

The pipes that transport CO_2 working fluid can be very expensive due to the large flowrate of CO_2 and the elevated temperature and pressure of the fluid in some portions of the cycle. The four pipe lengths with the most severe service are the pipe from the CO_2 turbine to the HTR, the combined syngas and recycle CO_2 pipe to the oxy-combustor, the recycle CO_2 pipe from the HTR to the syngas cooler, and the syngas pipe from the syngas cooler. For the purposes of this economic assessment, the pipe lengths are assumed to be 30.5 m (100 feet) except for the pipe run from the CO_2 turbine to the HTR, which is assumed to be 7.6 m (25 feet). The pipe inside diameter was calculated based on the actual working fluid volumetric flow rate and an assumed fluid velocity of 45.7 m/sec (150 ft/sec). The selection of pipe material and thickness was based on a NETL report. [41] The material capable of meeting the service temperature and pressure with the lowest estimated pipe cost was selected. A 60 percent installation factor was assumed.

6.1.8 High-Temperature Syngas Coolers

The high-temperature syngas coolers were scaled from the estimate for the reference IGCC plant syngas coolers based on the difference in heat duties. The portion of the syngas cooler used for heating sCO_2 accounts for 27 percent of the overall syngas cooler heat duty.

6.2 Economic Analysis Results

6.2.1 Reference IGCC Case

The capital cost estimate and economic analysis for the reference IGCC plant are reproduced in this section to facilitate a comparison with the results from this study. Exhibit 6-1 shows the capital cost estimate for the reference plant.

Exhibit 6-1 Capital cost estimate for reference IGCC plant

Case:		B1B – Shell IGCC w/ CO_2					Estimate Type:	Conceptual			
Plant Size (MW,net):		497					Cost Base:	Jun 2011			
Item No.	Description	Equipment Cost	Material Cost	Labor		Bare Erected Cost	Eng'g CM H.O.& Fee	Contingencies		Total Plant Cost	
				Direct	Indirect			Process	Project	$/1,000	$/kW
1		Coal & Sorbent Handling									
1.1	Coal Receive & Unload	$4,425	$0	$2,133	$0	$6,558	$656	$0	$1,443	$8,656	$17
1.2	Coal Stackout & Reclaim	$5,718	$0	$1,367	$0	$7,086	$709	$0	$1,559	$9,353	$19
1.3	Coal Conveyors & Yd Crush	$5,316	$0	$1,353	$0	$6,669	$667	$0	$1,467	$8,803	$18
1.4	Other Coal Handling	$1,391	$0	$313	$0	$1,704	$170	$0	$375	$2,249	$5
1.9	Coal & Sorbent Hnd. Foundations	$0	$2,955	$7,723	$0	$10,677	$1,068	$0	$2,349	$14,094	$28
	Subtotal	**$16,851**	**$2,955**	**$12,889**	**$0**	**$32,694**	**$3,269**	**$0**	**$7,193**	**$43,156**	**$87**
2		Coal & Sorbent Prep & Feed									
2.1	Coal Crushing & Drying	$50,700	$3,058	$7,286	$0	$61,043	$6,104	$0	$13,430	$80,577	$162
2.2	Prepared Coal Storage & Feed	$2,401	$577	$371	$0	$3,350	$335	$0	$737	$4,422	$9
2.3	Dry Coal Injection System	$79,030	$911	$7,239	$0	$87,180	$8,718	$0	$19,180	$115,078	$232
2.4	Misc. Coal Prep & Feed	$1,321	$965	$2,842	$0	$5,127	$513	$0	$1,128	$6,767	$14
2.9	Coal & Sorbent Feed Foundation	$0	$4,844	$4,156	$0	$9,000	$900	$0	$1,980	$11,880	$24
	Subtotal	**$133,452**	**$10,354**	**$21,894**	**$0**	**$165,700**	**$16,570**	**$0**	**$36,454**	**$218,724**	**$440**
3		Feedwater & Miscellaneous BOP Systems									
3.1	Feedwater System	$2,970	$5,126	$2,687	$0	$10,784	$1,078	$0	$2,372	$14,234	$29
3.2	Water Makeup & Pretreating	$857	$89	$471	$0	$1,416	$142	$0	$467	$2,024	$4
3.3	Other Feedwater Subsystems	$1,670	$552	$493	$0	$2,715	$271	$0	$597	$3,584	$7
3.4	Service Water Systems	$501	$999	$3,443	$0	$4,942	$494	$0	$1,631	$7,068	$14
3.5	Other Boiler Plant Systems	$2,699	$1,009	$2,483	$0	$6,191	$619	$0	$1,362	$8,172	$16
3.6	FO Supply Sys & Nat Gas	$17,717	$675	$625	$0	$19,017	$1,902	$0	$4,184	$25,103	$51
3.7	Waste Treatment Equipment	$1,159	$0	$718	$0	$1,877	$188	$0	$619	$2,683	$5
3.8	Misc. Power Plant Equipment	$1,261	$168	$655	$0	$2,085	$208	$0	$688	$2,981	$6
	Subtotal	**$28,834**	**$8,617**	**$11,575**	**$0**	**$49,026**	**$4,903**	**$0**	**$11,921**	**$65,849**	**$133**
4		Gasifier & Accessories									
4.1	Syngas Cooler Gasifier System	$171,383	$0	$73,493	$0	$244,876	$24,488	$33,487	$46,617	$349,467	$704
4.2	Syngas Cooler	w/4.1	$0	w/ 4.1	$0	$0	$0	$0	$0	$0	$0
4.3	ASU & Oxidant Compression	$207,843	$0	w/equip.	$0	$207,843	$20,784	$0	$22,863	$251,490	$506
4.4	LT Heat Recovery & FG Saturation	$30,655	$0	$11,647	$0	$42,303	$4,230	$0	$9,307	$55,840	$112
4.5	Misc. Gasification Equipment	w/4.1&4.2	$0	w/4.1&4.2	$0	$0	$0	$0	$0	$0	$0
4.6	Flare Stack System	$0	$1,694	$685	$0	$2,379	$238	$0	$523	$3,141	$6
4.8	Major Component Rigging	w/4.1&4.2	$0	w/4.1&4.2	$0	$0	$0	$0	$0	$0	$0
4.9	Gasification Foundations	$0	$9,672	$5,768	$0	$15,440	$1,544	$0	$4,246	$21,230	$43
	Subtotal	**$409,881**	**$11,366**	**$91,593**	**$0**	**$512,841**	**$51,284**	**$33,487**	**$83,556**	**$681,168**	**$1,371**
5A		Gas Cleanup & Piping									
5A.1	Double Stage Selexol	$162,818	$0	w/equip.	$0	$162,818	$16,282	$32,564	$42,333	$253,996	$511
5A.2	Elemental Sulfur Plant	$12,076	$2,354	$15,473	$0	$29,902	$2,990	$0	$6,579	$39,471	$79
5A.3	Mercury Removal	$2,022	$0	$1,528	$0	$3,550	$355	$177	$816	$4,899	$10
5A.4	Shift Reactors	$8,880	$0	$3,550	$0	$12,429	$1,243	$0	$2,734	$16,406	$33
5A.5	Particulate Removal	w/4.1	$0	w/4.1	$0	$0	$0	$0	$0	$0	$0

Exhibit 6-1 Capital cost estimate for reference IGCC plant, continued

Case:		B1B – Shell IGCC w/ CO_2					Estimate Type:			Conceptual	
Plant Size (MW,net):		497					Cost Base:			Jun 2011	
Item No.	Description	Equipment Cost	Material Cost	Labor		Bare Erected Cost	Eng'g CM H.O.& Fee	Contingencies		Total Plant Cost	
				Direct	Indirect			Process	Project	$/1,000	$/kW
5A.6	Blowback Gas Systems	$2,562	$431	$241	$0	$3,234	$323	$0	$711	$4,269	$9
5A.7	Fuel Gas Piping	$0	$1,043	$683	$0	$1,726	$173	$0	$380	$2,278	$5
5A.9	HGCU Foundations	$0	$944	$636	$0	$1,581	$158	$0	$522	$2,261	$5
	Subtotal	**$188,356**	**$4,773**	**$22,111**	**$0**	**$215,240**	**$21,524**	**$32,741**	**$54,075**	**$323,580**	**$651**
5B		**CO_2 Compression**									
5B.2	CO_2 Compression & Drying	$39,421	$5,913	$16,551	$0	$61,885	$6,188	$0	$13,615	$81,688	$164
	Subtotal	**$39,421**	**$5,913**	**$16,551**	**$0**	**$61,885**	**$6,188**	**$0**	**$13,615**	**$81,688**	**$164**
6		**Combustion Turbine & Accessories**									
6.1	Combustion Turbine Generator	$111,210	$0	$7,881	$0	$119,091	$11,909	$11,909	$14,291	$157,201	$316
6.9	Combustion Turbine Foundations	$0	$923	$1,068	$0	$1,992	$199	$0	$657	$2,848	$6
	Subtotal	**$111,210**	**$923**	**$8,950**	**$0**	**$121,083**	**$12,108**	**$11,909**	**$14,948**	**$160,049**	**$322**
7		**HRSG, Ducting, & Stack**									
7.1	Heat Recovery Steam Generator	$29,630	$0	$5,739	$0	$35,369	$3,537	$0	$3,891	$42,796	$86
7.3	Ductwork	$0	$2,111	$1,480	$0	$3,591	$359	$0	$790	$4,740	$10
7.4	Stack	$4,074	$0	$1,520	$0	$5,594	$559	$0	$615	$6,769	$14
7.9	HRSG, Duct & Stack Foundations	$0	$776	$779	$0	$1,554	$155	$0	$513	$2,222	$4
	Subtotal	**$33,704**	**$2,887**	**$9,517**	**$0**	**$46,108**	**$4,611**	**$0**	**$5,809**	**$56,527**	**$114**
8		**Steam Turbine Generator**									
8.1	Steam TG & Accessories	$35,245	$0	$4,790	$0	$40,035	$4,003	$0	$4,404	$48,442	$98
8.2	Turbine Plant Auxiliaries	$199	$0	$453	$0	$651	$65	$0	$72	$788	$2
8.3	Condenser & Auxiliaries	$3,020	$0	$1,697	$0	$4,717	$472	$0	$519	$5,708	$11
8.4	Steam Piping	$13,533	$0	$5,869	$0	$19,402	$1,940	$0	$5,335	$26,677	$54
8.9	TG Foundations	$0	$937	$1,655	$0	$2,592	$259	$0	$855	$3,707	$7
	Subtotal	**$51,997**	**$937**	**$14,463**	**$0**	**$67,397**	**$6,740**	**$0**	**$11,185**	**$85,322**	**$172**
9		**Cooling Water System**									
9.1	Cooling Towers	$4,330	$0	$1,310	$0	$5,640	$564	$0	$931	$7,135	$14
9.2	Circulating Water Pumps	$2,088	$0	$154	$0	$2,242	$224	$0	$370	$2,836	$6
9.3	Circ. Water System Auxiliaries	$183	$0	$26	$0	$208	$21	$0	$34	$264	$1
9.4	Circ. Water Piping	$0	$8,098	$1,962	$0	$10,060	$1,006	$0	$2,213	$13,280	$27
9.5	Make-up Water System	$475	$0	$653	$0	$1,128	$113	$0	$248	$1,489	$3
9.6	Component Cooling Water Sys	$926	$1,107	$760	$0	$2,794	$279	$0	$615	$3,687	$7
9.9	Circ. Water System Foundations	$0	$2,651	$4,711	$0	$7,362	$736	$0	$2,429	$10,527	$21
	Subtotal	**$8,001**	**$11,857**	**$9,575**	**$0**	**$29,434**	**$2,943**	**$0**	**$6,840**	**$39,217**	**$79**
10		**Ash & Spent Sorbent Handling Systems**									
10.1	Slag Dewatering & Cooling	$19,503	$0	$9,552	$0	$29,055	$2,905	$0	$3,196	$35,156	$71
10.2	Gasifier Ash Depressurization	w/10.1	w/10.1	w/10.1	$0	$0	$0	$0	$0	$0	$0
10.3	Cleanup Ash Depressurization	w/10.1	w/10.1	w/10.1	$0	$0	$0	$0	$0	$0	$0
10.6	Ash Storage Silos	$658	$0	$711	$0	$1,368	$137	$0	$226	$1,731	$3
10.7	Ash Transport & Feed Equipment	$905	$0	$211	$0	$1,117	$112	$0	$184	$1,413	$3
10.8	Misc. Ash Handling Equipment	$1,362	$1,670	$495	$0	$3,527	$353	$0	$582	$4,462	$9
10.9	Ash/Spent Sorbent Foundation	$0	$55	$73	$0	$128	$13	$0	$42	$183	$0
	Subtotal	**$22,428**	**$1,725**	**$11,042**	**$0**	**$35,195**	**$3,519**	**$0**	**$4,230**	**$42,945**	**$86**

Exhibit 6-1 Capital cost estimate for reference IGCC plant, continued

Case:		B1B – Shell IGCC w/ CO_2					Estimate Type:			Conceptual	
Plant Size (MW,net):		497					Cost Base:			Jun 2011	
Item No.	Description	Equipment Cost	Material Cost	Labor		Bare Erected Cost	Eng'g CM H.O.& Fee	Contingencies		Total Plant Cost	
				Direct	Indirect			Process	Project	$/1,000	$/kW
11		Accessory Electric Plant									
11.1	Generator Equipment	$1,096	$0	$1,067	$0	$2,162	$216	$0	$238	$2,616	$5
11.2	Station Service Equipment	$5,293	$0	$487	$0	$5,780	$578	$0	$636	$6,994	$14
11.3	Switchgear & Motor Control	$9,770	$0	$1,816	$0	$11,586	$1,159	$0	$1,912	$14,657	$30
11.4	Conduit & Cable Tray	$0	$4,964	$15,302	$0	$20,266	$2,027	$0	$5,573	$27,866	$56
11.5	Wire & Cable	$0	$9,571	$5,823	$0	$15,394	$1,539	$0	$4,233	$21,167	$43
11.6	Protective Equipment	$0	$798	$2,963	$0	$3,761	$376	$0	$621	$4,758	$10
11.7	Standby Equipment	$263	$0	$262	$0	$525	$53	$0	$87	$664	$1
11.8	Main Power Transformers	$18,593	$0	$162	$0	$18,756	$1,876	$0	$3,095	$23,726	$48
11.9	Electrical Foundations	$0	$170	$462	$0	$632	$63	$0	$209	$904	$2
	Subtotal	**$35,016**	**$15,503**	**$28,345**	**$0**	**$78,864**	**$7,886**	**$0**	**$16,603**	**$103,353**	**$208**
12		Instrumentation & Control									
12.1	IGCC Control Equipment	w/4.1	$0	w/4.1	$0	$0	$0	$0	$0	$0	$0
12.2	Combustion Turbine Control	w/6.1	$0	w/6.1	$0	$0	$0	$0	$0	$0	$0
12.3	Steam Turbine Control	w/8.1	$0	w/8.1	$0	$0	$0	$0	$0	$0	$0
12.4	Other Major Component Control	$1,274	$0	$868	$0	$2,143	$214	$107	$370	$2,834	$6
12.5	Signal Processing Equipment	w/12.7	$0	w/12.7	$0	$0	$0	$0	$0	$0	$0
12.6	Control Boards, Panels & Racks	$293	$0	$192	$0	$484	$48	$24	$111	$669	$1
12.7	Computer & Accessories	$6,798	$0	$222	$0	$7,020	$702	$351	$807	$8,880	$18
12.8	Instrument Wiring & Tubing	$0	$2,617	$4,953	$0	$7,570	$757	$379	$2,176	$10,882	$22
12.9	Other I & C Equipment	$4,544	$0	$2,251	$0	$6,796	$680	$340	$1,172	$8,987	$18
	Subtotal	**$12,909**	**$2,617**	**$8,487**	**$0**	**$24,013**	**$2,401**	**$1,201**	**$4,637**	**$32,252**	**$65**
13		Improvements to Site									
13.1	Site Preparation	$0	$118	$2,686	$0	$2,804	$280	$0	$925	$4,010	$8
13.2	Site Improvements	$0	$2,101	$2,970	$0	$5,072	$507	$0	$1,674	$7,252	$15
13.3	Site Facilities	$3,765	$0	$4,227	$0	$7,992	$799	$0	$2,637	$11,429	$23
	Subtotal	**$3,765**	**$2,219**	**$9,883**	**$0**	**$15,868**	**$1,587**	**$0**	**$5,236**	**$22,691**	**$46**
14		Buildings & Structures									
14.1	Combustion Turbine Area	$0	$317	$179	$0	$496	$50	$0	$109	$655	$1
14.2	Steam Turbine Building	$0	$2,481	$3,532	$0	$6,014	$601	$0	$992	$7,607	$15
14.3	Administration Building	$0	$1,027	$745	$0	$1,772	$177	$0	$292	$2,242	$5
14.4	Circulation Water Pumphouse	$0	$193	$102	$0	$295	$29	$0	$49	$373	$1
14.5	Water Treatment Buildings	$0	$704	$686	$0	$1,391	$139	$0	$229	$1,759	$4
14.6	Machine Shop	$0	$526	$360	$0	$885	$89	$0	$146	$1,120	$2
14.7	Warehouse	$0	$849	$548	$0	$1,397	$140	$0	$230	$1,767	$4
14.8	Other Buildings & Structures	$0	$508	$396	$0	$904	$90	$0	$199	$1,193	$2
14.9	Waste Treating Building & Str.	$0	$1,137	$2,171	$0	$3,307	$331	$0	$728	$4,366	$9
	Subtotal	**$0**	**$7,742**	**$8,718**	**$0**	**$16,460**	**$1,646**	**$0**	**$2,975**	**$21,081**	**$42**
	Total	**$1,095,825**	**$90,388**	**$285,594**	**$0**	**$1,471,807**	**$147,181**	**$79,338**	**$279,277**	**$1,977,603**	**$3,981**

Exhibit 6-2 shows the Owner's costs for the reference IGCC plant and Exhibit 6-3 summarizes the O&M costs. Exhibit 6-4 shows the component and aggregate (with and without T&S) COE.

Exhibit 6-2 Owner's costs for reference IGCC plant

Description	$/1,000	$/kW
Pre-Production Costs		
6 Months All Labor	$15,919	$32
1 Month Maintenance Materials	$3,587	$7
1 Month Non-fuel Consumables	$682	$1
1 Month Waste Disposal	$434	$1
25% of 1 Months Fuel Cost at 100% CF	$2,910	$6
2% of TPC	$39,552	$80
Total	**$63,083**	**$127**
Inventory Capital		
60-day supply of fuel and consumables at 100% CF	$24,228	$49
0.5% of TPC (spare parts)	$9,888	$20
Total	**$34,116**	**$69**
Other Costs		
Initial Cost for Catalyst and Chemicals	$16,739	$34
Land	$900	$2
Other Owner's Costs	$296,640	$597
Financing Costs	$53,395	$107
Total Overnight Costs (TOC)	**$2,442,476**	**$4,917**
TASC Multiplier (IOU, high-risk, 35 year)	1.140	
Total As-Spent Cost (TASC)	**$2,784,423**	**$5,605**

Exhibit 6-3 Operating and maintenance costs for reference IGCC plant

Case:	B1B – Shell IGCC w/ CO_2				Cost Base:	Jun 2011
Plant Size (MW,net):	497	Heat Rate-net (Btu/kWh):		10,927	Capacity Factor (%):	80
Operating & Maintenance Labor						
Operating Labor				**Operating Labor Requirements per Shift**		
Operating Labor Rate (base):	39.70	$/hour		Skilled Operator:		2.0
Operating Labor Burden:	30.00	% of base		Operator:		10.0
Labor O-H Charge Rate:	25.00	% of labor		Foreman:		1.0
				Lab Tech's, etc.:		3.0
				Total:		**16.0**
Fixed Operating Costs						
					Annual Cost	
					($)	**($/kW-net)**
Annual Operating Labor:					$7,233,658	$14.562
Maintenance Labor:					$18,236,067	$36.711
Administrative & Support Labor:					$6,367,431	$12.818
Property Taxes and Insurance:					$39,552,053	$79.623
Total:					**$71,389,208**	**$143.715**
Variable Operating Costs						
					($)	**($/MWh-net)**
Maintenance Material:					$34,437,835	$9.89265
Consumables						
	Consumption				**Cost ($)**	
	Initial Fill	**Per Day**	**Per Unit**	**Initial Fill**		
Water (/1000 gallons):	0	4,070	$1.67	$0	$1,989,343	$0.57146
Makeup and Waste Water Treatment Chemicals (lbs):	0	24,247	$0.27	$0	$1,896,308	$0.54474
Carbon (Mercury Removal) (lb):	201,639	345	$5.50	$1,109,016	$554,508	$0.15929
Shift Catalyst (ft^3):	6,470	4.43	$771.99	$4,994,685	$998,937	$0.28696
Selexol Solution (gal):	289,068	92	$36.79	$10,635,172	$989,212	$0.28416
Claus Catalyst (ft^3):	w/equip.	1.93	$203.15	$0	$114,583	$0.03292
Subtotal:				**$16,738,872**	**$6,542,891**	**$1.87952**
Waste Disposal						
Spent Mercury Catalyst (lb.):	0	345	$0.65	$0	$65,542	$0.01883
Flyash (ton):	0	0	$0.00	$0	$0	$0.00000
Slag (ton):	0	559	$25.11	$0	$4,099,990	$1.17777
Subtotal:				**$0**	**$4,165,532**	**$1.19660**
By-Products						
Sulfur (tons):	0	140	$0.00	$0	$0	$0.00000
Subtotal:				**$0**	**$0**	**$0.00000**
Variable Operating Costs Total:				**$16,738,872**	**$45,146,258**	**$12.96876**
Fuel Cost						
Illinois Number 6 (ton):	0	5,583	$68.54	$0	$111,739,739	$32.09848
Total:				**$0**	**$111,739,739**	**$32.09848**

Exhibit 6-4 COE breakdown for reference IGCC plant

Component	Value, $/MWh	Percentage
Capital	87.0	57%
Fixed O&M	20.5	13%
Variable O&M	13.0	8%
Fuel	32.1	21%
Total (Excluding T&S)	**152.6**	**N/A**
CO_2 T&S	9.8	6%
Total (Including T&S)	**162.4**	**N/A**

6.2.2 Direct-fired sCO_2 Case

Exhibit 6-5 shows the capital cost estimate for the direct-fired sCO_2 case. Exhibit 6-6 shows the owner's costs for the direct-fired sCO_2 plant and Exhibit 6-7 summarizes the O&M costs. Exhibit 6-8 shows the component and aggregate (with and without T&S) COE.

Exhibit 6-5 Capital cost estimate for direct-fired sCO_2 plant

Case:		Coal-fired direct-fire sCO2 Baseline Plant					Estimate Type: Conceptual				
Plant Size (MW, net):		580					Cost Base: Jun 2011				
Item No.	Description	Equipment Cost	Material Cost	Labor		Bare Erected Cost	Eng'g CM H.O. & Fee	Contingencies		Total Plant Cost	
				Direct	Indirect			Process	Project	$/1,000	$/kW
1		Coal & Sorbent Handling									
1.1	Receive & unload	$4,291	$0	$2,061	$0	$6,353	$635	$0	$1,398	$8,385	$15
1.2	Coal stackout & reclaim	$5,546	$0	$1,322	$0	$6,868	$687	$0	$1,511	$9,066	$16
1.3	Conveyors & crushers	$5,156	$0	$1,308	$0	$6,464	$646	$0	$1,422	$8,532	$15
1.4	Other coal handling	$1,349	$0	$303	$0	$1,652	$165	$0	$363	$2,180	$4
1.9	Foundations	$0	$2,847	$7,464	$0	$10,312	$1,031	$0	$2,269	$13,611	$24
	Subtotal	**$16,343**	**$2,847**	**$12,458**	**$0**	**$31,648**	**$3,165**	**$0**	**$6,962**	**$41,775**	**$74**
2		Coal & Sorbent Prep & Feed									
2.1	Coal crushing & drying	$48,717	$2,931	$7,026	$0	$58,675	$5,867	$0	$12,908	$77,451	$138
2.2	Storage & feed (prepped coal)	$2,277	$546	$353	$0	$3,176	$318	$0	$699	$4,193	$7
2.3	Lock hopper feed system	$74,865	$876	$0	$0	$75,740	$7,574	$0	$16,663	$99,977	$178
2.4	Misc coal prep & feed	$1,268	$925	$2,740	$0	$4,932	$493	$0	$1,085	$6,510	$12
2.9	Foundations	$0	$4,659	$4,008	$0	$8,667	$867	$0	$1,907	$11,440	$20
	Subtotal	**$127,127**	**$9,936**	**$14,127**	**$0**	**$151,190**	**$15,119**	**$0**	**$33,262**	**$199,571**	**$355**
3		Feedwater & Miscellaneous BOP Systems									
3.1	Feedwater system	$285	$437	$227	$0	$948	$95	$0	$209	$1,252	$2
3.2	Water make-up & pretreating	$834	$86	$458	$0	$1,378	$138	$0	$455	$1,971	$4
3.3	Other feedwater subsystems	$146	$51	$41	$0	$238	$24	$0	$52	$315	$1
3.4	Service water systems	$489	$972	$3,352	$0	$4,813	$481	$0	$1,588	$6,883	$12
3.5	Other boiler plant systems	$866	$325	$799	$0	$1,989	$199	$0	$438	$2,626	$5
3.6	FO supply sys and nat gas	$388	$733	$679	$0	$1,801	$180	$0	$396	$2,377	$4
3.7	Waste treatment equipment	$1,128	$0	$699	$0	$1,827	$183	$0	$603	$2,612	$5
3.8	Misc power plant equipment	$1,358	$182	$709	$0	$2,249	$225	$0	$742	$3,216	$6
	Subtotal	**$5,496**	**$2,785**	**$6,964**	**$0**	**$15,244**	**$1,524**	**$0**	**$4,483**	**$21,252**	**$38**
4		Gasifier & Accessories									
4.1	Gasifier	$165,669	$0	$70,524	$0	$236,193	$23,619	$33,386	$44,844	$338,042	$601
4.2	Syngas cooler	$126,122	$0	$58,684	$0	$184,807	$18,481	$26,122	$35,087	$264,497	$470
4.3	ASU & oxidant compression	$157,647	$0	$128,984	$0	$286,631	$28,663	$0	$31,529	$346,824	$617
4.4	Syngas cooling	$20,964	$0	$7,915	$0	$28,879	$2,888	$0	$6,353	$38,121	$68
4.5	Fluff gas compressor	$222	$155	$232	$0	$609	$61	$0	$0	$670	$1
4.6	Flare stack system	$0	$1,169	$472	$0	$1,641	$164	$0	$0	$1,805	$3
4.9	Foundations	$0	$10,975	$6,594	$0	$17,569	$1,757	$0	$4,831	$24,157	$43
	Subtotal	**$470,625**	**$12,299**	**$273,406**	**$0**	**$756,329**	**$75,633**	**$59,508**	**$122,645**	**$1,014,116**	**$1,803**
5A		Gas Cleanup & Piping									
5A.1	Acid gas removal	$41,886	$0	$35,290	$0	$77,176	$7,718	$0	$16,979	$101,872	$181
5A.2	Elemental sulfur plant	$11,520	$2,249	$14,753	$0	$28,522	$2,852	$0	$6,275	$37,650	$67
5A.3	Mercury removal	$1,092	$0	$826	$0	$1,918	$192	$95	$441	$2,646	$5
5A.4	COS hydrolysis reactor	$3,690	$0	$4,786	$0	$8,476	$848	$0	$1,865	$11,189	$20
5A.6	Blowback gas systems	$1,717	$289	$161	$0	$2,167	$217	$0	$477	$2,860	$5
5A.7	Fuel gas piping	$0	$964	$630	$0	$1,594	$159	$0	$351	$2,104	$4
5A.9	Foundations	$0	$919	$619	$0	$1,537	$154	$0	$507	$2,199	$4
	Subtotal	**$59,906**	**$4,419**	**$57,066**	**$0**	**$121,391**	**$12,139**	**$95**	**$26,894**	**$160,519**	**$285**
5B		Gas Cleanup & Piping									
5B.1	CO2 Removal System	$0	$0	$0	$0	$0	$0	$0	$0	$0	$0
5B.2	CO2 Compression & Drying	$26,091	$0	$19,818	$0	$45,910	$4,591	$0	$10,100	$60,601	$108
	Subtotal	**$26,091**	**$0**	**$19,818**	**$0**	**$45,910**	**$4,591**	**$0**	**$10,100**	**$60,601**	**$108**

Exhibit 6-5 Capital cost estimate for direct-fired sCO_2 plant (continued)

Case:		Coal-fired direct-fire sCO2 Baseline Plant					Estimate Type: Conceptual				
Plant Size (MW, net):		580					Cost Base: Jun 2011				
Item No.	Description	Equipment Cost	Material Cost	Labor		Bare Erected Cost	Eng'g CM H.O. & Fee	Contingencies		Total Plant Cost	
				Direct	Indirect			Process	Project	$/1,000	$/kW
6		sCO_2 Combustion Turbine and Accessories									
6.1	Oxy-turbine generator	$40,688	$0	$0	$0	$40,688	$4,069	$2,059	$4,699	$51,515	$92
6.2	High temperature recuperator	$9,159	$0	$0	$0	$9,159	$916	$0	$1,008	$11,083	$20
6.3	Low temperature recuperator	$7,303	$0	$0	$0	$7,303	$730	$0	$803	$8,837	$16
6.4	CO□pre-cooler	$1,401	$0	$0	$0	$1,401	$140	$0	$154	$1,696	$3
6.5	CO□pre-compressor	$39,488	$0	$0	$0	$39,488	$3,949	$0	$8,687	$52,124	$93
6.6	CO□cooler/condenser	$5,833	$0	$0	$0	$5,833	$583	$0	$642	$7,058	$13
6.7	CO□pumpressor	$17,906	$0	$0	$0	$17,906	$1,791	$0	$3,939	$23,636	$42
6.8	O□compressor	$13,200	$9,160	$13,740	$0	$36,100	$3,610	$0	$3,971	$43,681	$78
6.9	Syngas compressor	$10,500	$7,320	$10,980	$0	$28,800	$2,880	$0	$3,168	$34,848	$62
6.10	Piping	$0	$9,811	$5,887	$0	$15,698	$1,570	$0	$4,317	$21,585	$38
6.11	Foundations	$0	$1,902	$2,105	$0	$4,007	$401	$0	$1,322	$5,730	$10
	Subtotal	**$145,479**	**$28,193**	**$32,712**	**$0**	**$206,384**	**$20,638**	**$2,059**	**$32,711**	**$261,793**	**$465**
7		HRSG, Ducting, & Stack									
7.1	HRSG	$0	$0	$0	$0	$0	$0	$0	$0	$0	$0
7.2	SCR	$0	$0	$0	$0	$0	$0	$0	$0	$0	$0
7.3	Ductwork	$0	$0	$0	$0	$0	$0	$0	$0	$0	$0
7.4	Stack	$0	$0	$0	$0	$0	$0	$0	$0	$0	$0
7.9	Foundations	$0	$0	$0	$0	$0	$0	$0	$0	$0	$0
	Subtotal	**$0**	**$0**	**$0**	**$0**	**$0**	**$0**	**$0**	**$0**	**$0**	**$0**
8		Steam Turbine Generator									
8.1	Heat exchangers	$14,676	$0	$2,829	$0	$17,506	$1,751	$0	$1,926	$21,182	$38
8.4	Steam piping	$6,344	$0	$2,752	$0	$9,095	$910	$0	$2,501	$12,506	$22
8.9	Foundations	$0	$245	$273	$0	$518	$52	$0	$171	$740	$1
	Subtotal	**$21,020**	**$245**	**$5,854**	**$0**	**$27,119**	**$2,712**	**$0**	**$4,598**	**$34,428**	**$61**
9		Cooling Water System									
9.1	Cooling tower	$4,335	$0	$1,333	$0	$5,668	$567	$0	$935	$7,170	$13
9.2	Circ water pumps	$2,090	$0	$153	$0	$2,243	$224	$0	$370	$2,837	$5
9.3	Circ water system auxiliaries	$183	$0	$26	$0	$209	$21	$0	$34	$264	$0
9.4	Circ water piping	$0	$8,149	$1,967	$0	$10,115	$1,012	$0	$2,225	$13,352	$24
9.5	Make-up water system	$467	$0	$640	$0	$1,107	$111	$0	$243	$1,461	$3
9.6	Component cooling water sys	$932	$1,115	$765	$0	$2,812	$281	$0	$619	$3,712	$7
9.9	Foundations	$0	$2,659	$4,842	$0	$7,501	$750	$0	$2,475	$10,727	$19
	Subtotal	**$8,007**	**$11,922**	**$9,725**	**$0**	**$29,655**	**$2,965**	**$0**	**$6,903**	**$39,523**	**$70**
10		Ash & Spent Sorbent Handling Systems									
10.1	Slag cooling	$18,963	$0	$9,289	$0	$28,253	$2,825	$0	$3,108	$34,186	$61
10.2	Gasifier ash depressurization	$0	$0	$0	$0	$0	$0	$0	$0	$0	$0
10.3	Cleanup ash depressurization	$0	$0	$0	$0	$0	$0	$0	$0	$0	$0
10.4	High temp ash piping	$0	$0	$0	$0	$0	$0	$0	$0	$0	$0
10.5	Other ash recovery equipment	$0	$0	$0	$0	$0	$0	$0	$0	$0	$0
10.6	Ash Storage Silos	$639	$0	$690	$0	$1,329	$133	$0	$219	$1,681	$3
10.7	Ash transport & feed	$882	$0	$205	$0	$1,087	$109	$0	$179	$1,376	$2
10.8	Misc ash handling	$1,323	$1,621	$481	$0	$3,425	$342	$0	$565	$4,332	$8
10.9	Foundations	$0	$54	$71	$0	$124	$12	$0	$41	$177	$0
	Subtotal	**$21,807**	**$1,675**	**$10,736**	**$0**	**$34,218**	**$3,422**	**$0**	**$4,113**	**$41,753**	**$74**

Exhibit 6-5 Capital cost estimate for direct-fired sCO_2 plant (continued)

Case:		Coal-fired direct-fire sCO2 Baseline Plant					Estimate Type: Conceptual				
Plant Size (MW, net):		580					Cost Base: Jun 2011				
Item No.	Description	Equipment Cost	Material Cost	Labor		Bare Erected Cost	Eng'g CM H.O. & Fee	Contingencies		Total Plant Cost	
				Direct	Indirect			Process	Project	$/1,000	$/kW
11		Accessory Electric Plant									
11.1	Generator equip	$1,187	$0	$1,159	$0	$2,347	$235	$0	$258	$2,839	$5
11.2	Station service equip	$5,784	$0	$535	$0	$6,319	$632	$0	$695	$7,645	$14
11.3	Switchgear & motor control	$10,741	$0	$1,997	$0	$12,738	$1,274	$0	$2,102	$16,113	$29
11.4	Conduit & cable tray	$0	$5,469	$16,827	$0	$22,295	$2,230	$0	$6,131	$30,656	$55
11.5	Wire & cable	$0	$10,521	$6,401	$0	$16,922	$1,692	$0	$4,653	$23,267	$41
11.6	Protective equipment	$0	$818	$3,040	$0	$3,859	$386	$0	$637	$4,881	$9
11.7	Standby equipment	$281	$0	$281	$0	$562	$56	$0	$93	$711	$1
11.8	Main power transformers	$20,468	$0	$179	$0	$20,647	$2,065	$0	$3,407	$26,119	$46
11.9	Foundations	$0	$186	$512	$0	$698	$70	$0	$230	$999	$2
	Subtotal	**$38,461**	**$16,994**	**$30,930**	**$0**	**$86,386**	**$8,639**	**$0**	**$18,206**	**$113,231**	**$201**
12		Instrumentation & Control									
12.1	Plant control equip	$0	$0	$0	$0	$0	$0	$0	$0	$0	$0
12.2	GT control equipment	$0	$0	$0	$0	$0	$0	$0	$0	$0	$0
12.3	Steam turbine control	$0	$0	$0	$0	$0	$0	$0	$0	$0	$0
12.4	Other major equip control	$1,336	$0	$911	$0	$2,247	$225	$124	$388	$2,984	$5
12.5	Signal processing	$0	$0	$0	$0	$0	$0	$0	$0	$0	$0
12.6	Boards, panels & racks	$307	$0	$201	$0	$509	$51	$28	$118	$705	$1
12.7	Computer & accessories	$7,128	$0	$233	$0	$7,361	$736	$405	$850	$9,352	$17
12.8	Instrument wiring & tubing	$0	$2,750	$5,197	$0	$7,947	$795	$437	$2,290	$11,469	$20
12.9	Other I&C equipment	$4,764	$0	$2,362	$0	$7,127	$713	$392	$1,231	$9,462	$17
	Subtotal	**$13,536**	**$2,750**	**$8,904**	**$0**	**$25,190**	**$2,519**	**$1,385**	**$4,877**	**$33,972**	**$60**
13		Improvements to Site									
13.1	Site prep	$0	$125	$2,837	$0	$2,961	$296	$0	$977	$4,235	$8
13.2	Site improvements	$0	$2,220	$3,138	$0	$5,357	$536	$0	$1,768	$7,661	$14
13.3	Site facilities	$3,977	$0	$4,463	$0	$8,441	$844	$0	$2,785	$12,070	$21
	Subtotal	**$3,977**	**$2,344**	**$10,438**	**$0**	**$16,759**	**$1,676**	**$0**	**$5,531**	**$23,966**	**$43**
14		Buildings & Structures									
14.1	GT area	$0	$318	$180	$0	$497	$50	$0	$109	$656	$1
14.2	Steam turbine building	$0	$0	$0	$0	$0	$0	$0	$0	$0	$0
14.3	Administration building	$0	$1,072	$778	$0	$1,850	$185	$0	$305	$2,340	$4
14.4	Circ water pumphouse	$0	$199	$105	$0	$304	$30	$0	$50	$385	$1
14.5	Water treatment buildings	$0	$685	$640	$0	$1,325	$132	$0	$219	$1,676	$3
14.6	Machine shop	$0	$539	$372	$0	$911	$91	$0	$150	$1,153	$2
14.7	Warehouse	$0	$871	$561	$0	$1,432	$143	$0	$236	$1,811	$3
14.8	Other buildings & structures	$0	$521	$405	$0	$926	$93	$0	$204	$1,222	$2
14.9	Waste treatment building	$0	$1,164	$2,224	$0	$3,388	$339	$0	$745	$4,472	$8
	Subtotal	**$0**	**$5,366**	**$5,265**	**$0**	**$10,631**	**$1,063**	**$0**	**$2,019**	**$13,713**	**$24**
	Total	**$957,876**	**$101,777**	**$498,402**	**$0**	**$1,558,055**	**$155,805**	**$63,048**	**$283,303**	**$2,060,211**	**$3,663**

Exhibit 6-6 Owner's costs for direct-fired sCO_2 plant

Owners' Costs ($K)		
Preproduction Costs		
6 Months Fixed O&M	$17,836	
1 Month Variable O&M	$4,737	
25% of 1 Month's Fuel Cost	$2,731	
2% of TPC	$41,204	
Inventory Capital		
60 Day Supply of Fuel and Consumables	$22,247	
0.5% of TPC for Spare Parts	$10,301	
Other Costs		
Initial Catalyst and Chemicals	$5,525	
Land (300 acres)	$900	
Other Owners' Costs	$309,032	
Financing Costs	$55,626	
Total Owners' Costs		$470,139
Total Overnight Cost		$2,530,350
Total As-Spent Cost (TASC)		$2,884,600

Exhibit 6-7 Operating and maintenance costs for direct-fired sCO_2 plant

Annual O&M Costs ($) @80 % Capacity Factor				
Fuel Cost			**($/yr)**	**($/MW-hr)**
	Bituminous Coal		104,866,720	26.61
Total Fuel			**104,866,720**	**26.61**
Fixed Operating Cost		**Unit Cost**	**($/yr)**	**($/kW)**
	Operating Labor	39.7 $/hr	7,233,658	13
	Maintenance Labor		21,304,529	38
	Administrative & Support Labor		7,134,547	13
	Total Labor		35,672,733	63
	Taxes & Insurance		41,204,229	73
Total Fixed O&M			**76,876,962**	**137**
Variable O&M Cost		**Unit Cost**	**($/yr)**	**($/MW-hr)**
	Maintenance Materials		38,214,973	9.70
	Water		1,190,088	0.30
	Chemicals			
	Water Treatment	0.27 $/lb	1,817,194	0.46
	Carbon (Mercury Removal)	1.63 $/lb	41,304	0.01
	AGR Solvent	36.79 $/gal	32,088	0.01
	COS Catalyst	3751.7 $/m3	211,610	0.05
	Claus Catalyst	203.15 $/ft3	107,799	0.03
	Total Chemicals		2,209,995	0.56
	Waste Disposal			
	Spent Mercury Sorbent	0.65 $/lb	16,471	0.00
	Slag	25.11 $/lb	3,847,816	0.98
	Total Waste Disposal		3,864,287	0.98
Total Variable O&M			**45,479,343**	**11.54**

Exhibit 6-8 COE breakdown for direct-fired sCO_2 plant

Component	Value, $/MWh	Percentage
Capital	79.6	58%
Fixed O&M	19.5	14%
Variable O&M	11.5	8%
Fuel	26.6	19%
Total (Excluding T&S)	**137.3**	**N/A**
CO_2 T&S	8.8	6%
Total (Including T&S)	**146.1**	**N/A**

An account-level breakdown of the TPC for the baseline direct-fired sCO_2 plant is shown in Exhibit 6-9. This is dominated by the costs in the Gasifier & Accessories account, which comprises 49 percent of the TPC for the plant, compared to 13 percent for the sCO_2 cycle, the next largest account. The breakout pie chart shows that this account comprises the Gasifier, Syngas Cooler, and ASU & Oxygen Compression sub-accounts, with the remaining sub-accounts lumped into the Gasifier Accessories item. The most significant opportunities for reducing the capital costs of the baseline sCO_2 plant, therefore, lie in selecting a more cost-effective gasifier, or in reducing syngas cooler or ASU costs, rather than in reducing costs of the sCO_2 cycle components, which are shown separately in Exhibit 6-10. The sCO_2 cycle TPC is dominated by costs for compressors and pumps, which account for about 59 percent of the overall account, compared to only 20 percent for the sCO_2 turbine. Recuperator and cooler costs only account for about 11 percent of the cycle TPC, due in large part to the larger log-mean temperature differences between the hot and cold sides (see Exhibit 5-9), which allow for more compact heat exchangers.

Exhibit 6-9 Relative account costs for the direct-fired sCO2 plant TPC

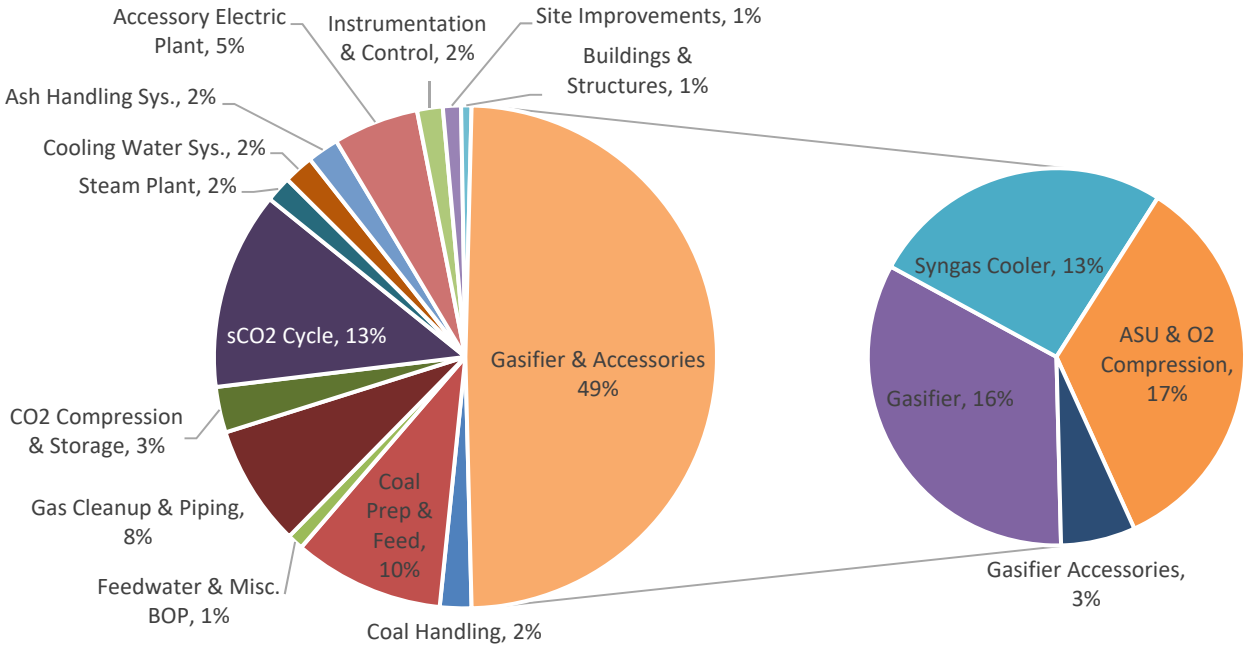

Exhibit 6-10 Relative sub-account component costs for the sCO_2 Cycle Account

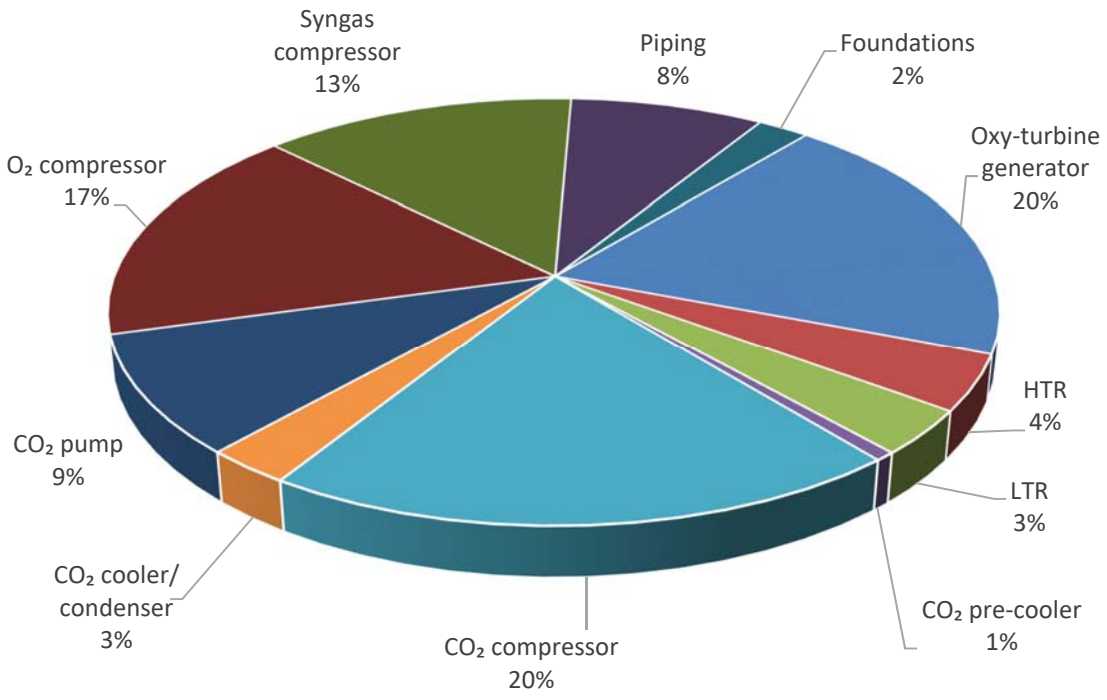

6.2.3 Comparison of Direct-fired sCO_2 Case with Reference Case

Compared to the reference IGCC plant, the direct-fired sCO_2 plant produces 13 percent more net power using 6 percent less coal, resulting in a 21 percent higher HHV efficiency. The expected effect on the capital cost estimate is that the BOP components related to fuel processing and cleanup should be on the order of 6 percent lower for the sCO_2 plant. An exception to this is the high-temperature syngas cooler, which has an approximately 25 percent higher duty in the sCO_2 case and a proportionally higher capital cost. Because the direct-fired sCO_2 plant is oxy-fired, the ASU cost would be expected to be much higher than the reference IGCC plant, but the oxy-fired plant can generate a raw CO_2 product stream at pressure resulting in a significant cost savings in the CO_2 purification unit due to the elimination of the feed stream compressor. Further, the oxy-fired plant does not require a CO_2 capture unit. Because the power islands are so different in the two cases, the difference in their relative cost cannot be anticipated based on overall plant performance. However, the 13 percent higher net power output suggests that the sCO_2 power island cost could be on the order of 13 percent higher than the reference IGCC power island cost (including boiler feedwater processing) without adversely impacting the COE.

Exhibit 6-11 compares the account level TPC between the sCO_2 plant and the reference IGCC plant. Exhibit 6-12 compares the annual O&M costs between the two plants and Exhibit 6-13 compares the COE between the two plants. Additional economic comparisons are made to other sCO_2 and IGCC studies in Section 7.

Exhibit 6-11 Comparison of capital cost between the sCO_2 and IGCC plants

Account	sCO_2 Plant		Reference IGCC Plant, Case B1B	
	TPC ($1000)	TPC ($/kW)	TPC ($1000)	TPC ($/kW)
Coal Handling System	41,775	74	43,156	87
Coal Prep and Feed	199,571	355	218,724	440
Feedwater and Miscellaneous BOP	21,252	38	65,849	133
Gasifier and Accessories	1,014,116	1,803	681,168	1,371
Gas Cleanup & Piping	160,519	285	323,580	651
CO_2 Compression & Storage	60,601	108	81,688	164
sCO_2 Cycle /Combustion Turbine & Acc.	261,793	465	160,049	322
HRSG Ductwork & Stack	0	0	56,527	114
Steam Plant	34,428	61	85,322	172
Cooling Water System	39,523	70	39,217	79
Ash/Spent Sorbent Handling Sys.	41,753	74	42,945	86
Accessory Electric Plant	113,231	201	103,353	208
Instrumentation and Control	33,972	60	32,252	65
Improvements to Site	23,966	43	22,691	46
Buildings and Structures	13,713	24	21,081	42
Total	**2,060,211**	**3,663**	**1,977,603**	**3,981**

Exhibit 6-12 Comparison of annual O&M costs between the sCO_2 and IGCC plants

Account	sCO_2 Plant		Reference IGCC Plant	
	$1000/yr	$/MW-hr	$1000/yr	$/MW-hr
Fixed O&M	76,877	19.5	71,389	20.5
Variable O&M	45,479	11.5	45,146	13.0
Fuel	104,867	26.6	111,740	32.1

Exhibit 6-13 Comparison of COE between the sCO_2 and IGCC plants

COE Component	sCO_2 Plant $/MWh	Reference IGCC Plant $/MWh
Capital	79.6	87.0
Fixed O&M	19.5	20.5
Variable O&M	11.5	13.0
Fuel	26.6	32.1
Total (Excluding T&S)	**137.3**	**152.6**
CO_2 T&S	8.8	9.8
Total (Including T&S)	**146.1**	**162.4**

The relative differences in the TPC for the capital cost accounts in Exhibit 6-11 qualitatively follow the expected trends. The Coal Handling, Coal Prep, and Ash Handling accounts show a relative decrease compared to the reference IGCC plant proportional to the decrease in coal feed rate. The increase in relative TPC for Accounts Accessory Electric Plant, Instrumentation & Control, and Improvements to Site reflect the larger plant output and larger TPC of the sCO_2 plant compared to the reference IGCC plant. The TPC for the Gasifier account is 49 percent higher for the sCO_2 plant; this is due to a combination of effects including the larger ASU needed to produce oxygen for the oxy-combustor and the larger syngas cooler to preheat the sCO_2 feed to the oxy-combustor. The impact of the higher ASU TPC in the sCO_2 plant is more than offset by a reduction in the gas cleanup cost (due to not having to capture the CO_2) and the CO_2 compression cost (since the CO_2 is delivered to the CPU at pressure).

The sCO_2 power island TPC is 64 percent higher than a combustion turbine generator for the reference IGCC plant but it is 2 percent lower than the aggregate power island TPC for the IGCC plant (including HRSG and Steam Plant accounts). Overall, the TPC for the sCO_2 plant is 4 percent higher than the reference IGCC plant. However, when comparing on a $/kW basis, the sCO_2 capital cost accounts are all significantly lower than the IGCC plant accounts, except for the gasifier (32 percent higher). Overall, on a $/kW basis, the TPC for the sCO_2 plant is 8 percent less than the reference IGCC plant.

Per Exhibit 6-13, the COE for the sCO_2 plant is 10 percent lower than the COE for the reference IGCC plant both with and without T&S costs. This decrease in COE is primarily due to the higher efficiency of the sCO_2 plant.

6.3 SENSITIVITY ANALYSES

6.3.1 Sensitivity Analysis to Total Plant Cost

Given that many of the components of the sCO_2 cycle have never been built at commercial scale, there is considerable uncertainty in the capital cost estimates for these components. Although contingencies have been added, they may not fully account for the cost uncertainty. A rough sensitivity analysis was performed on the TPC and it was determined that for the sCO_2 plant, if the TPC increases by 296 MM$ (14.4 percent), the COE without T&S will rise to the same value as for the reference IGCC plant, $152.6/MWh. If the TPC increases by 316 MM$ (15.3 percent), the COE with T&S will rise to the same value as for the reference IGCC plant, $162.4/MWh. These results are shown in Exhibit 6-14, which plots the COE (with and without T&S) as a function of the increase in TPC above the value shown in Exhibit 6-5. The horizontal dashed lines denote the COE values for the reference IGCC plant. Given that the TPC for the sCO_2 cycle components totals 262 MM$, there is a considerable buffer in the sCO_2 cycle component cost estimates for the baseline sCO_2 plant to show economic benefits relative to the reference IGCC plant.

Exhibit 6-14 Sensitivity of COE to increase in TPC for the sCO_2 plant

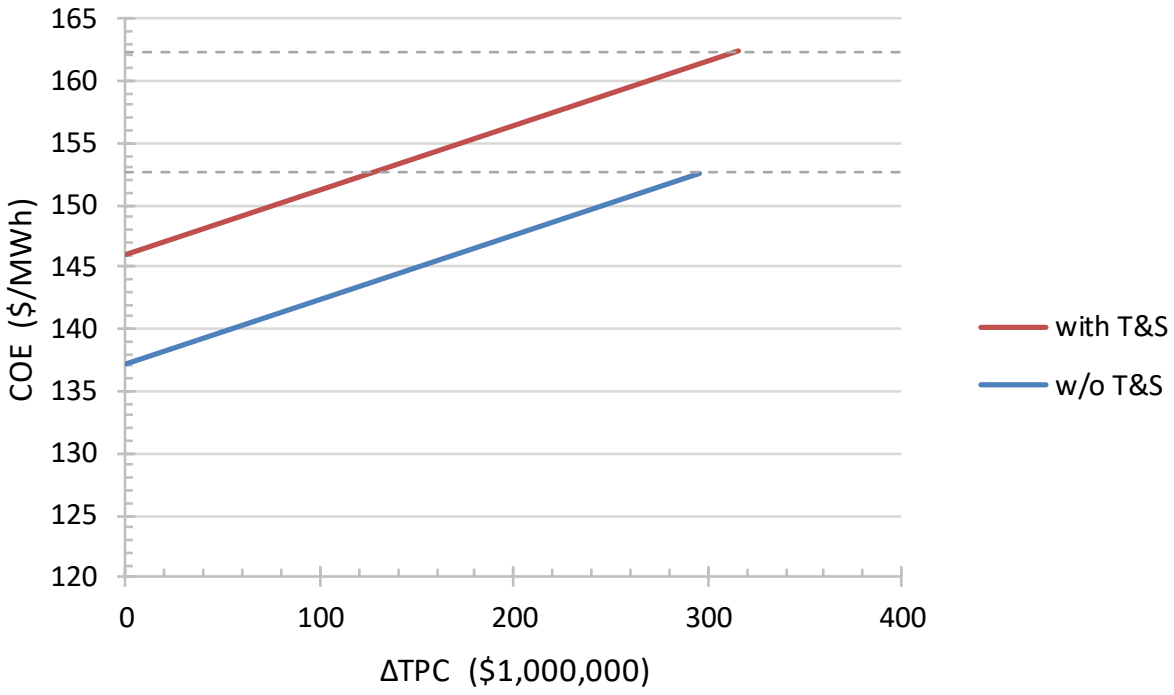

6.3.2 Sensitivity Analysis to CO_2 Preheating

Preheating the CO_2 feed stream to the oxy-combustor is advantageous from an efficiency standpoint. However, the only high-quality heat source available to perform this preheating is from the syngas cooler. Due to its high temperature and pressure, this heat exchanger is

relatively costly, accounting for 13 percent of the plant's TPC per Exhibit 6-9. To determine whether this preheating configuration is economically advantageous, a sensitivity analysis was performed on the baseline case in which no preheating was performed on the CO_2 feed stream to the oxy-combustor. Preheating of the syngas fuel to the oxy-combustor by the syngas cooler was maintained. Exhibit 6-15 shows the results from that case compared to the baseline case.

Elimination of the preheating results in a loss of approximately 57 MW of thermal input to the cycle, which results in a 31.5 MW drop in net plant output and a drop in overall process efficiency of 2.1 percentage points. However, the reduction in the syngas cooler size resulted in a drop in TPC of 172 MM$. The COE without T&S was reduced by 1.3 $/MWh (0.9 percent) and the COE with T&S was reduced 0.8 $/MWh (0.5 percent). This suggests that while preheating the CO_2 feed to the oxy-combustor with the syngas cooler improves efficiency significantly, it is not economically advantageous.

Exhibit 6-15 Sensitivity of baseline case to CO_2 preheating

Item	sCO_2 Baseline	sCO_2 w/o CO_2 preheat
Performance Results		
Gross Power (kWe)	777,080	745,068
Net Auxiliary Load (kWe)	-214,659	-214,135
Net Plant Power (kWe)	562,421	530,903
Net Plant Efficiency (HHV, %)	37.7	35.6
Thermal Input (kW_t)	1,492,815	1,492,815
Carbon Captured (%)	98.1	98.1
Captured CO_2 Purity (%)	99.8	99.8
Economic Results		
Total plant cost ($1,000)	2,060,211	1,888,264
Total plant cost ($/kW)	3,663	3,557
COE without T&S ($/MWh)	137.3	136.0
COE with T&S ($/MWh)	146.1	145.3

7 COMPARISON TO OTHER STUDIES

A comparison of these performance results against other gasification-based sCO_2 [3] [4] and IGCC [2] [5] plant design studies is shown in Exhibit 7-1 and Exhibit 7-2, while comparison of economic results is shown in Exhibit 7-3 and Exhibit 7-4.

Exhibit 7-1 Plant design and performance comparison

Item	sCO_2 Baseline	EPRI Case 3 [3]	8 Rivers Case 1 [4]	Reference IGCC Shell Gasifier [2]	Reference IGCC GE Gasifier [2]	IGCC-AHT [5]	IGCC-THT [5]
Coal Type	Illinois #6	PRB	Illinois #6	Illinois #6	Illinois #6	Illinois #6	Illinois #6
Coal Feed	Dry	Dry	Dry	Dry	Water Slurry	Water Slurry	Water Slurry
Gasifier Type	Shell	Shell	Shell	Shell	GE-RGC	GE-RGC	GE-RGC
Syngas Heat Recovery	Syngas cooler	Syngas cooler	Syngas cooler	Syngas cooler	Radiant Syngas cooler	Radiant Syngas cooler	Radiant Syngas cooler
Other Processes	Steam plant	Steam power cycle	None	Gas turbine steam cycle	Gas turbine steam cycle	AHT + steam cycle	THT + steam cycle
Sulfur Removal	AGR	AGR	DeSNOx	AGR	AGR	AGR	AGR
Turbine Cooling	Yes	No	?	Yes	Yes	Yes	Yes
Turbine Inlet Temp. (°C)	1204	1123	1150	1337	1337	1450	1700
Net Plant Power (MWe)	562	583	~280	497	543	771	1057
Net Plant Efficiency (HHV, %)	37.7	39.6	49.6	31.2	32.6	35.7	38.0
Carbon Captured (%)	97.6	99.2	~100	90.0	90.0	90.0	90.0
Captured CO_2 Purity (%)	99.8	98.1	?	99.4	99.5	99.5	99.5

Exhibit 7-2 Net plant efficiency comparison

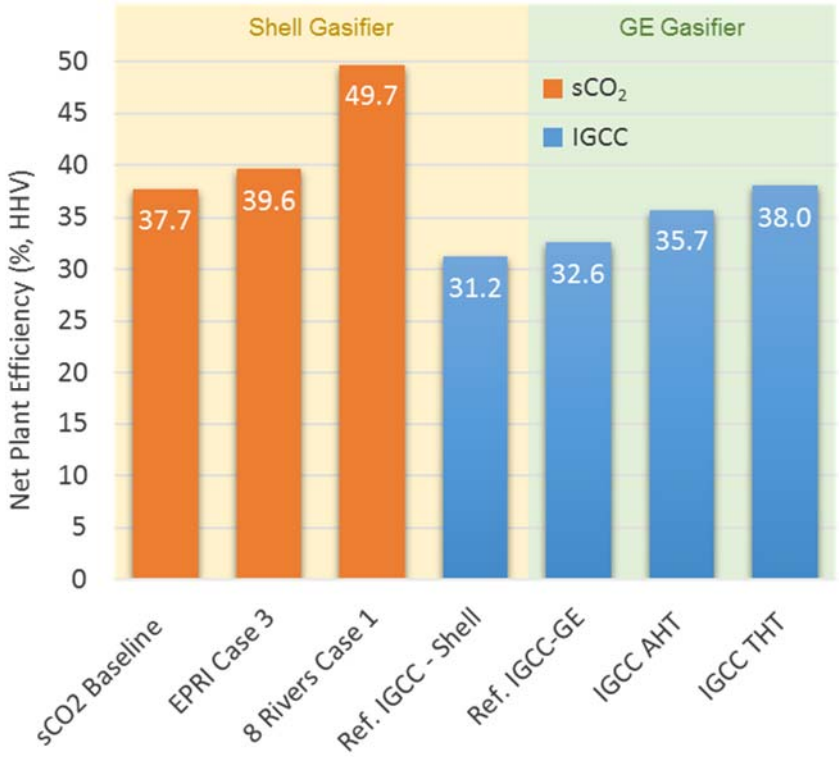

Exhibit 7-3 Cost of electricity comparison

Component COE ($/MWh)	sCO_2 Baseline	EPRI Case 3	Reference IGCC- Shell	Reference IGCC-GE	IGCC AHT	IGCC THT
Capital	79.6	85.8	87.0	74.2	61.0	53.6
Fixed O&M	19.5	13.0	20.5	18.2	14.6	12.5
Variable O&M	11.5	13.0	13.0	12.2	10.2	9.1
Fuel	26.6	15.8	32.1	30.7	28.1	26.4
Total (w/o T&S)	**137.3**	**127.6**	**152.6**	**135.4**	**114.0**	**101.6**
CO_2 T&S	8.8	8.3	9.8	9.2	8.4	7.9
Total (w / T&S)	146.1	135.9	162.4	144.7	122.4	109.5

Exhibit 7-4 Cost of electricity breakdown

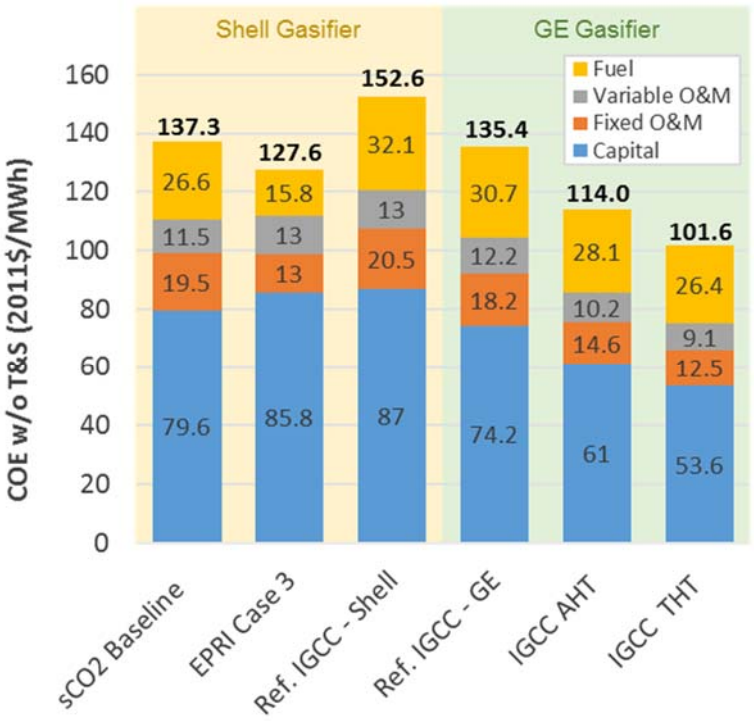

The thermal efficiency and COE of the baseline sCO_2 plant calculated in this study are similar to that from the EPRI study. [3] Per Exhibit 7-1, both studies include the use of a Shell gasifier, dry coal feeding, syngas heat recovery, an acid gas removal (AGR) process for sulfur removal, high-purity oxygen, and CO_2 coal transport fluid to minimize nitrogen impurities in the sCO_2 cycle. There are several notable differences between these two studies that contribute to the differences in plant performance. The largest of these differences is in the fuel gasified, where EPRI uses a low-sulfur sub-bituminous Powder River Basin (PRB) coal, and the present study uses a higher value bituminous coal (Illinois No. 6). Additional differences in the baseline sCO_2 plant design that contribute to reduced efficiency relative to EPRI's Case 3 plant design include the inclusion of turbine cooling streams, high combustor pressure drops, and a carbon purification system. EPRI's steam bottoming cycle, which generates power from the thermal energy from the gasification train, may further improve plant efficiency at the expense of higher capital cost. Differences in the baseline sCO_2 plant design expected to contribute to improved plant efficiency relative to the EPRI study include: a higher sCO_2 TIT, inclusion of syngas preheating, and a lower cold sCO_2 temperature (26.7 °C vs. 29.5 °C) for reduced sCO_2 compression power. All told, the baseline sCO_2 plant has a lower efficiency relative to the EPRI study, but includes a more detailed plant model. [3]

The economics for the EPRI study have been updated from June 2014 dollars to June 2011 dollars used in this study, and most other NETL baseline studies, by applying a CEPCI scaling factor of 1.022. While absolute comparisons are difficult due to differing cost accounting methods and economic assumptions used between the two studies, a few general comparisons can be made. The total plant cost in Case 3 of the EPRI study is $2.8 billion dollars

(2011 basis), compared to $2.06 billion in the current study. The largest differences are in the gasifier + ASU account, where EPRI's costs are $420 million higher, and in the sCO_2 cycle costs, where about 48 percent in process and project contingencies has been added for first-of-a-kind technology, compared to about 15 percent in the present study, which is more representative of n^{th}-of-a-kind technology. Comparing the COE results between the two studies, the COE for the sCO_2 baseline plant of the present study ($137.3/MWh, w/o CO_2 T&S) is very comparable to that of the EPRI study ($127.7/MWh, w/o T&S). The contribution of capital costs is shown to be higher in the EPRI study, as shown in Exhibit 7-4 and discussed above, while significant fuel savings are realized in the EPRI study due to the use of low rank sub-bituminous coal. [3]

A study of the influence of several gasification types on overall plant performance was performed by 8 Rivers Capital. [13] [4] Among the cases studied, Case 1 is the most similar to the current study, employing a high-purity ASU to minimize nitrogen and argon diluent in the sCO_2 cycle, a Shell gasifier with dry feed of Illinois No. 6 coal, and a syngas cooler for high- and low-grade heat recovery. The efficiency of this case is 49.7 percent, compared to 37.7 percent in the baseline sCO_2 plant of this study. [4]

The modeled cases from 8 Rivers Capital represent a large departure in configuration and thermal integration from the current study. These cases hinge on successfully being able to move the syngas sulfur and nitrogen cleanup processes from the gasification train to the sCO_2 cycle. This eliminates the need for a large AGR plant, as well as its associated steam requirements, and allows for utilization of the energy content of the sulfur-bearing species in the syngas within the sCO_2 plant. [4] This is contingent on the development and demonstration of this strategy, as well as on a careful consideration of the corrosion effects on the sCO_2 cycle components and materials. Additional efficiency and cost savings benefits are claimed by proposing water quench syngas cooling, with recovery of low-grade thermal energy through cooling and condensation of the steam content in the post-quench syngas. [4] Considering the significant cost of the syngas coolers in the present work, this may be an attractive option to pursue in future studies.

Another interesting comparison can be made between the baseline sCO_2 plant of the current study and the Transformational Turbines Supplement to NETL's IGCC Pathway Study. [5] [27] As discussed in Section 2.7, this study considered the effects of hydrogen turbines and other advances on the performance and cost of an IGCC plant. Two hydrogen turbines were considered, an AHT with a firing temperature of 1449 °C (2640 °F) and a pressure ratio of 23.8, and a THT, with a firing temperature of 1704 °C (3100 °F) and a pressure ratio of 30.4. The effects of replacing the conventional hydrogen turbine (1137 °C firing temperature, 17.6 pressure ratio) with the AHT and THT are considered individually for an IGCC plant based on a GE gasifier with a radiant syngas cooler. [5]

These two cases are shown in Exhibit 7-1, as well as the reference IGCC case with the GE gasifier. Differences between the cases are more clearly shown in Exhibit 7-2, where the Shell gasifier cases on the left are contrasted with the GE gasifier cases on the right. Note that the GE gasifier results in a reference IGCC plant with CCS that is 1.4 percentage points more efficient than the corresponding Shell gasifier plant. [2] Even with this advantage, the Shell-

gasifier baseline sCO_2 plant from this study outperforms the AHT turbine case by 2 percentage points, and is comparable to the THT turbine case, despite lower TITs for the sCO_2 turbine. [5]

Comparing the economics in Exhibit 7-3 and Exhibit 7-4, the baseline GE gasifier IGCC case produces electricity at a cost that is $17.2/MWh (w/o T&S) lower than the baseline Shell gasifier IGCC case. [2] Replacing the GE gasifier conventional turbine for the AHT and THT results in $114.0/MWh and $101.6/MWh, respectively, without T&S [5] These cases produce electricity at a lower cost than the sCO_2 baseline plant design, though one might expect the sCO_2 baseline cycle to be competitive with the AHT IGCC case if the two cases were compared using the same gasifier train.

8 CONCLUSIONS AND FUTURE WORK

A conceptual design for a commercial-scale, baseline coal-fueled direct-fired sCO_2 power plant has been developed. This was done by first analyzing the gasifier technologies and choosing one that would pair well with the direct-fired sCO_2 Brayton cycle, followed by a detailed analysis of the degrees of freedom in the sCO_2 cycle. Based on a review of the literature on coal-fueled direct-fired sCO_2 power plants and an analysis of Brayton cycles done previously at NETL, an initial cycle configuration and state point was selected.

Following this, significant efforts were directed towards improving the accuracy and performance of the cycle model. An extensive analysis was performed on the accuracy of various EOSs for coal-fueled direct sCO_2 gas mixtures, which resulted in a change in Aspen physical property models from PR-BM (based in the Peng-Robinson EOS, as used in the preliminary study) to LK-PLOCK (based on the Lee-Kessler-Plöcker EOS). Further, for the TIT proposed for the initial baseline, it was deemed necessary to incorporate blade cooling flows in the turbine. The cooling bleed stream was taken from the outlet of the LTR. The amount of cooling required was calculated by correlating data from the literature. [1] An algorithm was derived to distribute the cooling bleed between turbine stages based on the inlet temperature of the working fluid at each blade.

Several sensitivity analyses were performed to guide potential improvements in the plant configuration or state point. It was determined that significant improvements to process efficiency can be realized by adding three stages of intercooling to the pre-compressor, lowering the CO_2 cooler temperature to 26.7 °C (80 °F), and increasing the CO_2 TIT to 1204 °C (2200 °F). A change in the oxidant insertion point was examined as a way to extract additional high-quality heat from the syngas coolers. While it was found to slightly increase process efficiency, there were many secondary impacts that indicate that such a change is not advisable. Finally, the impact of eliminating the costly high-temperature syngas coolers was examined. An initial screening level assessment indicated that this would result in a process efficiency reduction of approximately 2 percentage points, but improve COE slightly.

Based on the results from the sensitivity analyses, a final sCO_2 cycle and plant configuration was developed and the performance of the plant was estimated from an Aspen model. The results showed a net plant efficiency of 37.7 percent on a HHV basis, which includes capture of 98.1 percent of the input carbon at a purity of 99.8 percent. This is significantly higher than the reference Shell IGCC plant efficiency of 31.2 percent, which includes a carbon capture rate of 90 percent.

An economic analysis was performed on the commercial-scale sCO_2 plant, though with a high degree of uncertainty in the results, given that a successful pilot-scale demonstration of this technology has not yet been performed. Compared to the reference IGCC plant, the absolute TPC was 4 percent higher for the sCO_2 plant, though the TPC on a $/kW basis was 8 percent lower. The TPC of the sCO_2 plant was dominated by the capital costs of the gasifier, syngas coolers, and ASU, rather than by sCO_2 cycle components. The COE for the sCO_2 plant is 10 percent lower than for the reference IGCC plant both with and without CO_2 T&S costs. Both

the decrease in TPC on a $/kW basis and the decrease in COE are primarily due to the higher efficiency of the sCO_2 plant.

Overall, the proposed direct sCO_2 cycle studied here provides a significant efficiency benefit compared to other coal-based power generation processes with CCS. The sensitivity analyses, and further comparisons to similar studies, show significant room for improvement in the cycle design to maximize plant efficiency and minimize COE, which will be pursued in future studies. In particular, additional consideration of thermal integration between the recuperators and gasifier processes, while also incorporating oxygen preheating, should further improve plant efficiency and reduce COE. Other types of gasifiers may also be considered in future work. Quench-style gasifiers have been shown to be cost-effective in the studies of 8 Rivers Capital [13], while GE gasifiers have shown efficiency and capital cost benefits over Shell gasifiers in IGCC studies, despite lower cold gas efficiencies. [2] Further, a catalytic gasifier may be very well suited to direct sCO_2 cycles, as cold gas efficiencies are very high for these gasifiers, and the additional syngas methane content that is problematic to achieving high IGCC carbon capture efficiencies is easily handled by the direct sCO_2 cycle.

9 REFERENCES

[1] International Energy Agency Greenhouse Gas (IEAGHG), "Oxy-combustion Turbine Power Plants," Cheltenham, United Kingdom, August 2015.

[2] National Energy Technology Laboratory (NETL), "Cost and Performance Baseline for Fossil Energy Plants Volume 1b: Bituminous Coal (IGCC) to Electricity Revision 2b – Year Dollar Update," Pittsburgh, Pennsylvania, 2015.

[3] Electric Power Research Institute (EPRI), "Performance and Economic Evaluation of Supercritical CO2 Power Cycle Coal Gasification Plant," (3002003734), Palo Alto, California, December, 2014.

[4] X. Lu., B. Forrest, S. Martin, J. Fetvedt, M. McGroddy and D. Freed, "Integration and Optimization of Coal Gasification Systems with a Near Zero Emissions Supercritical Carbon Dioxide Power Cycle," in *ASME Turbo Expo*, Seoul, South Korea, June 13-17, 2016.

[5] W. W. Shelton, R. Ames, R. Dennis, C. W. White, J. Plunkett, J. Fisher and R. Dalton, "Advanced and Transformational Hydrogen Turbines for Integrated Gasification Combined Cycles," in *ASME Turbo Expo, ASME Paper: GT2016-57723*, Seoul, South Korea, June 13-17, 2016.

[6] W. Shelton, N. Weiland, C. White, J. Plunkett and D. Gray, "Oxy-Coal-Fired Circulating Fluid Bed Combustion with a Commercial Utility-Size Supercritical CO2 Power Cycle," in *The 5th International Symposium - Supercritical CO2 Power Cycles*, San Antonio, Texas, March 29-31, 2016.

[7] B. Purgert and J. Shingledecker, "Update on U.S. DOE/OCDO Advanced Ultra-supercritical Steam Boiler and Turbine Consortium," in *Presented at the DOE-FE Cross-Cutting Review Meeting*, Pittsburgh, PA, April 29, 2015.

[8] R. Allam, "NET Power: Carbon Capture & Utilization from Power Generation," in *NEPIC International Bioresources Conference*, Newcastle, UK, June 19, 2014.

[9] R. Allam, M. R. Palmer, G. W. Brown Jr., J. Fetvedt, D. Freed, H. Nomoto, M. Itoh, N. Okita and C. Jones Jr, "High Efficiency and Low Cost of Electricity Generation from Fossil Fuels While Eliminating Atmospheric Emissions, Including Carbon Dioxide," *Energy Procedia,* vol. 37, pp. 1135-1149, 2013.

[10] R. Allam, J. Fetvedt, B. Forrest and D. Freed, "The Oxy-Fuel, Supercritical CO2 Allam Cycle: New Cycle Developments to Produce Even Lower-Cost Electricity from Fossil Fuels without Atmospheric Emissions," in *ASME Turbo Expo*, Düsseldorf, Germany, 2014.

[11] A. McClung, K. Brun and J. Delimont, "Comparison of Supercritical Carbon Dioxide Cycles for Oxy-Combustion," in *ASME Turbo Expo*, Montréal, Canada, 2015.

[12] Shell Global, "CANSOLV carbon dioxide (CO2) capture system," [Online]. Available: http://www.shell.com/business-customers/global-solutions/shell-cansolv-gas-absorption-solutions/cansolv-co2-capture-system.html. [Accessed 11 March 2017].

[13] X. Lu, "Flexible Integration of the sCO2 Allam Cycle with Coal Gasification Low-Cost Emission-Free Electricity Generation," GTC, 2014.

[14] N. Weiland, W. Shelton, C. White and D. Gray, "Performance baseline for direct-fired sCO2 cycles," in *5th International Supercritical CO2 Power Cycles Symposium*, San Antonio, Texas, March 29-31, 2016.

[15] C. W. White and N. T. Weiland, "Evaluation of Property Methods for Modeling Direct-Supercritical CO2 Power Cycles," in *Proceedings of ASME Turbo Expo 2017: Turbomachinery Technical Conference and Exposition: GT2017-64261*, Charlotte, NC, June 26-30, 2017.

[16] National Energy Technology Laboratory (NETL), "Cost and Performance Baseline for Fossil Energy Plants Volume 1: Bituminous Coal and Natural Gas to Electricity, Revision 3," June 2015.

[17] National Energy Technology Laboratory (NETL), "Quality Guidelines for Energy System Studies, Cost Estimation Methodology for NETL Assessments of Power Plant Performance," January 2013.

[18] National Energy Technology Laboratory (NETL), "Quality Guidelines for Energy System Studies -- Fuel Prices for Selected Feedstocks in NETL Studies," Pittsburgh, Pennsylvania, November, 2012.

[19] National Energy Technology Laboratory (NETL), "Quality Guidelines for Energy System Studies: Estimating Carbon Dioxide Transport and Storage Costs," Pittsburgh, Pennsylvania, March, 2013.

[20] National Energy Technology Laboratory (NETL), "Quality Guidelines for Energy System Studies: Carbon Dioxide Transport and Storage Costs in NETL Studies," Pittsburgh, Pennsylvania, September, 2013.

[21] National Energy Technology Laboratory (NETL), "Quality Guidelines for Energy System Studies -- Process Modeling Design Parameters," Pittsburgh, Pennsylvania, May, 2014.

[22] National Energy Technology Laboratory (NETL), "Quality Guidelines for Energy System Studies -- Detailed Coal Specifications," Pittsburgh, PA, January, 2012.

[23] National Energy Technology Laboratory (NETL), "Quality Guidelines for Energy System Studies -- CO2 Impurity Design Parameters," Pittsburgh, Pennsylvania, August, 2013.

[24] National Energy Technology Laboratory (NETL), "Quality Guidelines for Energy System Studies -- Capital Cost Scaling Methodology," Pittsburgh, Pennsylvania, January, 2013.

[25] AACE International Recommended Practice Number 16R-90, "Conducting Technical and Economic Evaluations -- As Applied for the Process and Utility Industries; TCM Framework 7.3 -- Cost Estimating and Budgeting," AACE, 2003.

[26] National Energy Technology Laboratory (NETL), "FE/NETL CO2 Saline Storage Cost Model, DOE/NETL-2014/1669," Pittsburgh, PA, July, 2014.

[27] National Energy Technology Laboratory (NETL), "A Pathway Study on IGCC R&D with Carbon Capture Using Bituminous Coal Supplemental Chapter: Transformational Turbines," DOE/NETL-2014/1639, Pittsburgh, PA, June 23, 2015.

[28] National Energy Technology Laboratory (NETL), "Cost and Performance Baseline for Fossil Energy Plants Volume 3a: Low Rank Coal to Electricity: IGCC Cases," DOE/NETL-2010/1399, Pittsburgh, PA, May, 2011.

[29] Q. Zhao, M. Mecheri, T. Neveux, R. Privat and J.-N. Jaubert, "Thermodynamic model investigation for supercritical CO2 Brayton cycle for coal-fired power plant application," in *5th International Supercritical CO2 Power Cycles Symposium*, San Antonio, Texas, March 29-31, 2016.

[30] National Institute of Standards and Technology (NIST), *NIST Reference Fluid Thermodynamic and Transport Properties - REFPROP,* U.S. Department of Commerce, 2007.

[31] National Energy Technology Laboratory (NETL), "CO2 Compressor Simulation User Manual," Carbon Capture Simulation Initiative, October 6, 2013.

[32] D. Thimsen, "Regen-SCOT: Rocket Engine-Derived High Efficiency Turbomachinery for Electric Power Generation," EPRI Report 3002006513.

[33] H. Maeda, T. Tashima, S. Iwai, N. Okizono, I. Sato, K. Tsuruta and N. Okamura, "Turbine and Operating Method of the Same". USA Patent 2014/0023478 A1, 23 January 2014.

[34] Modern Power Systems, "sCO2 turbine for Allam Cycle," 4 August 2016. [Online]. Available: http://www.modernpowersystems.com/features/featuresco2-turbine-for-allam-cycle-4970656/. [Accessed 12 December 2016].

[35] N. T. Weiland and D. Thimsen, "A Practical Look at Assumptions and Constraints for Steady State Modeling of sCO2 Brayton Power Cycles," in *5th International Supercritical CO2 Power Cycles Symposium*, San Antonio, Texas, March 29-31, 2016.

[36] Y. Iwai and et al, "Gas Turbine Facility". USA Patent 2015/0020497 A1, 22 January 2015.

[37] M. T. Breslin, "Heavy Shell Casings Design/Operation and Repair Criteria," in *Proceedings of the 18th Turbomachinery Symposium*, 1989.

[38] Gas Turbine World, "GTW Handbook 2009," *Gas Turbine World,* pp. 72-91, 2009.

[39] Aerojet Rocketdyne, "Turbine Technology Program Phase III - Task 2(b): Supercritical CO2 Turbomachinery (SCOT) System Studies Recuperator Development," DOE Contract No. DE-FE0004002, August 13, 2014.

[40] R. Turton, R. C. Bailie, W. B. Whiting and J. A. Shaeiwitz, Analysis, Synthesis, and Design of Chemical Processes, 2nd Edition, Prentice Hall, 2003.

[41] National Energy Technology Laboratory (NETL), "Report on Newly Developed A-USC Materials," August 1, 2014.

10 APPENDIX A: PERFORMANCE BASELINE FOR DIRECT-FIRED sCO_2 CYCLES

The 5th International Symposium - Supercritical CO_2 Power Cycles
March 29-31, 2016, San Antonio, Texas
NETL-PUB-20257

PERFORMANCE BASELINE FOR DIRECT-FIRED sCO_2 CYCLES

Nathan Weiland
Engineer
National Energy Technology Laboratory
Pittsburgh, PA U.S.
Nathan.Weiland@NETL.DOE.GOV

Wally Shelton
Engineer
National Energy Technology Laboratory
Morgantown, WV U.S.
Walter.Shelton@NETL.DOE.GOV

Charles White
Senior Principal
Noblis
Falls Church, VA U.S.
Charles.White@noblis.org

David Gray
Senior Principal
Noblis
Falls Church, VA U.S.
DGray@noblis.org

Dr. Nathan Weiland is an engineer in the Systems Engineering & Analysis group at the National Energy Technology Laboratory (NETL), where he where he performs systems studies of supercritical CO_2 power cycles and oxy-fuel magneto-hydrodynamics (MHD) power plants. Prior to joining the systems analysis group he was a research professor at West Virginia University, where he worked with NETL on low-NOx hydrogen combustion, coal/biomass co-gasification, ash deposition processes in gasification systems, oxy-combustion plasmas for MHD power, and chemical looping combustion. He has received a BS (Purdue University), MS, and PhD (Georgia Tech) in Mechanical Engineering.

Walter Shelton is an engineer in the Systems Engineering & Analysis group at NETL supporting research/process development projects. Focused on the analysis and development of processes based on fossil fuels spanning both existing and emerging technologies that produce electrical power or a combination of power and chemicals. Key aspects involve performing system process studies that determine the efficiency, economic, regulatory and environmental impacts. The process studies are targeted to contribute to formulating and determining government/public policy. He received a BS (SUNYAB) and MS (U. of Minnesota) in Chemical Engineering.

Charles White is a senior principal engineer at Noblis, where he performs modeling, simulation, and systems analysis of fossil-fueled processes for producing electric power and transportation fuels. He has provided energy systems analysis modeling and simulation support to NETL since 1985. He received a PhD in chemical engineering from the University of Pennsylvania.

Dr. Gray is a senior principal engineer at Noblis. He has extensive experience in conversion of coal into electric power, fuels and chemicals and has provided research and development (R&D) guidance to NETL in those areas for many years. Prior to coming to the U.S. he worked in South Africa where he was an R&D manager operating pilot plants for alternative transportation fuels production. He has served on the National Academies of Sciences Committee on America's Energy Future and as a subject matter expert on the National Petroleum Council Study on Future Transportation Fuels. He received a PhD in physical chemistry from the University of Southampton in the United Kingdom.

ABSTRACT

Direct supercritical CO_2 (sCO_2) power cycles have recently received interest as a potentially lower-cost, fossil-fueled power source with inherent amenability to carbon capture. In this cycle, heat addition occurs via fossil fuel combustion with oxygen, while sCO_2 is recycled back to the combustor to limit combustion temperatures. This high-temperature and high-pressure working fluid is then expanded through a turbine. After water is condensed from the working fluid, a portion of the CO_2 is exhausted from the cycle, purified as needed, and pressurized for enhanced oil recovery (EOR) or storage.

NETL has conducted an evaluation of the performance and emissions for a direct coal-fired sCO_2 power plant. This study describes a baseline coal-fired cycle configuration, where coal is first gasified and cleaned in order to avoid introducing sulfur and particulate matter into the sCO_2 cycle, with the sCO_2 cycle's oxy-combustor operating on syngas. The baseline sCO_2 plant design yields a net plant thermal efficiency of 37.7% (HHV), with 98.1% CO_2 capture at 99.4% purity. This compares favorably to the reference IGCC plant, which has a 31.2% net HHV thermal efficiency, and 90.1% CO_2 capture rate at 99.99% purity. The sensitivity of the sCO_2 plant's performance to its process variables is discussed, as well as their effect on plant operability and cost surrogate variables.

1 Introduction

The United States (U.S.) Department of Energy's (DOE) Clean Coal and Carbon Management Program (CCCMP) provides a worldwide leadership role in the development of advanced coal-based energy conversion technologies, with a focus on electric power generation with carbon capture and storage (CCS). As part of DOE's Office of Fossil Energy (FE), the National Energy Technology Laboratory (NETL) implements research, development, and demonstration (RD&D) programs that address the challenges of reducing greenhouse gas emissions. To meet these challenges, FE/NETL evaluates advanced power cycles that will maximize system efficiency and performance, while minimizing CO_2 emissions and the costs of CCS.

To this end, NETL has recently been investigating direct-fired supercritical CO_2 (sCO_2) power cycles, which are attractive due to their high efficiency and inherent ability to capture CO_2 at storage-ready pressures. In these cycles, fuel is combusted with oxygen in a highly dilute sCO_2 environment, with the combustion products driving an expansion turbine to generate power. The thermal energy in the turbine exhaust is recuperated in a compact heat exchanger to heat the CO_2 diluent flow to the combustor, followed by condensation of water out of the product stream. A portion of this stream is sent to a purification unit for CO_2 storage, while the bulk of the fluid is compressed for return to the combustor. Most of these processes occur at elevated pressures of 200-400 bars in the combustor and 10-80 bars at the condenser, which leads to a high-power density cycle with a reduced footprint relative to conventional power generation technologies. Resulting capital costs are somewhat offset by the need to contain the high pressures, but combined with the high efficiencies, direct-fired sCO_2 power plants are expected to be comparable to, or better than, conventional combined cycle plants with CCS, on a cost of electricity basis.

Several analyses of direct sCO2 power cycles are available in the literature, including those of Allam and colleagues (12, 13), who are pursuing commercialization of this technology through the construction of a 25 MWe demonstration plant over the next few years. In their natural gas-fired version of this cycle, they suggest that net plant thermal efficiencies of 53% (higher heating value [HHV]) are achievable (12) with near 100% carbon capture (13). Foster Wheeler's modeling of this system under slightly different assumptions yields a plant thermal efficiency of 50% (HHV), with 90% carbon capture (15). Southwest Research Institute has evaluated alternative natural gas-fired direct sCO_2 cycles, and have reported plant thermal efficiencies of 48% (14). For comparison, baseline natural gas combined cycle (NGCC) plants with 90% carbon capture can achieve a plant efficiency of 45.7% (19).

NET Power has also developed a coal-fired version of their direct sCO_2 cycle, in which coal is first gasified and cleaned before syngas is burned in the sCO_2 cycle combustor (12). In the baseline system, an entrained flow, dry-fed, slagging gasifier is used with a water quench, which produces a claimed net plant thermal efficiency of 47.8% (HHV) on bituminous coal (6). Variations in coal type, gasifier type, and heat recovery processes yield a range of HHV efficiencies from 43.3% to 49.7% (6).

The Electric Power Research Institute (EPRI) has also studied a syngas-fired direct sCO_2 power plant based on coal gasification in a slagging, entrained flow gasifier (4). The study includes Shell's dry-fed gasifier design (including a steam bottoming cycle powered by the syngas cooler's thermal input) and investigates the effects of oxygen purity and coal carrier gas on the purity of the CO_2 in the power cycle's turbomachinery. The study concludes that high oxygen purity (99.5%) and CO_2 carrier gas are required to produce a storage-ready stream with sufficient CO_2 purity (98.1%) for permanent sequestration. Plant thermal efficiency for this case was 39.6% (HHV), with 99.2% CO_2 capture rate, compared to 31.1% plant efficiency with 87% CO_2 capture in the integrated gasification combined cycle (IGCC) reference plant. Cost of electricity was also estimated at 133 $/MWh, compared to 138 $/MWh for the IGCC plant with capture, though significant uncertainty in the sCO_2 capital cost was noted (4).

Building on the studies found in the literature, the objective of the present study is to develop a performance baseline for a syngas-fired direct sCO_2 power plant using coal gasification, and to analyze the sensitivity of its net thermal efficiency and cost indicators to variations in operating parameter assumptions. These results will be utilized in future studies that will include capital cost estimation and plant optimization to minimize cost of electricity.

2 Coal-Fired Direct-sCO_2 Power Plant Design

As noted above, the objective of this study is to determine the extent to which the open Brayton cycle based on sCO_2 offers advantages compared to other coal-fired power plant technologies in the NETL research and development (R&D) portfolio. The study is intended as an initial assessment and does not represent the definitive coal-fired sCO_2 conceptual plant design or an optimized configuration. Nevertheless, in making selections for the conceptual design and plant configuration, the overriding objective was to maximize the plant efficiency within the constraints imposed by component and sub-system limitations. Where appropriate, heuristics and results from prior IGCC studies were used to guide these selections.

The plants in this study are assumed to be located at a generic plant site in Midwestern U.S. at zero elevation and with ambient conditions that are the same as International Organization for Standardization (ISO) conditions, i.e., barometric pressure 0.10 MPa, dry bulb and wet bulb temperatures of 15 °C and 11 °C, respectively, and 60 percent relative humidity. The fuel source selected for the power plant in this study is Illinois No. 6 bituminous coal, which is used as a reference fuel in many of NETL's systems studies (16, 17). For the most part, IGCC plants can attain a higher plant efficiency using bituminous coal than by using lower rank coals.

The specific fuel source for the sCO_2 power cycle is syngas from a gasifier suitable for an IGCC plant. Many gasifiers could be suitable for this application, but for this study the dry feed entrained flow gasifier based on the Shell gasifier design was selected. Other gasification systems considered include: General Electric Energy (GEE) gasifier with radiant syngas cooler, GEE gasifier with quench, Siemens gasifier, Chicago Bridge & Iron Company's (CB&I) E-Gas gasifier, and Kellogg Brown & Root's (KBR) transport integrated gasifier (TRIG). The Shell gasifier was selected because it has a relatively high cold gas efficiency and a commercial offering with high temperature syngas heat recovery from the syngas. Both of these factors were deemed advantageous in a direct-fired sCO_2 power cycle application.

Figure 1 shows a simplified block flow diagram (BFD) for the coal-fired direct-fired sCO_2 power plant. The following sections provide more detailed descriptions of the conceptual plant design and component configuration.

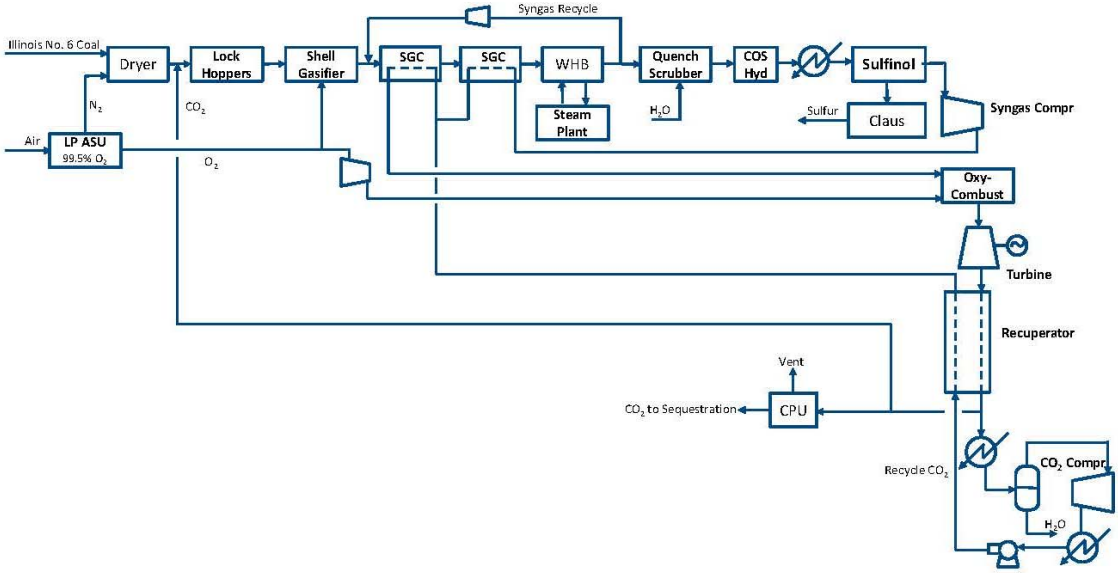

Figure 1 Coal-fired direct-fired sCO_2 power plant

2.1 Gasifier Train Conceptual Design

A low pressure cryogenic air separation unit (ASU) provides oxygen for the single-stage, entrained flow, oxygen-blown gasifier and the pressurized oxy-syngas combustor. The ASU is sized to provide sufficient oxygen to the gasifier and combustor, plus a small slipstream of oxygen used in the Claus furnace for acid gas treatment. Some of the N_2 by-product is heated in a syngas-fired furnace and sent to a fluidized bed dryer to dry the bituminous coal (11.12 percent moisture as received) to 5 percent moisture for dry-feeding to the gasifier (2).

The Shell gasifier operates at a temperature of 1,454 °C and is assumed to achieve 99.5 percent carbon conversion. (2) A syngas recycle stream mixes with raw syngas to reduce the gasifier exit temperature to 1,093 °C to minimize ash agglomeration during heat recovery.

After passing through the syngas cooler, the syngas passes through a cyclone and a raw gas candle filter where a majority of the fine particles are removed and returned to the gasifier with the coal fuel. Fines produced by the gasification system are recirculated to extinction. The ash that is not carried out with the gas forms slag and runs down the interior walls, exiting the gasifier in liquid form. The slag is solidified in a quench tank for disposal.

After passing through the cyclone and ceramic candle filter array, the syngas is further cooled by raising intermediate pressure (IP) steam. The raw syngas exiting the final raw gas cooler then enters the quench scrubber for removal of chlorides, SO_2, NH_3, and remaining particulates. The quenched syngas is then reheated to 232 °C for carbonyl sulfide (COS) hydrolysis. Following the exothermic COS hydrolysis reaction, the gas passes through several low temperature syngas coolers to reduce the syngas temperature to 35 °C. The fuel gas enters packed carbon bed absorbers to remove mercury, followed by

a Sulfinol process that absorbs H_2S from the fuel gas. H_2S is sent to the Claus plant for sulfur purification. (2)

The Claus plant converts H_2S to elemental sulfur through a series of reactions. Sulfur is condensed, and tail gas is hydrogenated to convert residual SO_2 back into H_2S, which can be captured when the tail gas is recycled to the Sulfinol absorber. A small slipstream of clean fuel gas is used for the hydrogenation reaction (2). The fuel gas exits the Sulfinol absorber at 31 °C, and is sent to the sCO_2 power cycle.

The process includes a steam plant to raise high-pressure (HP), IP, and low-pressure (LP) steam by recovering waste heat from the gasifier water wall, syngas, Claus unit, and scrubber. The steam is used in the process as a feed to the gasifier and for assorted process steam requirements including for the ASU, Sulfinol reboiler, and sour water stripper reboiler. Surplus steam generation for a steam power island is not considered, as this would increase the complexity and cost of the plant. All available process heat not needed in the steam plant is used to heat recycle CO_2 and fuel gas.

2.2 sCO_2 Brayton Cycle

The sCO_2 power cycle is a direct-fired open Brayton cycle. Although multiple potential configurations are possible and have been studied in the literature, none of those studies present a convincing analysis showing what configuration is optimal. The configuration selected for this study represents a synthesis of conceptual designs presented in earlier work (4-11) and is intended as a starting point for future optimization and to identify potential areas of RD&D.

Referring again to Figure 1, the clean syngas from the Sulfinol unit is compressed to the combustor pressure and preheated to the maximum extent possible based on a pinch analysis using the high temperature syngas cooler downstream of the gasifier. Oxygen is compressed and delivered to the combustor with the syngas and recycle CO_2. The combustor is assumed to be adiabatic with a combustion efficiency of 100 percent, 1% excess oxygen, and a pressure drop of 0.7 bar. The target combustor temperature is 1149 °C, which was selected to yield a turbine outlet temperature of 760 °C at the chosen pressure ratio.

The combustor effluent enters the sCO_2 turbine where it is expanded and power is generated. For this study, a turbine blade cooling model is not implemented. Future studies will develop one or more recuperative cooling strategies which will allow blade cooling without incurring a significant drop in cycle or process efficiency.

The effluent from the sCO_2 turbine enters the hot side of the CO_2 recuperator. With the selected combustor temperature and cycle pressure ratio this temperature will be approximately 760 °C, which is roughly the temperature limit of nickel alloys used in the exhaust piping at these pressures. The hot side stream is cooled to within the minimum temperature approach of the cold side feed temperature, which is equal to the final stage recycle CO_2 compressor exit temperature. After the hot side CO_2 has been cooled to the maximum extent possible in the recuperator, a portion of the stream is split off to provide both a CO_2 purge and a CO_2 stream used as transport gas in the gasifier. The purge stream is sent to a CO_2 purification unit to purify and compress it to pipeline specification (3).

The remaining CO_2 exiting the hot side of the recuperator is cooled to 27 °C, based on the available cooling water temperature and assumed temperature approach (18), to knock-out of most of the H_2O in the stream. The non-condensing portion of the stream is compressed to 75.8 bar and cooled again to 27 °C. The fluid pressure is finally increased to 300 bar and recycled to the cold side of the CO_2 recuperator. The CO_2 stream exiting the cold side of the recuperator is then sent to the high temperature syngas coolers where it is heated to a final temperature of 692 °C in the baseline case before entering the combustor.

2.3 sCO_2 Brayton Cycle Parameters

Table 1 shows the parameters for the baseline sCO_2 power cycle configuration. The plant was sized to produce approximately 600 MW net output. The turbine and compressor efficiencies represent reasonable estimates for nth-of-a-kind units of the proposed scale. The minimum temperature approach and pressure drops are relatively aggressive settings but still attainable in a commercial plant. For the most part, these baseline parameters are arbitrary and represent a reasonable starting point for the sensitivity analyses that examine how the cycle performance changes with changes to the parameter values.

The sCO_2 cycle was modeled using Aspen Plus® (Aspen) and the Peng-Robinson-Boston-Mathias (PR-BM) property method. The Reference Fluid Thermodynamic and Transport Properties Database (REFPROP) is considered the most accurate property model to use for CO_2 near its critical point; however, the Aspen REFPROP implementation could not be used for this system due to the presence of certain impurities including HCl and NH_3. Within the Aspen model, the flow rate of recycle CO_2 was varied in order to attain the specified turbine inlet temperature.

Table 1 Baseline sCO_2 cycle parameters used in Aspen Plus® simulations

Parameter	Value
Heat source	Pressurized oxy-syngas combustor
Cycle thermal input	1315.0 MW (4486.8 MMBtu/hr)
Turbine exit pressure	30.0 bar (435.1 psia)
Cooler exit temperature	27 °C (80 °F)
Turbine inlet temperature	1149 °C (2100 °F)
Turbine isentropic efficiency	0.927
Compressor isentropic efficiency	0.85
Recuperator maximum temperature	760 °C (1400 °F)
Recuperator pressure drop per side	1.4 bar (20 psia)
Combustor pressure drop	0.7 bar (10 psia)
CO_2 cooler pressure drop	1.4 bar (20 psia)
Minimum recuperator temperature approach	10 °C (18 °F)
Nominal compressor pressure	300.0 bar (4351 psia)
Nominal compressor pressure ratio	11.0

2.4 Reference case: IGCC with advanced hydrogen turbine and carbon capture

Figure 2 shows a simplified BFD for an IGCC process based on the Shell gasifier and with carbon capture. This is used as a reference case for the current study, and is described in the Bituminous Baseline Study Rev 2 as Case 6. (2)

The gasifier island and gas cleanup sections in the IGCC are very similar to the corresponding sections in the coal-fired direct-fired sCO_2 power plant with a few notable differences. The IGCC plant utilizes an elevated pressure cryogenic ASU designed to produce 95 percent purity oxygen. In the sCO_2 plant, the ASU is low pressure and is designed to produce 99.5 percent purity oxygen to minimize argon and nitrogen contaminants in the sCO_2 cycle. Other systems studies have shown that the resulting reduction in CO_2 compression power due to higher sCO_2 purity more than offsets the increase in ASU power required to deliver higher purity oxygen to the cycle (4, 15).

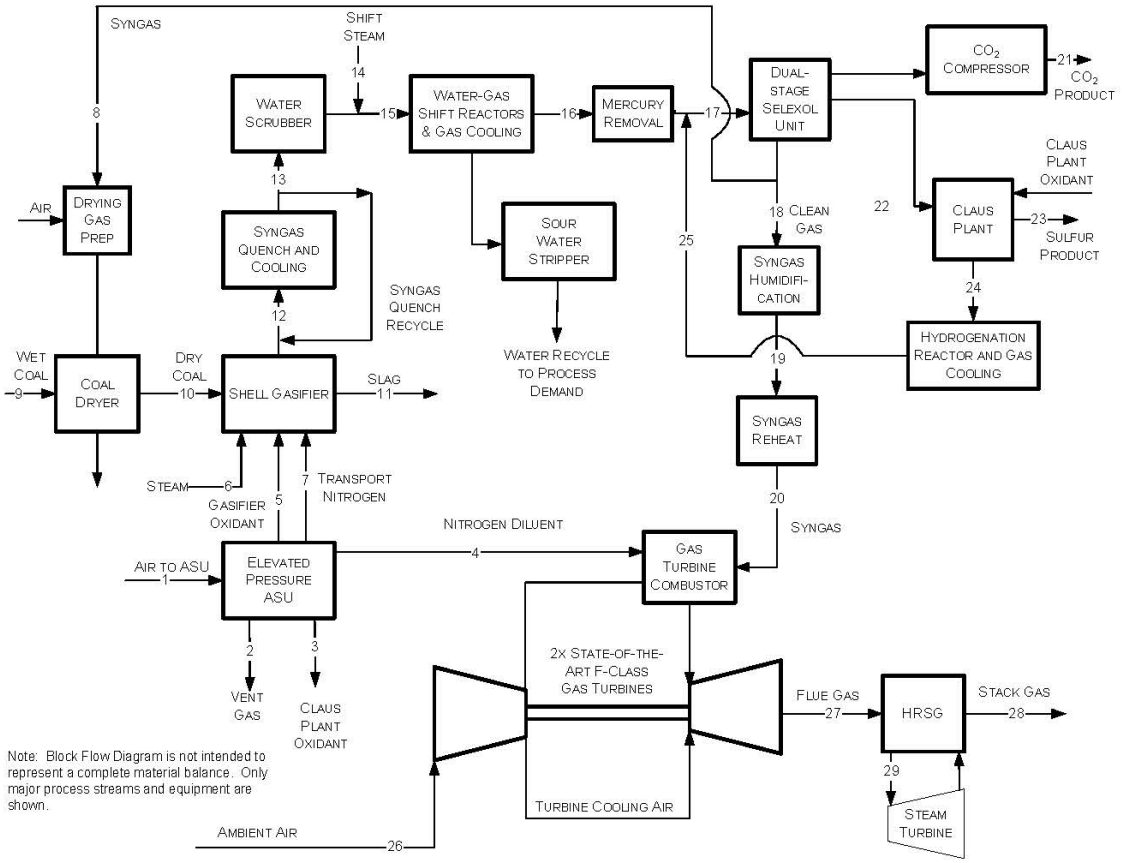

Figure 2 Reference IGCC power plant with carbon capture

In the IGCC plant, decarbonization requires water gas shift reactors, which are located downstream of the COS hydrolysis reactor. The acid gas removal is a two-stage Selexol process that removes both H_2S and CO_2 as separate product streams. Finally, the IGCC plant uses nitrogen as the transport gas for the dry feed lock hopper system, whereas the sCO_2 plant uses CO_2 to improve sCO_2 purity and, hence, cycle performance (4).

The IGCC plant's power island uses a combined cycle with F-frame gas turbines operated on hydrogen-rich syngas and a sub-critical Rankine bottoming cycle. The gas turbine efficiency is estimated from the Aspen Plus model, and is within the range of turbine efficiencies obtained from vendor quotes. In the IGCC plant, there is further process integration with the use of byproduct nitrogen from the ASU as fuel gas diluent for power augmentation and NO_x control in the gas turbine (2).

3 Baseline Performance Results

Table 2 shows the performance comparison between the IGCC plant and the coal-fired direct-sCO_2 plant, and Table 3 compares their auxiliary power requirements.

Table 2 Performance comparison between IGCC and sCO_2 plants

Parameter	IGCC	sCO_2 Cycle
Coal flow rate (kg/hr)	211,040	198,059
Oxygen flow rate (kg/hr)	160,514	391,227
sCO_2 flow rate (kg/hr)	---	6,608,538
Carbon capture fraction (%)	90.1	98.1
Captured CO_2 purity (mol% CO_2)	99.99	99.44
Net plant efficiency (HHV %)	**31.2**	**37.7**
sCO_2 power cycle efficiency (%)	---	53.1
F-frame gas turbine efficiency (HHV %)	35.9	---
Steam power cycle efficiency (%)	39.0	---
Raw water withdrawal (m^3/s)	0.355	0.360
Carbon conversion (%)	99.5	99.5
Power summary (kW)		
Coal thermal input (HHV)	1,591,000	1,493,000
Steam turbine power output	209,400	0
Gas turbine power output	464,000	0
sCO_2 turbine power output	0	758,215
Gross power output	673,400	758,215
Total auxiliary power load	176,540	195,643
Net power output	**496,860**	**562,572**

Table 3 Auxiliary power comparison between IGCC and sCO_2 plants

Auxiliary Load (kW)	IGCC	sCO_2 Cycle
Coal milling & handling, slag handling	3,180	2,976
Air separation unit auxiliaries	1,000	1,000
Air separation unit main air compressor	59,740	78,999
Gasifier oxygen compressor	9,460	19,917
sCO_2 oxygen compressor	---	25,743
Nitrogen compressors	32,910	---
Fuel gas compressor	---	34,197
CO_2 compressor (including CPU)	30,210	17,042
Boiler feedwater pumps	3,500	87
Syngas recycle compressor	790	869
Circulating water pump	4,370	3,559
Cooling tower fans	2,260	2,303
Acid gas removal	18,650	457
Gas/sCO_2 turbine auxiliaries	1,000	1,000
Claus plant TG recycle compressor	1,830	594
Miscellaneous balance of plant	5,110	4,069
Transformer losses	2,530	2,831
TOTAL	**176,540**	**195,643**

In comparing the performance results between the two cases, it is apparent that the sCO_2 plant achieves a significantly greater efficiency and a significantly greater carbon capture fraction than an IGCC plant using the same gasification technology. The sCO_2 plant generates almost 13 percent more power and requires 6 percent less coal than the IGCC plant. This difference is due almost entirely to the difference in cycle efficiencies in the power cycles between the two plants. Similar results have been obtained in a study by EPRI with a slightly different configuration, yielding a net HHV plant efficiency of 39.6% with 99.2% CO_2 capture at 98.1% purity (4).

The auxiliary power in the sCO_2 cycle is almost 26 percent of the net power generated in the sCO_2 turbine. This compares closely to the IGCC plant for which the auxiliary power is just over 26 percent of the net power generated. Both plants require approximately the same amount of parasitic power per kW of net power generated. The IGCC plant has higher CO_2 purification unit (CPU) power requirements (since the incoming CO_2 is at lower pressure), higher acid gas removal power (due to the need to remove CO_2 from the syngas), and nitrogen compression power (which is not needed in the sCO_2 cycle). These auxiliary power requirements are offset in the sCO_2 plant with syngas compression needs and higher ASU and oxygen compression power requirements due to higher demand.

The sCO_2 turbine output shown in Table 2 is the net output after subtracting the compression power for the low pressure (109,304 kW) and high pressure (71,838 kW) sCO_2 compressors, as well as the generator loss. The amount of compression power as a percentage of gross turbine output is considerably less in the sCO_2 cycle (<20 percent) than for the F-frame gas turbine (>30 percent). This contributes greatly to the significantly higher simple cycle efficiency for the sCO_2 cycle compared to the gas turbine cycle.

The increase in carbon capture fraction attained by the sCO_2 plant over the IGCC plant is due to the use of oxy-combustion in the sCO_2 plant. In the IGCC plant, a significant amount of CO_2 fails to be captured due to limitations in conversion of the water gas shift reaction plus limitations in capture by the Selexol unit. The sCO_2 plant is not impacted by such limitations.

4 Sensitivity Analyses

As noted previously, the cycle configuration and state point used for the baseline sCO_2 plant did not result from a formal optimization. To determine whether opportunities for improving the plant efficiency exist by modifying the plant configuration or state point, a series of sensitivity analyses was performed in which several of the key operating parameters in Table 1 were adjusted to determine the impact on process efficiency (i.e., net plant efficiency on an HHV basis) and indirect indicators of system cost. In many cases, this indirect cost measure is specific power, which is the net cycle power output divided by the mass of working fluid through the turbine.

The results of these sensitivity analyses are presented and discussed in the following sections.

4.1 Sensitivity to Turbine Exit Pressure

Figure 3 shows a plot of process efficiency versus the turbine exit pressure. All other cycle configuration parameters were the same as shown in Table 1. The dashed line indicates the baseline parameter value of 30 bar from Table 1.

As turbine exit pressures are increased from 24 bar, the turbine inlet temperature was kept constant at 1149 °C, and the turbine exit temperature was allowed to increase with pressure to the predetermined limit of 760 °C at a turbine exit pressure of 28.6 bar. The increase in turbine exit temperature with pressure leads to a greater recuperator duty and heating of the recycle CO_2 stream, thereby increasing process efficiency. For increases in turbine exit pressure beyond 28.6 bar, the turbine inlet temperature is lowered below 1149 °C with a constant turbine exit temperature of 760 °C to keep from exceeding the

recuperator temperature limits. The lower the turbine inlet temperature, the lower the cycle efficiency and process efficiency.

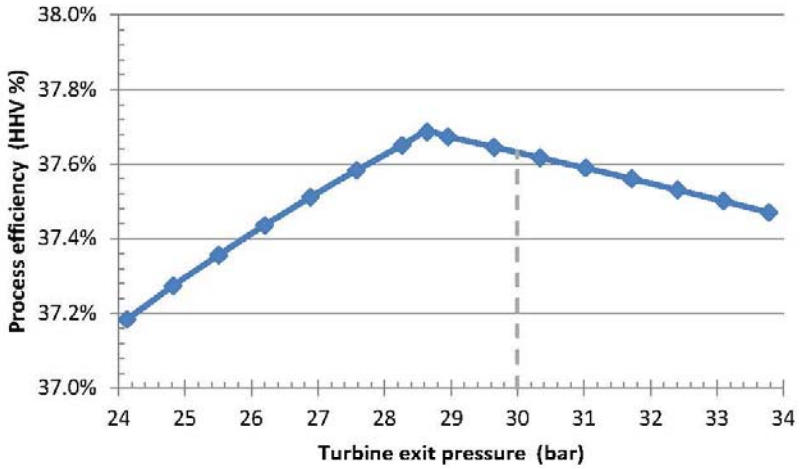

Figure 3 Efficiency versus turbine exit pressure

The specific power and recuperator duty, both indirect capital cost indicators, are shown in Figure 4. The specific power decreases monotonically as the turbine exit pressure increases, since the turbine pressure ratio and turbine output both decrease. With the increase in recuperator duty with turbine exit pressure, these results suggest that the cycle capital cost will increase with turbine exit pressure, and that the optimum turbine exit pressure is 28.6 bar or lower. However, that lower exit pressure increases the volume flow through the low pressure side of the recuperator, which must lead to either an increased pressure drop, adversely affecting the cycle efficiency, or an increase in the recuperator's size, increasing its cost. Neither of these effects are considered in this study, but must be included in a detailed plant optimization to minimize the cost of electricity.

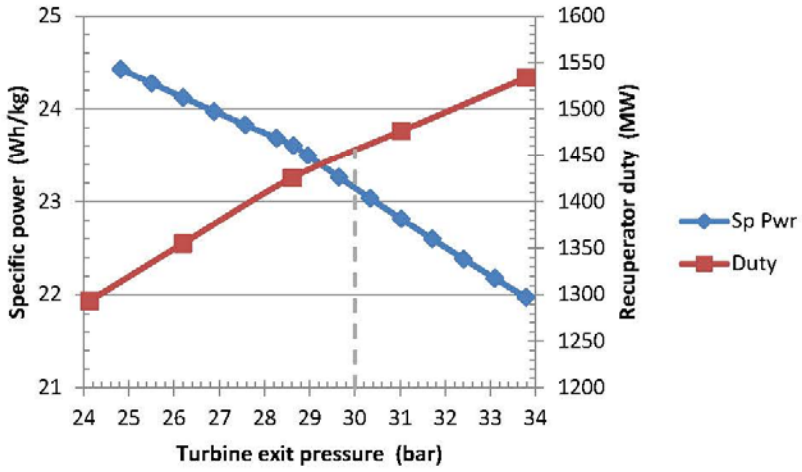

Figure 4 Specific power and recuperator duty versus turbine exit pressure

4.2 Sensitivity to CO_2 Compressor Pressure

Figure 5 shows a plot of process efficiency and specific power as a function of CO_2 compressor pressure. As with all other sensitivity analyses, the cycle configuration parameters have the same values shown in Table 1 except for the sensitivity variable itself and the turbine exit pressure, which was adjusted to simultaneously meet the turbine inlet temperature maximum of 1149 °C and the turbine exit temperature maximum of 760 °C. The dashed line indicates the baseline parameter value of 300 bar from Table 1.

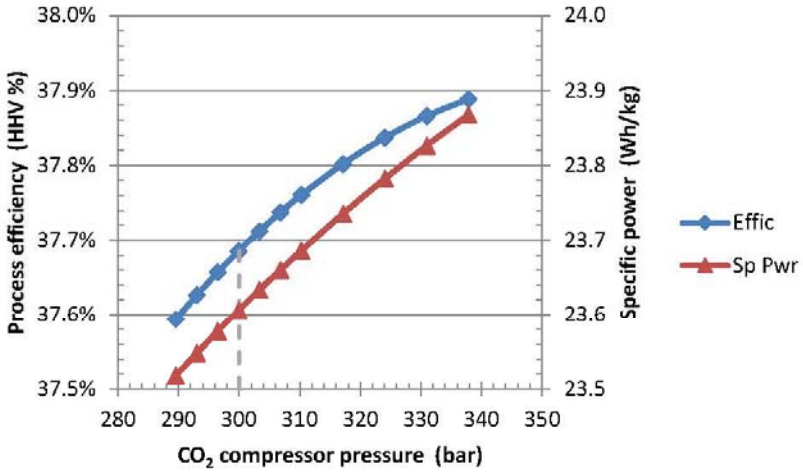

Figure 5 Process efficiency and specific power versus CO_2 compressor pressure

The process efficiency and specific power increase with an increase in the compressor pressure, though the efficiency dependence on compressor pressure is reduced at elevated pressures. The upper range of the compressor pressure was kept below 345 bar as a likely economic limitation. These results suggest that there would be a modest improvement in process performance (higher efficiency and lower cost) if the compressor pressure were increased closer to 345 bar. However, predicting the impact of operating pressure on cost is difficult. Higher pressure operation generally means smaller vessel and pipe sizes, but elevated pressure requires thicker walls and a more costly vessel on a dollars per volume basis. Ultimately, detailed equipment designs will be needed to ascertain the economically optimal compressor pressure. This is especially true in the high temperature areas of the cycle where pressure increases could force the selection of expensive materials of construction, particularly for the piping between the recuperator, syngas cooler (SGC), oxy-combustor, and sCO_2 turbine.

4.3 Sensitivity to Turbine Inlet Temperature

Figure 6 shows the process efficiency and specific power as a function of turbine inlet temperature. The turbine exit pressure was adjusted to attain a turbine exit temperature of 760 °C. As the turbine inlet temperature increases, the process efficiency rises parabolically until it reaches a maximum at a turbine inlet temperature of 1400 °C. This is due in part to higher cycle pressure ratios required to meet the 760 °C turbine exit temperature limitation. In addition, increased combustion temperatures require more fuel and oxidizer and less recycle CO_2, resulting in sCO_2 combustion product diluents that increase the cycle compressor power requirements (4). These efficiency estimates are somewhat optimistic in that turbine blade cooling is not accounted for in the model, and it would adversely impact process efficiency and plant cost of electricity (15).

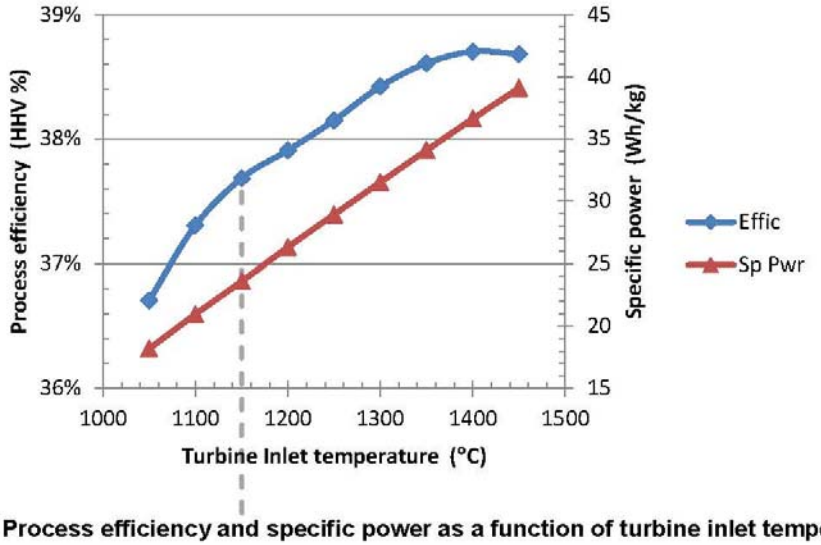

Figure 6 Process efficiency and specific power as a function of turbine inlet temperature

The specific power increases considerably with turbine inlet temperature, due in large part to decreasing turbine exit pressures and increased power output. While this suggests that the cycle cost will be lower at higher turbine inlet temperatures, the turbine cost itself is expected to increase with higher turbine inlet temperatures due to the need for more expensive materials for such high temperature service.

4.4 Sensitivity to CO_2 Cooler Pressure

The portion of the CO_2 exiting the hot side of the recuperator that is recycled is cooled prior to raising its pressure to the nominal cycle pressure of 300 bar. It was found that a significant reduction in the power needed to raise the fluid's pressure can be realized if the cooling is done in multiple stages. As shown in Figure 1, the first cooling stage removes most of the condensable water. The CO_2 pressure is increased to an intermediate point and the CO_2 stream is cooled again before raising its pressure to the final level. Plant performance is strongly dependent on the pressure in the first stage of compression.

Figure 7 shows the process efficiency and specific power as a function of the second-stage CO_2 cooler pressure, also the pressure of the first-stage CO_2 compressor. The process efficiency shows a maximum at the baseline CO_2 cooler pressure of 75.8 bar, shown with the dashed line in Figure 7. The minimum CO_2 cooler pressure was 73.1 bar, which is just below the CO_2 critical pressure of 73.9 bar. The specific power follows the same trends as the process efficiency except that the maximum in specific power occurs at a pressure of 74.5 bar, just slightly less than the pressure used in the baseline case.

Both the process efficiency and specific power curves are relatively flat in the region of cooler pressures between 73.1 bar and 79.3 bar. Although the results suggest that the baseline cooler pressure is optimal, plant operability considerations may favor increasing this pressure closer to 79 bar as the plant will be more stable to perturbations in the operating point. Note also that there is significant uncertainty in these results, due to the use of the PR-BM property method in Aspen around the CO_2 critical point.

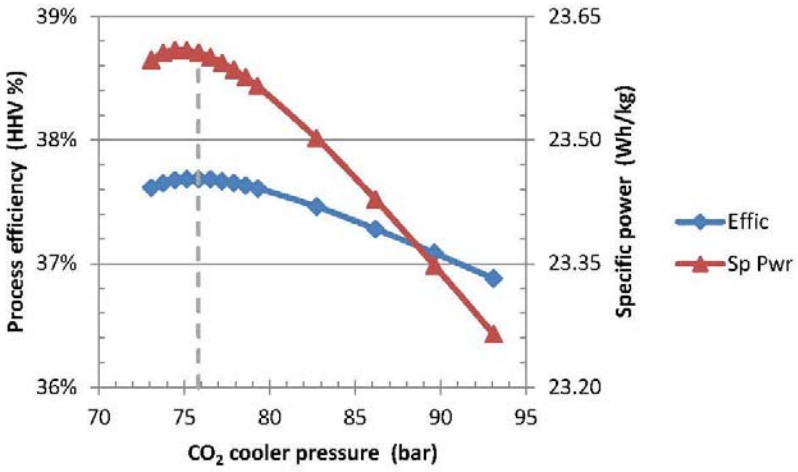

Figure 7 Process efficiency versus CO_2 cooler pressure

4.5 Sensitivity to CO_2 Cooling Temperature

Figure 8 shows the process efficiency and specific power as a function of CO_2 cooling temperature. The process efficiency decreases with increasing CO_2 cooler temperature. The plot shows two distinct regimes. At temperatures below 30 °C the process efficiency is significantly higher than for temperatures above 30 °C, and the efficiency versus temperature curve is a paraboloid with the efficiency plateauing at a cooler temperature below 15 °C. In this low-cooling temperature regime, the CO_2 is a dense phase fluid and can be pumped to its final pressure. To the left of the dashed line, which represents the baseline cooler temperature of 27 °C, the efficiencies do not include the auxiliary power requirement for the refrigeration that would be needed to attain such low temperatures relative to the cooling water temperature in this study. Mechanical draft cooling towers may also be employed to reduce cooling water temperatures and have been shown to benefit the process efficiency in spite of higher power requirements relative to natural draft cooling towers (15). At cooler temperatures above 30 °C, the relatively lower process efficiency curve is linear, showing a drop in process efficiency of approximately 0.1 percentage point for every 1 °C increase in cooler temperature. In this regime, the CO_2 mixture is above its dew point, and a compressor is needed to elevate its pressure, significantly increasing the auxiliary power requirement and resulting in a relatively low process efficiency.

The specific power follows the same trends as the process efficiency. While overall process performance improves with lower CO_2 cooler temperature, the benefit diminishes as the temperature decreases. As with the CO_2 cooling pressure, there is significant uncertainty with the use of the PR-BM property method in Aspen at these conditions.

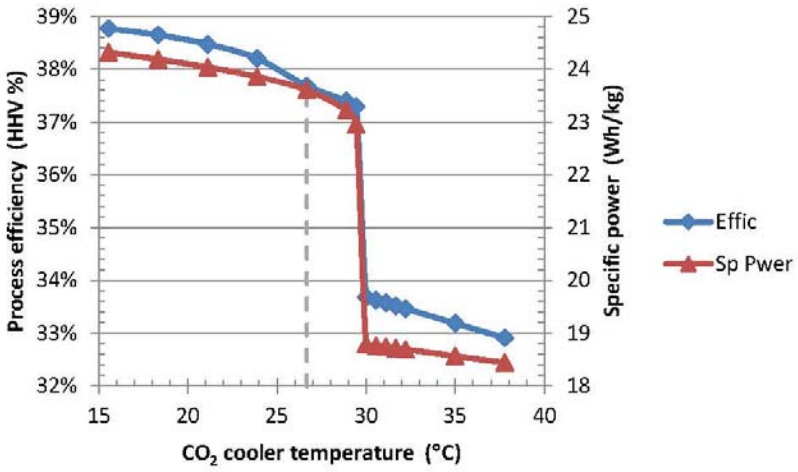

Figure 8 Process efficiency versus CO_2 cooler temperature

4.6 Sensitivity to Cycle Pressure Drop

The assumed pressure drop of 4.8 bar for the direct sCO_2 cycle is a rough estimate and not based on system optimization. The sensitivities of the process efficiency and specific power to the cycle pressure drop, as shown in Figure 9, are essentially linear. The process efficiency drops approximately 1 percentage point with every 6 bar increase in the pressure drop. This plot suggests that the cycle cost will decrease slightly as pressure drop decreases. However this apparent result is overshadowed by the sharp increase in capital cost required to design unit operations, especially heat exchangers, for very low pressure drops, which will be included in future efforts to optimize the plant for minimum cost of electricity .

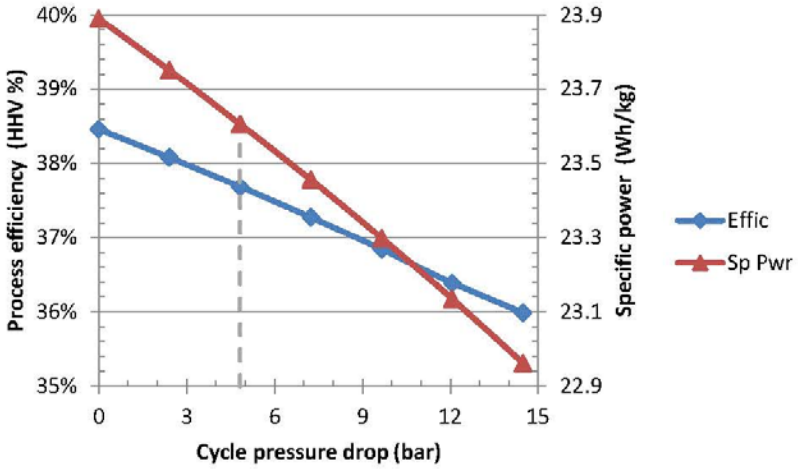

Figure 9 Process efficiency versus cycle pressure drop

4.7 Sensitivity to Minimum Approach Temperature

The minimum temperature approach in the recuperator of 10 °C used for the baseline configuration was an arbitrary target. A larger temperature approach would decrease cycle efficiency but may be worthwhile if it results in a substantial capital cost savings due to larger driving forces and smaller recuperators. Figure 10 shows the process efficiency versus minimum approach temperature. The vertical line on Figure 10 corresponds to the baseline configuration.

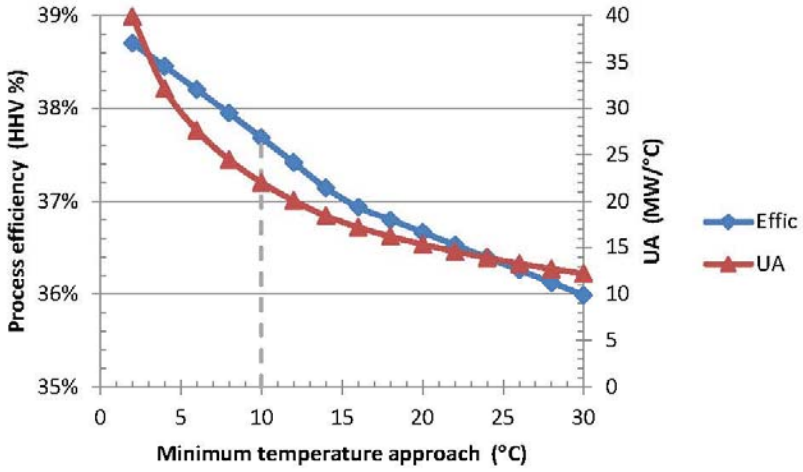

Figure 10 Process efficiency versus minimum approach temperature

Over the range examined, the process efficiency drops approximately 0.1 percentage points for every 1 °C increase in the minimum approach temperature, but is slightly nonlinear. The specific power is not dependent on the minimum approach temperature. Similar trends, with higher sensitivity of efficiency to approach temperature, are reported for the NG-fired direct sCO_2 cycle (15).

A more appropriate cost surrogate variable is the heat duty divided by the log mean temperature difference (LMTD), which is equal to the heat transfer coefficient times the required recuperator area (UA). This is a fairly direct indicator of relative cost for heat exchangers. Figure 10 shows that the recuperator UA decreases with increasing minimum temperature approach but at an ever decreasing rate as the minimum temperature approach increases. Doubling the minimum temperature approach from 10 °C to 20 °C results in a 30 percent reduction in the recuperator UA but also results in a nearly 1 percentage point drop in the process efficiency, highlighting the importance of recuperator efficiency/cost tradeoffs in sCO_2 cycle design.

4.8 Sensitivity to Excess O_2

Sensitivity analyses performed on the percentage of excess oxygen fed to the combustor show that both process efficiency and specific power drop approximately 0.01 percentage point for every 1 percentage point increase in the excess oxygen. Though not shown on this study, these performance indicators show that the process is relatively insensitive to the amount of excess oxygen at levels up to 5 percent.

4.9 Sensitivity to Additional Intercooling

A variation of the baseline process configuration was evaluated to determine if additional intercooling during the final stage of dense fluid compression is advantageous. During this final operation to increase the fluid pressure, the pressure increases from 75.8 bar to 300 bar. In the baseline configuration, this is done in a single stage. In the variation, the pressure increase is performed in two stages of approximately equal pressure ratio; between stages, the fluid is re-cooled to 27 °C. The results are summarized in Table 4, and show a significant increase in process efficiency of 0.45 percentage points from the use of the extra intercooling. This efficiency gain is due almost entirely to the 8 percent drop in the sCO_2 cycle compression power required. While intercooling entails two additional process units, the aggregate cooling duty and compressor power duty both decrease. This is an attractive option to pursue in future studies.

Table 4: Effect of sCO_2 pump intercooling on plant performance

Parameter	Baseline sCO_2 Cycle	Additional Intercooling
Process efficiency (HHV %)	37.69	38.14
CO_2 cooler duty (MW)	559.6	558.7
CO2 cycle compression power (MW)	181.1	166.9
Thermal input to cycle (MW)	1,315	1,314

5 Summary and Conclusions

A detailed model of a direct, syngas-fired sCO_2 cycle has been constructed and exercised in this study. The model uses a high-purity ASU; the gasification of coal in a slagging, dry-fed Shell gasifier; a thermal integration with syngas coolers; and a Sulfinol unit for sulfur recovery. The sCO_2 cycle includes a high-pressure oxy-combustor at 300 bar, feeding sCO_2 at 1149 °C to a turbine with a pressure ratio of 10. Some of the exhaust is captured and purified for CO_2 storage, while the remaining recycle stream is compressed and preheated in a recuperator prior to return to the combustor.

The baseline direct-sCO_2 plant design yields a net power output of 562.6 MW_e and net plant thermal efficiency of 37.7% (HHV), with 98.1% CO_2 capture at 99.4% purity. This compares very favorably to the reference IGCC plant, which has a 496.9 MW_e net power output, 31.2% net HHV thermal efficiency, and 90.1% CO_2 capture rate at 99.99% purity. The sCO_2 plant generates almost 13% more power and requires 6% less coal than the IGCC plant, due almost entirely to the difference in power cycle efficiencies between the two plants.

Sensitivity analyses were performed around most of the sCO_2 plant process variables, including cycle operating pressures, turbine inlet temperature, cooler operating temperature, sCO_2 cycle pressure drop, recuperator temperature approach, excess oxygen in the oxy-combustor, and CO_2 pump intercooling. Intercooling has been identified as a particularly fruitful option for further improving cycle and plant efficiency.

Given the promising performance results for the baseline plant, further work is planned to improve upon the plant design and to better understand its limitations. In particular, models for recuperative cooling strategies that allow turbine blade cooling without incurring a significant drop in cycle or process efficiency will be investigated. In addition, detailed recuperator models will be developed to better understand the interaction between heat exchanger performance and its capital cost, so that optimization of the plant for reduced cost of electricity can be performed. As this implies, cost estimation and evaluation of the overall cost of electricity for the plant will be performed, to be followed by analysis of natural gas-fired direct-sCO_2 plants.

NOMENCLATURE

Aspen = Aspen Plus®
ASU = Air separation unit
bar = 100,000 Pa, approximately 1 atmosphere
BFD = Block flow diagram
Btu = British thermal unit
Btu/hr = British thermal units per hour
CB&I = Chicago Bridge & Iron Company
CCCMP = Clean Coal Carbon Management Program
CCS = Carbon capture and storage
CO_2 = Carbon dioxide
Compr = Compressor
COS = Carbonyl sulfide
CPU = CO_2 purification unit
DOE = Department of Energy
EOR = Enhanced oil recovery
EPRI = Electric Power Research Institute
FE = Office of Fossil Energy
FE/NETL= Office of Fossil Energy/National Energy Technology Laboratory
GEE = General Electric Energy
h, hr = Hour
H_2O = Water
H_2S = Hydrogen sulfide
HCl - Hydrogen chloride
HHV = Higher heating value
HP = High pressure
HRSG = Heat recovery steam generator
Hyd = Hydrolysis
IGCC = Integrated gasification combined cycle
IP = Intermediate pressure
ISO = International Organization for Standardization
KBR = Kellogg Brown & Root
kg = Kilogram
kW = Kilowatt
LMTD = Log mean temperature difference
LP = Low pressure
m^3 = Cubic meter
MM = Million
MMBtu = Million British thermal units
MW = Megawatt
MW/°C = Megawatt per degree Celsius
N_2 = Nitrogen
NETL = National Energy Technology Laboratory
NGCC = Natural gas combined cycle
NH_3 = Ammonia
NOx = Nitrogen oxide
O_2 = Oxygen
Pa = Pascal, SI unit of pressure
PR-BM = Peng-Robinson-Boston-Mathias
psia = Pound per square inch absolute
R&D = Research and development
RD&D = Research, development, and demonstration
REFPROP= Reference Fluid Thermodynamic and Transport Properties Database
s = Second
sCO_2 = Supercritical carbon dioxide
SGC = Syngas cooler
SO_2 = Sulfur dioxide
T = Temperature
TG = Tail gas
TGTU = Tail gas treatment unit
TRIG = Transport integrated gasifier
U.S. = United States
UA = Heat transfer coefficient times surface are = Heat duty divided by LMTD
W = Watt
Wh/kg = Watt-hour per kilogram, unit of specific power
WHB = Waste heat boiler
°C = Degrees Celsius
°F = Degrees Fahrenheit

REFERENCES

1) White, C., Shelton, W., and Dennis, R. (2014, September 9-10). *An Assessment of Supercritical CO_2 Power Cycles Integrated with Generic Heat Sources*. 4th International Symposium – Supercritical CO_2 Power Cycles: Pittsburgh, Pennsylvania.
2) National Energy Technology Laboratory (NETL). (2010, November 2). *Cost and Performance Baseline for Fossil Energy Plants Volume 1: Bituminous Coal and Natural Gas to Electricity*. Pittsburgh, Pennsylvania.

3) National Energy Technology Laboratory (NETL). (2013, August). *Quality Guidelines for Energy System Studies, CO_2 Impurity Design Parameters* (DOE/NETL-341/011212). Pittsburgh, Pennsylvania.

4) Electric Power Research Institute (EPRI). (2014, December). *Performance and Economic Evaluation of Supercritical CO_2 Power Cycle Coal Gasification Plant* (3002003734). Palo Alto, California.

5) Electric Power Research Institute (EPRI). (2013, December). *Novel & Innovative Power Cycles* (3002000437). Palo Alto, California.

6) Lu, X. (2014). *Flexible Integration of the sCO_2 Allam Cycle with Coal Gasification for Low-Cost, Emission-Free Electricity Generation*. Raleigh-Durham, North Carolina: 8 Rivers Capital.

7) Aerojet Rocketdyne. (2014, September 9-10). *Recent Advances in Power Cycles Using Rotating Detonation Engines with Subcritical and Supercritical CO_2*. The 4th International Symposium – Supercritical CO_2 Power Cycles: Pittsburgh, Pennsylvania.

8) Aerojet Rocketdyne. (2014, September 9-10). *Supercritical CO_2 Turbomachinery Configuration and Controls for a Zero Emission Coal Fired Power Plant: System Off Design & Control of System Transients*. The 4th International Symposium – Supercritical CO_2 Power Cycles: Pittsburgh, Pennsylvania.

9) Aerojet Rocketdyne. (2013, June 1). *Turbine Technology Program Phase III – Task 1(a) & (b): Supercritical CO_2 Turbomachinery (SCOT) System Studies Incorporating Multiple Fossil Fuel Heat Sources and Recuperator Development* (DE-FE0004002 Subcontract S163-PWR-PPM4002 Mod 03).

10) McClung, A., Brun, K., Chordia, L. (2014, September 9-10). *Technical and Economic Evaluation of Supercritical Oxy-combustion for Power Generation*. The 4th International Symposium – Supercritical CO_2 Power Cycles: Pittsburgh, Pennsylvania: SwRI and Thar.

11) Brun, K., McClung, A., and Davis, J. (2014, April). SwRI, *Novel Supercritical Carbon Dioxide Power Cycle Utilizing Pressurized Oxy-combustion in Conjunction with Cryogenic Compression* (DE-FE0009395): SwRI and Thar.

12) Allam, R.J., Palmer, M.R., Brown Jr., G.W., Fetvedt, J., Freed, D., Nomoto, H., Itoh, M., Okita, N., Jones Jr., C. (2013). High Efficiency and Low Cost of Electricity Generation from Fossil Fuels While Eliminating Atmospheric Emissions, Including Carbon Dioxide. *Energy Procedia*, 37:1135–1149.

13) Allam, R.J., Fetvedt, J.E., Forrest, B.A., Freed, D.A. (2014, June 16-20). *The Oxy-Fuel, Supercritical CO2 Allam Cycle: New Cycle Developments to Produce Even Lower-Cost Electricity from Fossil Fuels without Atmospheric Emissions* (GT2014-26952). ASME Turbo Expo: Düsseldorf, Germany.

14) McClung, A., Brun, K., and Delimont, J. (2015, June 15-19). *Comparison of Supercritical Carbon Dioxide Cycles for Oxy-Combustion* (GT2015-42523). ASME Turbo Expo: Montréal, Canada.

15) International Energy Agency Greenhouse Gas (IEAGHG). (2015, August). *Oxy-combustion Turbine Power Plants* (2015/05). Cheltenham, United Kingdom.

16) National Energy Technology Laboratory (NETL). (2012, January). *Quality Guidelines for Energy System Studies, Specification for Selected Feedstocks* (DOE/NETL-341/011812). Pittsburgh, Pennsylvania.

17) National Energy Technology Laboratory (NETL). (2012, January). *Quality Guidelines for Energy System Studies, Detailed Coal Specifications* (DOE/NETL-401/012111). Pittsburgh, Pennsylvania.

18) National Energy Technology Laboratory (NETL). (2012, January). *Quality Guidelines for Energy System Studies, Process Modeling Design Parameters* (DOE/NETL-341/081911). Pittsburgh, Pennsylvania.

19) National Energy Technology Laboratory (NETL). (2015). *Cost and Performance Baseline for Fossil Energy Plants; Cost and Performance Baseline for Fossil Energy Plants; Volume 1a: Bituminous Coal (PC) and Natural Gas to Electricity, Revision 3*. Pittsburgh, Pennsylvania.

ACKNOWLEDGEMENTS

The authors wish to thank Travis Shultz and Richard Dennis for their support and input on this project. This work was completed under DOE NETL Contract Number DE-FE0004001.

11 APPENDIX B: EVALUATION OF PROPERTY METHODS FOR MODELING DIRECT-SUPERCRITICAL CO_2 POWER CYCLES

Proceedings of ASME Turbo Expo 2017: Turbomachinery Technical Conference and Exposition
GT2017
June 26-30, 2017, Charlotte, NC, USA

GT2017-64261

EVALUATION OF PROPERTY METHODS FOR MODELING DIRECT-SUPERCRITICAL CO2 POWER CYCLES

Charles W. White
KeyLogic Systems, Inc.
Fairfax, Virginia, USA

Nathan T. Weiland
National Energy Technology Laboratory
Pittsburgh, Pennsylvania, USA

ABSTRACT

Direct supercritical CO_2 (sCO_2) power cycles have received considerable attention in recent years as an efficient and potentially cost-effective method of capturing CO_2 from fossil-fueled power plants. These cycles combust natural gas or syngas with oxygen in a high pressure (200-300 bar), heavily-diluted sCO_2 environment, such that the fluid entering the turbine is 90-95% CO_2, with the balance composed primarily of H_2O, CO, O_2, N_2 and Ar. After recuperation of the turbine exhaust thermal energy, water is condensed from the cycle, and the remainder is recompressed for either return to the combustor or for enhanced oil recovery (EOR) or storage. The compression power requirements vary significantly, depending on the proximity of the operating conditions to the CO_2 critical point (31 °C, 73.7 bar), as well as to the level of working fluid dilution by minor components. As this has a large impact on cycle and plant thermal efficiency, it is crucial to correctly capture the appropriate thermo-physical properties of these sCO_2 mixtures when carrying out performance simulations of direct sCO_2 power plants. These properties are also important to determining how water is removed from the cycle, and for accurate modeling of the heat exchange within the recuperator.

This paper presents a quantitative evaluation of ten different property methods that can be used for modeling direct sCO_2 cycles in Aspen Plus®. REFPROP is used as the de facto standard for analyzing indirect sCO_2 systems, where the closed nature of the cycle leads to a high purity CO_2 working fluid. The addition of impurities due to the open nature of the direct-sCO_2 cycle, however, introduces uncertainty to the REFPROP predictions. There is a limited set of mixtures available for which REFPROP can be reliably used and there are a number of species present in a coal-fired direct-fired sCO_2 cycle that REFPROP cannot accommodate. Even with a relatively simplified system in which the trace components are eliminated, simulations made using REFPROP require computation times that often preclude its use in parametric studies of these cycles. Consequently, a series of comparative analyses were performed to identify the best physical property method for use in Aspen Plus® for direct-fired sCO_2 cycles. These property methods are assessed against several mixture property measurements, and offer a relative comparison to the accuracy obtained with REFPROP. This study also underscores the necessity of accurate property modeling, where cycle performance predictions are shown to vary significantly with the selection of the physical property method.

INTRODUCTION

Combustion of fossil fuels in oxygen results in combustion products that are primarily CO_2 and H_2O, from which the water can be condensed to yield a reasonably high purity CO_2 stream for use or storage. Although there are several power systems capable of operating under oxy-fuel conditions, those that employ open cycle turbines are attractive due to the potential to leverage high efficiencies common to modern gas turbine cycles. A recent report by the International Energy Agency Greenhouse Gas R&D Program compared several oxy-combustion turbine power plants, and found that the potential for highest plant efficiency and lowest cost of electricity came from direct-fired supercritical CO_2 (sCO_2) power plants [1]. This is due in part to the properties of CO_2 near its critical point of 31 °C and 73.7 bar, where its high density reduces the power required for compression to improve net power output. Further, these cycles are efficient due to their high degree of recuperation, and also produce a relatively high purity CO_2 stream near storage-ready pressures as a byproduct of the process. Direct-fired sCO_2 cycles are a fairly recent innovation, and are well described by the works of Allam and colleagues [2, 3].

A block flow diagram (BFD) of a simplified direct sCO_2 cycle is shown in Figure 1, with accompanying state points for the numbered streams shown in Table A-1 in Appendix A. This BFD is derived from a more detailed plant design that includes coal gasification, syngas cleanup, and thermal integration with the sCO_2 power cycle. Additional details about the process

configuration and balance of plant unit operations are provided by Weiland et al. [4]. Note that the BFD and state point table are not intended to represent a complete process, as only major process streams and equipment are shown.

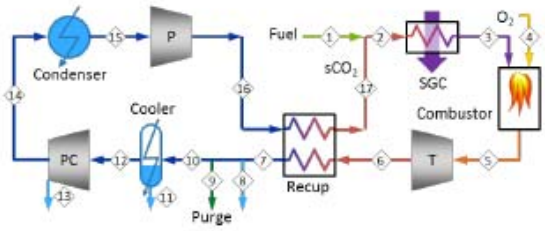

Figure 1: Block flow diagram of a simplified direct sCO_2 cycle

The sCO_2 cycle begins with the introduction of the fuel which in this case is a stream of cleaned and pressurized syngas that has been preheated in a syngas cooler (SGC). The syngas is mixed with the recycle working fluid that has been preheated by the recuperator. The mixed stream is further preheated in the SGC and fed to the oxy-combustor along with a stream of 99.5 mole percent oxygen from an air separation unit. The combustion products leave the oxy-combustor at 1149 °C and are expanded in the turbine (T) to generate electric power. The turbine exhaust preheats the portion of the working fluid that is recycled using a recuperator. The cooled stream leaving the recuperator (7) undergoes further cooling to knock out most of the water generated during combustion. The other products of combustion are removed in a purge stream that is sent to a CO_2 purification unit (CPU) in preparation for sequestration. At the final stage of cooling, the working fluid is liquefied and pumped to the peak cycle pressure and then preheated in the recuperator.

Coal-fueled systems in which coal is first gasified, and the resulting syngas is fired in the sCO_2 cycle, was proposed by Allam [2], and has recently been studied by Lu et al. [5], EPRI [6], and Weiland et al. [4] A few recent studies have also been undertaken in the area of natural-gas fired sCO_2 cycles, most notably those of Allam [2, 3], and IEAGHG [1].

Due to the high pressures throughout the cycle, and the already small size of the turbine, the development of small scale direct sCO_2 test units is all but cost prohibitive. As a result, modeling becomes a very cost-effective system design and component development tool, though there is a considerable lack of modeling experience in the temperature, pressure, and composition space required for this application.

Modeling of sCO_2 power cycles requires high accuracy in determining the physical properties of CO_2, particularly near its critical point. The Span-Wagner equation of state (EOS) [7] is the most accurate property method available for processes consisting of pure CO_2. [8] The Span-Wagner EOS is incorporated into the REFPROP physical property method developed by the National Institute of Standards and Technology (NIST), [9] and is used by most researchers in modeling indirect sCO_2 power cycles. For a direct-fired sCO_2 power cycle, however, the working fluid is not pure CO_2 and it changes composition at various points in the cycle. REFPROP was developed for a limited set of pure components and mixtures and the species set encountered in coal-fired direct sCO_2 cycles is not one of those mixtures. Using REFPROP on streams containing CO_2, O_2, H_2, N_2, Ar, H_2O, NH_3, and HCl generated severe errors in the Aspen physical property system. Furthermore, there are a number of species present in a coal-fueled direct-fired sCO_2 cycle which encounter temperature limitations in REFPROP's representation of those fluids. Per REFPROP's documentation, temperature limits for relevant species are: hydrogen, 727 °C; methane, 352 °C; carbon monoxide, 227 °C; ammonia, 427 °C; hydrogen sulfide, 487 °C; sulfur dioxide, 252 °C [9]. As a result of these temperature limits, computations fail if significant fuel preheating or incomplete combustion conditions are considered. Even with a relatively simplified system with the trace components eliminated and complete combustion assumed, simulations made using REFPROP required long computation times and are impractical for rapid parametric studies.

A series of comparative analyses were performed to identify the best physical property method in Aspen Plus® (Aspen) to use for direct-fired sCO_2 cycles. These analyses include assessment of property methods for matching saturated liquid and vapor states of pure CO_2, superheated CO_2 vapor properties, as well as vapor/liquid equilibria of CO_2-H_2O mixtures. Finally, the various property methods are compared against REFPROP as a standard in predicting the performance of various unit operations in a simplified direct sCO_2 cycle.

PROPERTY ASSESSMENT FOR PURE CO_2

Based on the recommendations in the Aspen physical property selection tool and the technical documentation (accessible through the Help system in the Aspen Plus software), 10 physical property methods were selected for detailed assessment. These methods are: REFPROP, LK-PLOCK, PR-BM, BWRS, BWR-LS, SRK, RKS, SR-POLAR, GRAYSON, and PC-SAFT. This set is similar to that examined in a previous NETL report. [10] Property methods used in other studies include PR-BM [4], the Peng-Robinson Equation of State (EOS) [1, 5], the Redlich-Kwong-Soave (RKS) EOS [5], and UNIFAC [6, 11], though little justification is given for these selections. UNIFAC uses the Redlich-Kwong EOS, and thus is expected to produce similar results to the RKS and SRK property methods used in this work.

Table 1 lists the basic features of the physical property methods examined. All of these methods are recommended for mixtures of light gases and all are significantly more accurate than the IDEAL (ideal gas) physical property method for conditions encountered in sCO_2 power cycles. No custom binary interaction parameters are used. Additional details on these physical property methods can be found in the Aspen Plus technical documentation.

Table 1: Aspen physical property methods examined

Aspen Name	Derived From	Type	Interaction Parameters	Least Accurate Region	Consistent in Critical Region
REFPROP	Span-Wagner EOS [7]	Custom	None	CP	Unspecified
LK-PLOCK	Lee-Kesler-Plöcker EOS	Virial	Binary, user adjust	CP	Yes
PC-SAFT	Perturbed-Chain Statistical Associating Fluid Theory	Specialty	Binary, 3 types, user adjust	Unspecified	Unspecified
RK-SOAVE	Redlich-Kwong-Soave EOS	Cubic	Binary, user adjust	CP	Yes
PR-BM	Peng Robinson EOS with Boston-Mathias alpha function	Cubic	Binary, undefaulted	CP	Yes
BWRS	Benedict-Webb-Rubin-Starling EOS	Virial	Binary, 2 sets, user adjust	Unspecified	Unspecified
BWR-LS	Benedict-Webb-Rubin-Lee-Starling EOS	Virial	Binary, 2 sets, user adjust	Unspecified	Unspecified
SRK	Soave-Redlich-Kwong EOS	Cubic	Optional binary (SRK-KD)	Unspecified	Unspecified
SR-POLAR	Schwarzentruber and Renon EOS	Cubic, elec	Binary, user adjust	CP	Unspecified
GRAYSON	Multiple	Custom	None	T<16C, P>21 MPa, CP	Unspecified

The initial evaluation is made using data from the pure CO_2 vapor-liquid saturation line, as shown in Table 2 [12]. The data in this table was generated using REFPROP and the Span-Wagner EOS, which has been shown to reproduce highly accurate saturated CO_2 density experimental data to within 0.01% below 293 K, and to within 0.5% up to the critical point [7]. The Aspen vapor-liquid flash is used to calculate the saturation line at the data points listed. The initial comparison is based on specific volume results of the vapor and liquid phases. Comparisons are based on root mean square (RMS) relative deviation from the data set of Table 2.

Table 2: Pure saturated CO_2 property data [12]

T (K)	P (MPa)	v_f (m^3/kg)	v_g (m^3/kg)	h_f (kJ/kg)	h_g (kJ/kg)
216.6	0.5180	0.000849	0.07267	80.0	430.4
220	0.5991	0.000858	0.06322	86.7	431.6
225	0.7351	0.000871	0.05192	96.6	433.2
230	0.8929	0.000886	0.04297	106.6	434.6
235	1.0747	0.000902	0.03582	116.6	435.7
240	1.2825	0.000918	0.03003	126.8	436.5
245	1.5185	0.000936	0.02532	137.2	437.0
250	1.7850	0.000956	0.02144	147.7	437.0
255	2.0843	0.000977	0.01822	158.5	436.7
260	2.4188	0.001001	0.01552	169.4	435.9
270	3.2033	0.001057	0.01132	192.4	432.6
275	3.6589	0.001092	0.00965	204.6	429.8
280	4.1607	0.001132	0.00821	217.3	425.9
290	5.3177	0.001243	0.00582	245.6	413.8
300	6.7131	0.001472	0.00372	283.4	387.1
304.2	7.3773	0.002139	0.00214	332.3	332.3

Figure 2 shows an example comparison of the REFPROP data against the calculated results for the LK-PLOCK property method. For this figure, the saturated vapor and liquid results are shown on the upper and lower portions of the curve, respectively. In general, results show very good agreement in calculating the specific volume of saturated liquid and vapor states, with significant error only at the critical point.

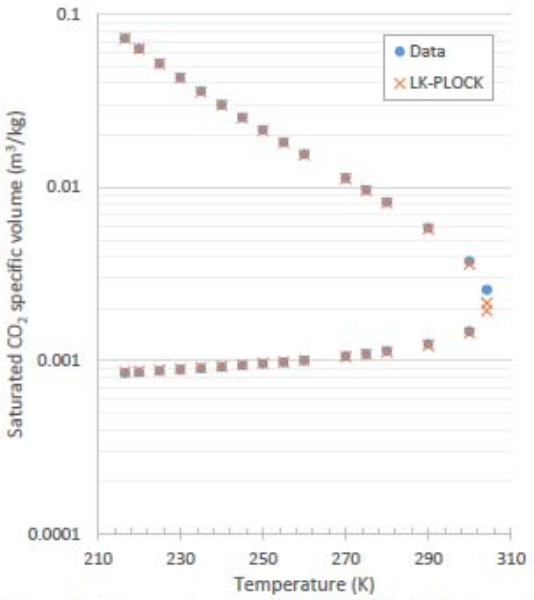

Figure 2: Comparison of LK-PLOCK calculations to saturated CO_2 vapor and liquid specific volume data

Figure 3 shows a comparison of the relative errors in predicting the data in Table 2 for each of the property methods studied. In general, vapor specific volumes are consistently over-predicted for the Grayson, PC-SAFT, SR-POLAR, RKS, and SRK property methods, though all methods have large error near the critical point for this property. The CO_2 liquid specific volume is poorly calculated throughout the temperature range by the SR-POLAR, SRK, and PR-BM property methods. Each of the remaining methods predict the liquid specific volume well, except for large deviations at the last two data points near the critical point (300 and 304.2 K).

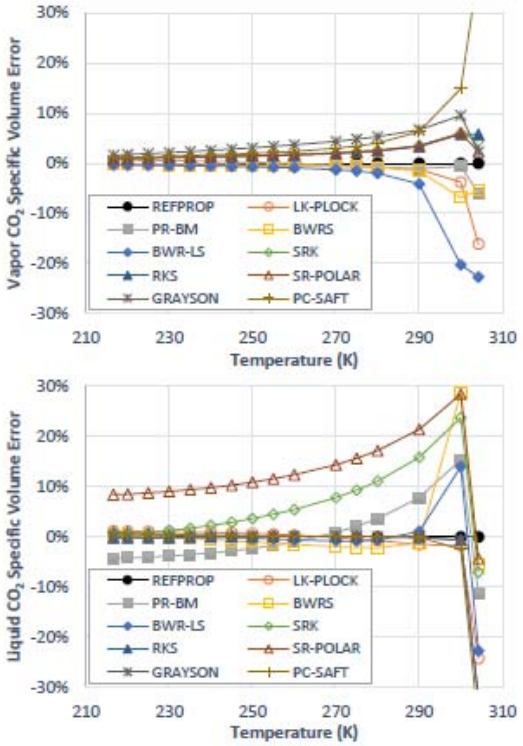

Figure 3: Relative errors of property methods in calculating saturated vapor (upper) and liquid (lower) CO_2 specific volumes

Table 3: Pure saturated CO_2 molar volume evaluation

Property Method	Relative RMS Δv (%) (no critical point)
LK-PLOCK	0.751
RKS	0.847
PC-SAFT	1.426
GRAYSON	1.489
BWR-LS	3.122
PR-BM	3.759
BWRS	5.696
SRK	6.488
SR-POLAR	9.063

Table 3 shows the average RMS relative deviations calculated for the saturated liquid and vapor molar volumes for all nine methods, sorted by increasing deviation. LK-PLOCK had the smallest deviation followed by RKS. The methods GRAYSON, and PC-SAFT had larger deviations due to difficulties noted above in calculating CO_2 saturated vapor specific volumes, but their accuracy is still deemed to be good.

The results are shown graphically in Figure 4 for the liquid and vapor states separately, and show the relative strengths and weaknesses of each of the property methods in modeling the liquid and vapor states of CO_2.

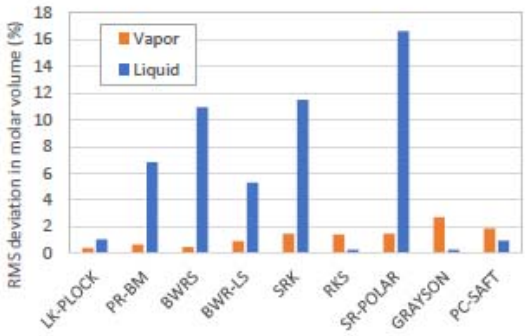

Figure 4: Pure saturated CO_2 vapor and liquid molar volume evaluation

An analogous comparison was made to a second pure CO_2 property data set of 84 points, based on REFPROP calculations for superheated CO_2. [12] The temperature range for the data was 300 – 1000 K and the pressure range was 3 - 30 MPa, focusing on sCO_2 cycle conditions of interest. The Aspen pure component property analysis feature was used to calculate superheated data at these conditions. In this case, only superheated vapor properties were calculated. Comparisons are based on average RMS deviation of the specific volume from REFPROP data. Table 4 lists the physical property methods ranked by the magnitude of the deviations.

Table 4: Pure superheated CO_2 property evaluation

Property Method	Relative RMS Δv (%) (no critical point)
BWR-LS	0.364
PC-SAFT	0.401
LK-PLOCK	0.521
PR-BM	0.652
SRK	1.108
RKS	1.154
GRAYSON	1.161
BWRS	1.214
SR-POLAR	1.429

For this second pure CO_2 property evaluation, the most accurate methods are BWR-LS, PC-SAFT, and LK-PLOCK. Figure 5 shows bubble plots of the relative error for these property methods as a function of temperature and pressure, which are useful for selecting the most accurate property methods for particular sCO_2 component operating conditions.

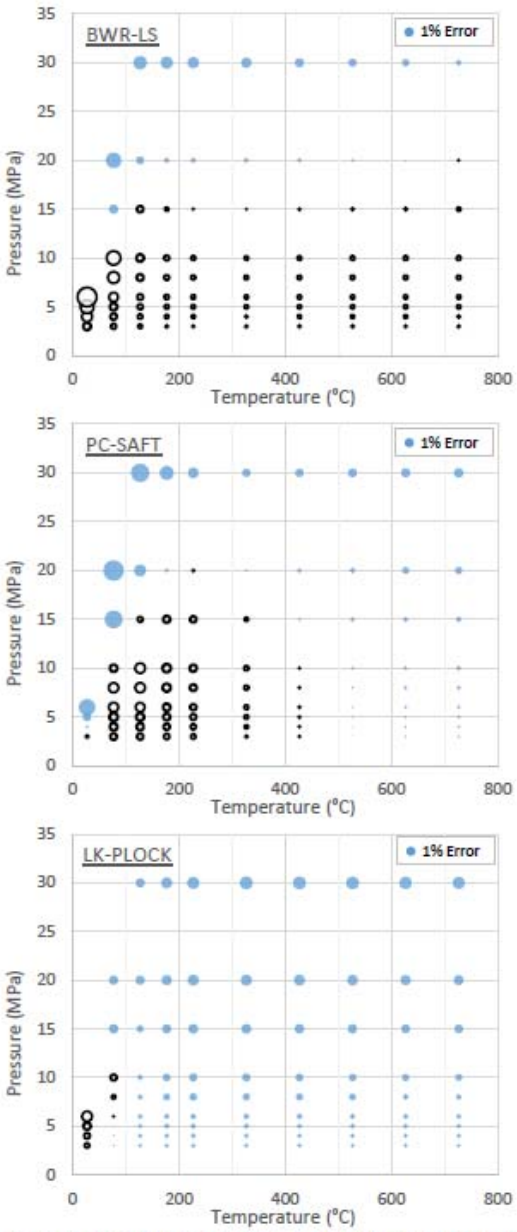

Figure 5: Relative error (bubble area) in superheated CO_2 molar volume. Solid bubbles are positive deviations from REFPROP, empty bubbles are negative deviations

PROPERTY ASSESSMENT FOR CO_2:H_2O BINARY MIXTURE

One area where direct sCO_2 cycle models may be challenged is in correctly calculating the water knock-out process on the low pressure side of the cycle. Depending on the fuel composition and CO_2 recycle conditions, the predominantly sCO_2 process fluid passing through the turbine and hot side of the recuperator may contain 2-7% water vapor by volume [1, 6]. As the process fluid is cooled, water vapor condenses out into liquid water, typically at temperatures ranging from 20 – 100 °C, and pressures from 2.5 – 4 MPa [1-6]. Accurate modeling of this process is required for two reasons. First, depending on cycle conditions, water may begin to condense out within the recuperator, which typically leads to an internal temperature pinch point that limits recuperator effectiveness and cycle efficiency. This can be managed to regain effectiveness if the onset and extent of the internal condensation are properly predicted. Second, following the water knock-out stage, the remaining water vapor in the sCO_2 process fluid acts as an impurity that increases the required cycle compression power, due to its much lower density than sCO_2 [6]. Accurate modeling of the remaining water vapor content will better predict the cycle's compression power requirements, and hence its efficiency.

Due to the importance of this process, another property evaluation was performed for the CO_2:H_2O binary mixture using experimental data taken from Ref. [10]. The data used are plotted in Figure 6, and show the saturated water content in a CO_2:H_2O mixture as a function of temperature and pressure. The calculated data were obtained by performing a vapor-liquid equilibrium two-phase flash in Aspen with the selected physical property method. Deviations from the experimental data were measured as average RMS of the differences in log10 of the ratio of moles of saturated H_2O per mole CO_2.

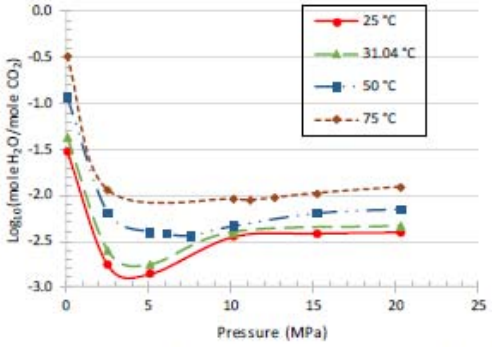

Figure 6: Data used for property assessment of CO_2:H_2O binary mixture [10]

Figures B-1 through B-10 in Appendix B show plots of the calculated data (as lines) compared to the experimental data (dots) for each of the physical property methods. Note that in some cases, the calculated data do not extend to the high pressures in the experimental data. This is because the flash calculation failed for those conditions. Of the 26 data points for which calculations were attempted, all property methods were able to calculate at least 20 data points, with BWRS, REFPROP, and SRK successfully calculating 23, 24, and 25 data points, respectively. Note that failed calculations are occurring at higher pressures than those presently employed in direct sCO_2 cycle water knockout stages.

Figure 7 plots the average RMS deviation from the data in Figure 6 for all ten physical property methods, in order of increasing error. In this case the most accurate methods are REFPROP, PR-BM, BWR-LS, RKS, and LK-PLOCK.

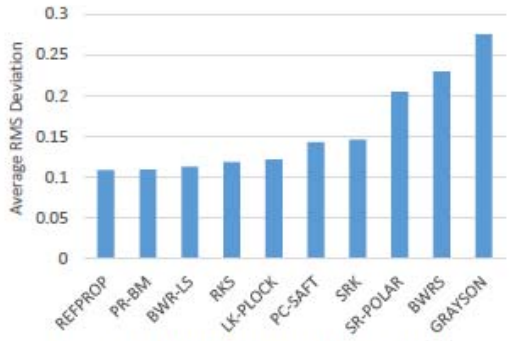

Figure 7: CO_2:H_2O binary property evaluation

CYCLE MODEL PROPERTY ASSESSMENT

As a final evaluation, a preliminary sCO_2 cycle [4] was modeled using different physical property methods and the results compared. In the absence of a model validation data set for a direct sCO_2 power cycle, comparisons are made to a single converged solution of the cycle model obtained using REFPROP with a reduced chemical species set (without HCl, NH_3, H_2S, and SOx), due to restrictions or error conditions from Aspen. The results for this baseline cycle are shown in Table A-1, and were compared to results using six physical property methods. These were LK-PLOCK, PC-SAFT, RK-SOAVE, PR-BM, BWRS, and BWRS-REF, a version of BWRS that used binary interaction parameters that were fit to REFPROP data. The latter model is included here for comparison to prior internal modeling efforts, while RK-SOAVE (RKS) and PR-BM are chosen due to their use in other studies [1, 5]. LK-PLOCK and PC-SAFT are included as the two best-performing property methods overall from the above analyses.

The comparison is based on a subset of stream data and unit operations block outputs that are considered important for accurately characterizing the performance of the system. To isolate the impact of deviations in the physical property model predictions, the feed stream to each process unit was set equal to the feed stream calculated in the converged REFPROP case.

Initially 26 process variables were examined, but it became apparent that most of the deviations were contained in 12 of the variables. As expected, the major differences arose for process units that operate near the CO_2 critical point, and negligible differences were seen between the property methods in the outputs of the turbine and oxy-combustion processes. Table 5 shows the list of 12 process variables used to quantitatively compare the six physical property methods.

Table 5: Process variables used to compare physical property models

No.	Process unit	Variable
1	Recuperator	Minimum temperature approach
2		Cold side stream vector
3		Hot side stream vector
4	CO_2 cooler	Mole fraction H_2O in outlet vapor
5	CO_2 pre-compressor	Outlet stream vector
6		Intercooler heat duty
7		Power requirement
8	Condenser	Outlet stream vector
9		Heat duty
10	Pump	Outlet stream vector
11		Exit temperature
12		Power requirement

For stream vector entries, an average RMS relative deviation was calculated for the enthalpy and density stream variables that were calculated by the physical property method.

Figure 8 shows the calculated relative deviation for the 12 key process variables listed in Table 5, for each of the six physical property methods tested. In this case, LK-PLOCK and PC-SAFT produced results most consistent with those from REFPROP.

In cases where the stream vector variable resulted in large discrepancies, differences in bulk fluid densities compared to those from REFPROP are generally the root cause. This is shown to be a problem for BWRS and BWRS-REF, which is consistent with BWRS's poor performance in predicting vapor molar volumes relative to the subset of property methods used in this analysis, per Figure 3. The large errors for all property methods for the pre-compressor stream vector results from the existence of a condensate stream per the REFPROP calculations (stream 13 in Figure 1 and Table A-1), which does not appear for any of the other property methods. As noted in Figures B-1 to B-10, water content is typically underpredicted at 25 °C and low pressures for most property methods, and often results in a failure to execute the calculation at higher pressures for this temperature. This is also consistent with the relative errors in the water vapor fraction exiting the CO_2 Cooler, where Figures 8 and B-10 show that PC-SAFT performs well at these conditions.

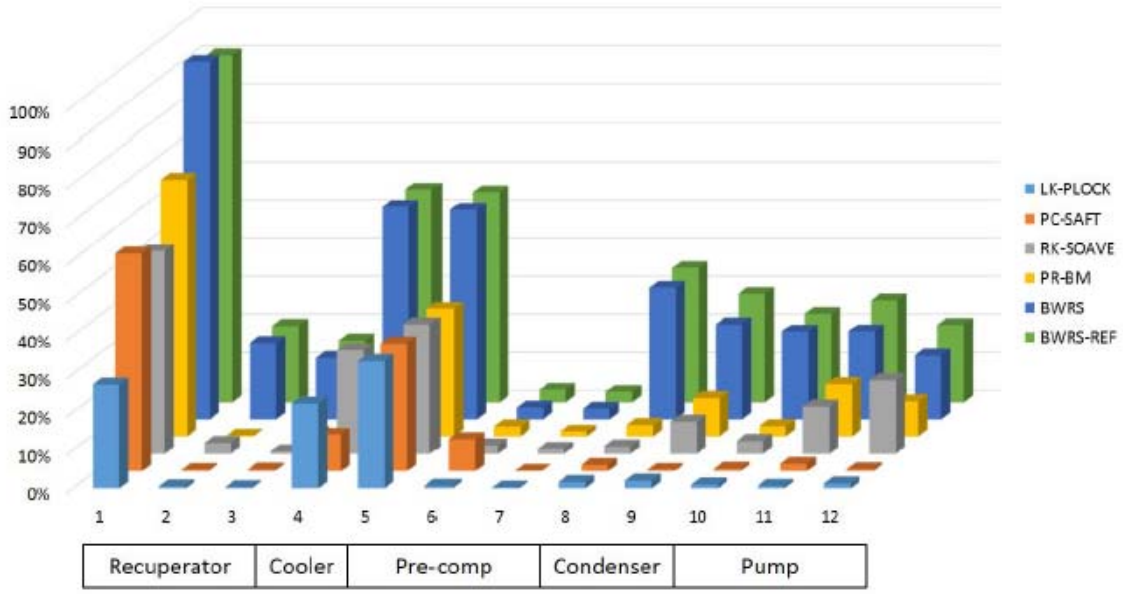

Figure 8: Relative differences in key performance variables from REFPROP. Numbered variables defined in Table 5.

Also shown in Figure 8 are large errors in the cold-end recuperator approach temperature relative to REFPROP, which is nominally 10 °C per Table A-1. PC-SAFT overestimated this approach temperature, but all other property methods underestimated it, with BWRS-based methods predicting about 1 °C approach temperature. This is due in large part to the fact that some water vapor condensation occurs within the recuperator (stream 8 in Figure 1 and Table A-1). The latent heat of vaporization affects the recuperator temperature profiles, underscoring the importance of accurate property methods for recuperator and cycle design purposes.

One final observation from Figure 8 is that the pump exit temperature is overpredicted by several property methods, which leads to errors in required pump power relative to REFPROP. Factoring this into the performance of a direct sCO_2 plant, a 10% error in the predicted pump power requirements roughly equates to 0.5 percentage points in the plant's net thermal efficiency [4]. This points again to the importance of utilizing accurate property methods in the modeling of direct sCO_2 power plants.

CONCLUSIONS

This work examines the ability of various physical property methods to accurately model fluid properties for direct sCO_2 power systems. General observations and recommendations are as follows:

1. For pure CO_2 process fluids at near-supercritical conditions, REFPROP is by far the best-performing property method, as concluded in other studies [8]. LK-PLOCK and PC-SAFT also perform well under these conditions.
2. In binary CO_2:H_2O mixtures, the most accurate methods for determining saturated water content at direct sCO_2 cycle conditions are REFPROP, PR-BM, BWR-LS, LK-PLOCK, and RKS. Most of these property methods, with the exception of REFPROP, give errors in Aspen Plus for conditions at or below the CO_2 critical temperature of 31.04 °C and above the critical pressure of 7.37 MPa., which may be problematic depending on the cycle design.
3. REFPROP is the recommended property method for direct sCO_2 power cycle modeling, however, it may not be compatible with the species set required for accurate modeling of syngas-fired direct sCO_2 cycles.
4. In these cases, performance indicators for various cycle processes were computed for several property methods and compared to REFPROP under a reduced species set. Results show that LK-PLOCK and PC-SAFT perform most similarly to REFPROP under the cycle conditions studied.
5. Given its superior performance in predicting saturated CO_2 properties and saturated water content in binary CO_2:H_2O mixtures, LK-PLOCK is the recommended property method if REFPROP cannot be used due to species compatibility or computational time constraints. LK-PLOCK has also been recommended for CO_2 compression studies [10, 13]. PC-SAFT is the next best option after LK-PLOCK, though it tends to under-predict saturated water content in sCO_2, whereas LK-PLOCK tends to over-predict this quantity.

Based on the results of this effort, the preliminary analysis of the direct sCO_2 power cycle by the authors in Ref. [4] is being modified to change the property method from PR-BM to LK-PLOCK to improve the accuracy of the results.

The property method analysis performed in this work is certainly not exhaustive, but should serve to guide the selection of property methods for modeling direct sCO_2 systems, particularly those with an expanded species set as encountered in syngas-fired systems. Additional comparisons to calorific data, where available, may also be pursued in future work to improve the utility of these results. The experimental data available for comparing property methods in this temperature, pressure, and composition space is sparse, however, particularly for CO_2 mixtures. Future analyses would benefit greatly from a more expansive data set at these conditions for model validation purposes, which will hopefully arise out of increased development and construction of these cycles in the coming years.

ACKNOWLEDGMENTS

This report was prepared under the Mission Execution and Strategic Analysis (MESA) Contract DE-FE00025912 for the United States Department of Energy (DOE), National Energy Technology Laboratory (NETL). This work was performed under MESA Activity 25912.02.2300.201.005. All images in the report are source NETL.

The authors wish to acknowledge the excellent guidance, contributions, and cooperation of the NETL staff, particularly: Richard Dennis, Walter Shelton, and Travis Shultz.

NOMENCLATURE

Ar	Argon
bar	100,000 Pascal
CO	Carbon monoxide
CO_2	Carbon dioxide
CP	Critical point
EOR	Enhanced oil recovery
EOS	Equation of state
H_2O	Water
H_2S	Hydrogen sulfide
HCl	Hydrogen chloride
h_f	Saturated liquid enthalpy
h_g	Saturated vapor enthalpy
K	Kelvin
kg	Kilogram
kJ	Kilojoule
m^3	Cubic meter
MPa	Megapascal
N_2	Nitrogen
NH_3	Ammonia
NIST	National Institute of Standards and Technology
O_2	Oxygen
P	Pressure, Pump
PC	Pre-compressor
psi	Pounds per square inch
Recup	Recuperator
REFPROP	Reference Fluid Thermodynamic and Transport Properties
RMS	Root mean square
sCO_2	Supercritical carbon dioxide
SGC	Syngas cooler
SOx	Sulfur oxides
T	Temperature, Turbine
v_f	Saturated liquid volume
v_g	Saturated vapor volume
°C	Degrees Celsius
°F	Degrees Fahrenheit

REFERENCES

[1] International Energy Agency Greenhouse Gas (IEAGHG), August 2015, "Oxy-combustion Turbine Power Plants," Cheltenham, United Kingdom.

[2] Allam, R.J., Palmer, M.R., Brown Jr., G.W., Fetvedt, J., Freed, D., Nomoto, H., Itoh, M., Okita, N., Jones Jr., C. (2013). "High Efficiency and Low Cost of Electricity Generation from Fossil Fuels While Eliminating Atmospheric Emissions, Including Carbon Dioxide." Energy Procedia, 37:1135–1149.

[3] Allam, R.J., Fetvedt, J.E., Forrest, B.A., Freed, D.A. (2014, June 16-20). "The Oxy-Fuel, Supercritical CO2 Allam Cycle: New Cycle Developments to Produce Even Lower-Cost Electricity from Fossil Fuels without Atmospheric Emissions," GT2014-26952. ASME Turbo Expo: Düsseldorf, Germany, pp. V03BT36A016; 9 pages.

[4] Weiland, N., Shelton, W., White, C. and Gray, D., "Performance baseline for direct-fired sCO2 cycles," in 5th International Supercritical CO2 Power Cycles Symposium, San Antonio, Texas, March 29-31, 2016.

[5] Lu., X., Forrest, B., Martin, S., Fetvedt, J., McGroddy, M., and Freed, D. (2016, June 13-17). "Integration and Optimization of Coal Gasification Systems with a Near Zero Emissions Supercritical Carbon Dioxide Power Cycle," GT2016-58066, ASME Turbo Expo: Seoul, South Korea, pp. V009T36A019; 9 pages.

[6] Electric Power Research Institute (EPRI). (2014, December). Performance and Economic Evaluation of Supercritical CO2 Power Cycle Coal Gasification Plant (3002003734). Palo Alto, California.

[7] Span, R. and Wagner, W., 1996, "A New Equation of State for Carbon Dioxide Covering the Fluid Region from the Triple-Point Temperature to 100 K at Pressures up to 800 MPa," J. Phys. Chem. Ref. Data, Vol 25, No. 6, pp. 1509-1596.

[8] Zhao, Q., Mecheri, M., Neveux, T., Privat, R. and Jaubert, J.-N., "Thermodynamic model investigation for supercritical CO2 Brayton cycle for coal-fired power plant application," in 5th International Supercritical CO2 Power Cycles Symposium, San Antonio, Texas, March 29-31, 2016.

[9] National Institute of Standards and Technology (NIST), 2007, NIST Reference Fluid Thermodynamic and Transport Properties - REFPROP, U.S. Department of Commerce.
[10] National Energy Technology Laboratory (NETL), October 6, 2013, "CO2 Compressor Simulation User Manual," Carbon Capture Simulation Initiative.
[11] Hume, Scott, January 20th, 2017, EPRI, Private Communication.
[12] Green, D.W., 2008, "Perry's Chemical Engineers' Handbook, 8th Ed," McGraw-Hill.
[13] Baltadjiev, NZ. D., 2012, "An Investigation of Real Gas Effects in Supercritical CO2 Compressors", M.S. Thesis, Massachusetts Institute of Technology, Cambridge, MA.

APPENDIX A: STATE POINT TABLE FOR DIRECT SCO_2 CYCLE

Referring to Figure 1, the fuel (Stream 1) adiabatically mixes with the heated recycle CO_2 (Stream 17) to form the partially preheated mixed fuel and sCO_2 (Stream 2). This stream is heated in the syngas cooler where zero heat loss is assumed to create the final preheated fuel and sCO_2 (Stream 3). This stream, along with the oxygen (Stream 4) enters the combustor where 100 percent conversion of the combustible species occurs. No heat loss is assumed in the combustor and the pressure drop is set at 0.69 MPa. One percent excess oxygen is fed to the combustor. The combustor effluent (Stream 5) is expanded in the turbine which has an isentropic efficiency of 0.927. The turbine effluent (Stream 6) passes through the hot side of the recuperator. The outlet (Stream 7) is partially condensed. After a small purge is taken (Stream 9) additional cooling and partial recompression removes most of the remaining water. The partially recompressed stream (Stream 14) is further cooled to 27 °C and recompressed to 30.0 MPa. Both compressors have isentropic efficiencies of 0.85. The high-pressure cool recycle sCO_2 (Stream 16) then enters the cold side of the recuperator to complete the cycle. The heat exchanger units in the cycle have a total of 0.45 MPa pressure drop.

Table A-1: State point table for direct sCO_2 cycle of Figure 1

Stream	1	2	3	4	5	6	7	8	9
V-L Mole Fraction									
CO_2	0.0442	0.8885	0.8885	0	0.9558	0.9558	0.9558	0.0006	0.9696
H_2O	0.0014	0.0015	0.0015	0	0.0299	0.0299	0.0299	0.9994	0.0158
Ar	0.0016	0.0047	0.0047	0.0044	0.0050	0.0050	0.0050	0	0.0050
O_2	0	0.0004	0.0004	0.9950	0.0005	0.0005	0.0005	0	0.0005
N_2	0.0063	0.0089	0.0089	0.0006	0.0089	0.0089	0.0089	0	0.0090
CO	0.6666	0.0676	0.0676	0	0	0	0	0	0
CH_4	0.0001	0	0	0	0	0	0	0	0
H_2	0.2797	0.0284	0.0284	0	0	0	0	0	0
Total	1.0000	1.0000	1.0000	1.0000	1.0000	1.0000	1.0000	1.0000	1.0000
V-L Flowrate (kg_{mole}/hr)	15,809	155,810	155,810	7,528	155,858	155,858	155,858	2,224	11,589
V-L Flowrate (kg/hr)	339,092	6,470,942	6,470,942	241,141	6,712,083	6,712,083	6,712,083	40,099	503,299
Vapor Fraction	0	1.0000	1.0000	1.0000	1.0000	1.0000	0.9857	0	1.0000
Temperature (°C)	679	677	699	139	1149	760	73	73	73
Pressure (MPa, abs)	29.99	29.86	29.86	30.06	29.17	2.92	2.78	2.78	2.78
Enthalpy (kJ/kg)	-3,314.18	-7,907.00	-7,878.58	78.88	-7,586.43	-8,095.14	-8,892.65	-15,650.94	-8,852.03
Density (kg/m^3)	60.4	145.8	142.4	262.5	99.2	14.6	46.3	976.3	46.0
V-L Molecular Weight	21.449	41.531	41.531	32.031	43.065	43.065	43.065	18.031	43.428

Stream	10	11	12	13	14	15	16	17
V-L Mole Fraction								
CO_2	0.9696	0.0003	0.9835	0.0004	0.9838	0.9838	0.9838	0.9838
H_2O	0.0158	0.9997	0.0018	0.9996	0.0015	0.0015	0.0015	0.0015
Ar	0.0050	0	0.0051	0	0.0051	0.0051	0.0051	0.0051
O_2	0.0005	0	0.0005	0	0.0005	0.0005	0.0005	0.0005
N_2	0.0090	0	0.0091	0	0.0091	0.0091	0.0091	0.0091
CO	0	0	0	0	0	0	0	0
CH_4	0	0	0	0	0	0	0	0
H_2	0	0	0	0	0	0	0	0
Total	1.0000	1.0000	1.0000	1.0000	1.0000	1.0000	1.0000	1.0000
V-L Flowrate (kg_{mole}/hr)	142,045	1,997	140,048	47	140,001	140,001	140,001	140,001
V-L Flowrate (kg/hr)	6,166,685	35,991	6,132,694	643	6,131,650	6,131,650	6,131,650	6,131,650
Vapor Fraction	1.0000	0	1.0000	0	1.0000	0	1.0000	1.0000
Temperature (°C)	73	27	27	27	47	27	63	679
Pressure (MPa, abs)	2.78	2.78	2.78	2.78	7.58	7.48	29.99	29.86
Enthalpy (kJ/kg)	-8,852.03	-15,849.83	-8,874.45	-15,847.23	-8,914.64	-9,068.74	-9,033.96	-8,160.98
Density (kg/m^3)	46.0	997.2	57.4	997.1	203.0	681.9	804.9	154.3
V-L Molecular Weight	43.428	18.023	43.790	18.026	43.799	43.799	43.799	43.799

APPENDIX B

COMPARISON OF CALCULATED AND EXPERIMENTAL SATURATED H_2O CONTENT IN CO_2:H_2O BINARY MIXTURES

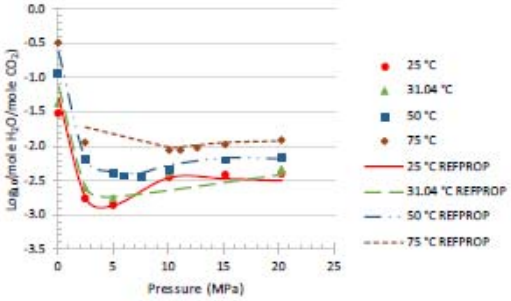

Figure B-1: Calculated versus experimental data for REFPROP

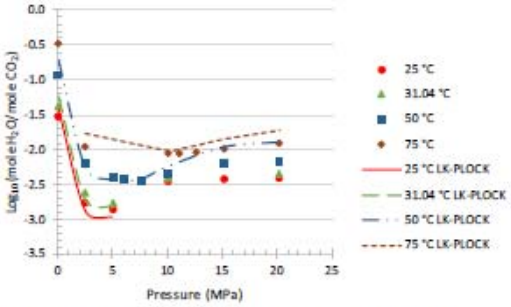

Figure B-2: Calculated versus experimental data for LK-PLOCK

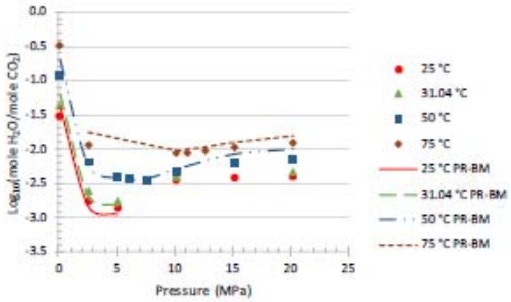

Figure B-3: Calculated versus experimental data for PR-BM

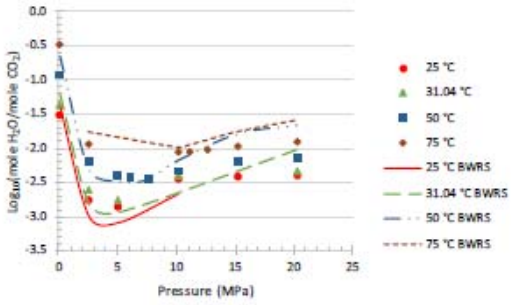

Figure B-4: Calculated versus experimental data for BWRS

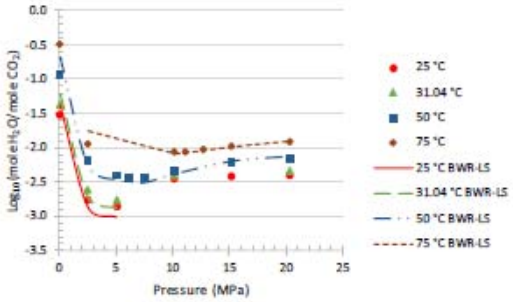

Figure B-5: Calculated versus experimental data for BWR-LS

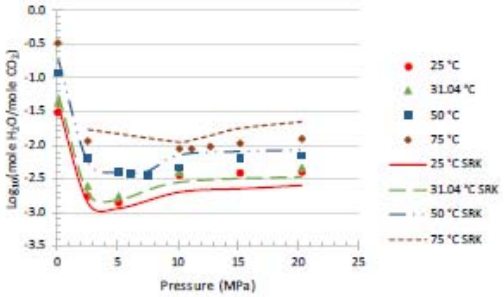

Figure B-6: Calculated versus experimental data for SRK

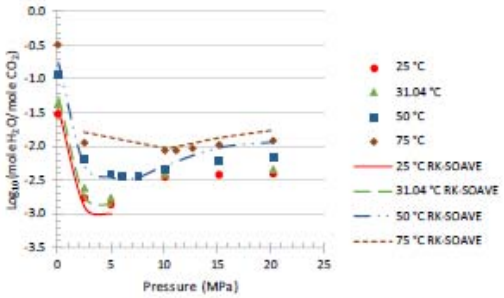

Figure B-7: Calculated versus experimental data for RK-SOAVE

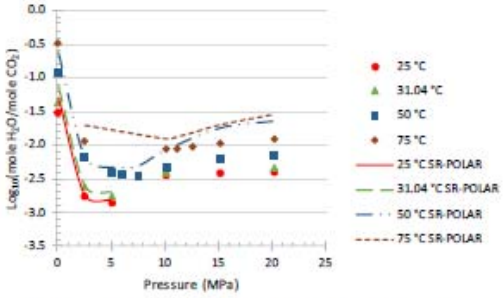

Figure B-8: Calculated versus experimental data for SR-POLAR

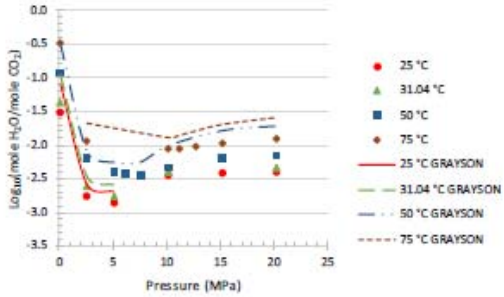

Figure B-9: Calculated versus experimental data for GRAYSON

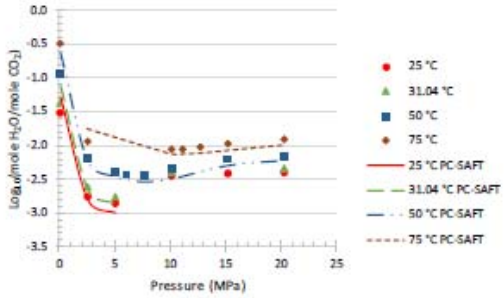

Figure B-10: Calculated versus experimental data for PC-SAFT

Nathan Weiland
nathan.weiland@netl.doe.gov

Mark Woods
mark.woods@netl.doe.gov

www.netl.doe.gov

Albany, OR • Anchorage, AK • Morgantown, WV • Pittsburgh, PA • Sugar Land, TX

(800) 553-7681

NATIONAL ENERGY TECHNOLOGY LABORATORY